Internet Congestion Control: Modeling and Stability Analysis

by

Lijun Wang

A thesis
presented to the University of Waterloo
in fulfillment of the
thesis requirement for the degree of
Doctor of Philosophy
in
Applied Mathematics

Waterloo, Ontario, Canada, 2008

I hereby declare that I am the sole author of this thesis. This is a true copy of the thesis, including any required final revisions, as accepted by my examiners.

I understand that my thesis may be made electronically available to the public.

Abstract

The proliferation and universal adoption of the Internet has made it become the key information transport platform of our time. Congestion occurs when resource demands exceed the capacity, which results in poor performance in the form of low network utilization and high packet loss rate. Internet congestion control is a topic that has drawn attentions of many researchers, and it has also become a facet of daily life for Internet users. The goal of congestion control mechanisms is to use the network resources as efficiently as possible, that is, attain the highest possible throughput while maintaining a low loss ratio and small delay. The research work in this thesis is centered on finding ways to address these types of problems and provide guidelines for predicting and controlling network performance, through the use of suitable mathematical tools and control analysis.

The first congestion collapse in the Internet was observed in 1980's, although the Internet was still in its early stage at that time. To solve the problem, Van Jacobson proposed the Transmission Control Protocol (TCP) congestion control algorithm based on the Additive Increase and Multiplicative Decrease (AIMD) mechanism in 1988. To be effective, a congestion control mechanism must be paired with a congestion detection scheme. To detect and distribute network congestion indicators fairly to all on-going flows, Active Queue Management (AQM), e.g., the Random Early Detection (RED) queue management scheme has been developed to be deployed in the intermediate nodes. The currently dominant AIMD congestion control, coupled with the RED queue in the core network, has been acknowledged as one of the key factors to the overwhelming success of the Internet.

In this thesis, the AIMD/RED system, based on the fluid-flow model, is systematically studied. In particular, we concentrate on the system modeling, stability analysis and bounds estimates. We first focus on the stability and fairness analysis of the AIMD/RED system with a single bottleneck. Stability results and fairness conditions are obtained for both homogeneous- and heterogeneous-flow systems with and without feedback delays. Then, we derive the theoretical estimates for the upper and lower bounds of homogeneous and heterogeneous AIMD/RED systems with feedback delays and further discuss the system performance when it is not asymptotically stable. Last, we develop a general mathematical model for a class of multiple-bottleneck networks and discuss the stability properties of such a system. Our analytical results are validated both numerically and by simulations. Theoretical and simulation results presented on this thesis provide important insights for in-depth understanding of the AIME/RED system and can also help predict and control the system performance for the Internet with higher data rate links multiplexed with heterogeneous flows.

Acknowledgments

First and foremost, I would like to express my gratitude to my advisors, Professor Xinzhi Liu and Professor Xuemin (Sherman) Shen, for bringing me into this area and giving me their invaluable guidance and help throughout my Ph.D. studies. The constant support and precious advice they provided in many ways during the preparation of this thesis are greatly appreciated.

I would like to thank Professor Nair. U. Ahmed, Professor Liangliang Xie, Professor Sue Ann Campbell and Professor Brian Ingalls for serving as my committee members. Their valuable comments and suggestions are very important for improving the quality of this thesis.

Special thanks go to Dr. Lin Cai, Dr. Junshan Zhang, Dr. Hiroaki Mukaidani and Dr. Yi Zhang. I have benefitted greatly from their thoughtful views and constructive advice through the collaborations and discussions with them. Many thanks to my friends and all members in Applied Mathematics for their friendship and support. Thanks for enriching my life with joy and happiness.

Thanks also go to University of Waterloo and the Natural Science and Engineering Council of Canada for their financial support. I am also grateful to the Department of Applied Mathematics for providing such a friendly and supportive research environment throughout my studies.

To my parents and fiance, Gabriel Esteves, my deepest gratitude goes. Thanks for being by my side whenever I needed it. I feel deeply indebted to my family for their unchanging love and encouragement through these many years.

To my dear parents

Contents

List of Tables

List of Figures

Chapter 1

Introduction

1.1 Problem Description and Motivations

The Internet is surely the second most extensive machine on the planet, after the public switched telephone network, and it is rapidly becoming as ubiquitous. As a decentralized system, network stability and integrity rely on the end-to-end congestion control algorithm, which is deployed in the dominant transport layer protocol, Transmission Control Protocol (TCP).

Internet congestion occurs when resource demands exceed the capacity. Congestion in the Internet can cause high packet loss rates, increased delays, and even break the whole system. Without congestion control, as shown in Fig. 1.1, when the offered load is larger than the network capacity, the network power (ratio of throughput to delay) will decrease sharply and the network will be driven to congestion collapse. The circled area in Fig. 1.1 is the desired operation area under congestion control. The main targets of TCP congestion control are to explore and fully utilize the available bandwidth for

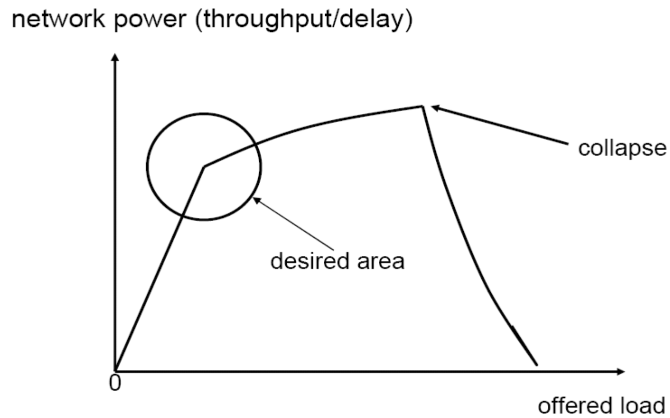

Figure 1.1: Objective of Congestion Control

a connection and to avoid severe congestions in the network, i.e., to make the network operating near the optimal area.

To deal with this problem, Van Jacobson proposed the Transmission Control Protocol (TCP) congestion control algorithm based on the Additive Increase and Multiplicative Decrease (AIMD) mechanism in 1988: when there is no congestion indication (no packet loss), the TCP congestion window size is increased linearly by one packet per round-trip time (RTT); otherwise, the TCP congestion window size is reduced by half upon the detection of packet loss. Since then, the TCP congestion control algorithm has been widely deployed in the end systems to respond to network congestion signals and avoid network congestion collapses.

Driven by new commercial demands and technological progress, the Internet is supporting differentiated services, e.g. a large amount of multimedia applications. Although it has been shown that TCP congestion control is very successful for bulk data transfer, its increase-by-one or decrease-by-half strategy produces a highly fluctuating sending rate which is undesirable for many applications that have very stringent delay requirement. For example, most multimedia traffic cannot tolerate its sending rate suddenly cut by half.

To overcome this limitations of TCP while maintaining all its advantages, a TCP-friendly Additive Increase and Multiplicative Decrease (AIMD) congestion control strategy has been proposed [11] to support heterogeneous services over the Internet. For each round trip time, the AIMD sender either increase its congestion window by α packets if no congestion occurs, or decrease the window to β times its current value when congestion signal is captured. For different traffic, appropriate pair of parameters (α, β) can be chosen according to the traffic characteristics to improve its quality of service (QoS). The protocol with this congestion control mechanism is called the AIMD(α, β) protocol. Without any modifications to the core networks, the AIMD protocol can be a scalable solution to support differentiated services. [11] also showed that AIMD can be efficient on bandwidth utilization, fairly share the network resources with ordinary TCP flows, and provide better QoS.

TCP/AIMD has no information of network mechanisms contributing to packet loss, which is taken as an indicator of congestion in the wired network. To effectively control the congestion in the Internet, a congestion control mechanism must be paired with a congestion detection scheme. To detect and distribute network congestion indicators fairly to all on-going flows, Active Queue Management (AQM), e.g., the Random Early Detection (RED) queue management scheme has been developed to be deployed in the intermediate nodes. The currently dominant AIMD congestion control, coupled with the RED queue management that is widely deployed in the core network, has been acknowledged as one of the key factors to the overwhelming success of the Internet [40, 41].

With the rapid advances in optical and wireless communications, Internet is becoming an even more diversified system. It will contain heterogeneous wireless and wired links with speeds varying from tens of Kbps to tens of Gbps, with flow round-trip delays varying from ms to seconds. It will also support various multimedia applications with different throughput, delay, and jitter requirements. A critical and immediate question is whether the AIMD/RED system is a stable, fair, and efficient system, independent of the heterogeneity of the link capacity, end-to-end delay, and network topology. In other words, should we re-design the Internet congestion control mechanism to accommodate future killer applications over the ever-diversified Internet, or can we take an incremental approach of engineering the existing congestion control mechanism and routers' queue management parameters to achieve the same objective?

With large time delays or link capacities, the AIMD/RED system as a whole may not be asymptotically stable [9]. However, It has been understandable that as long as the system operates near its desired equilibrium, small oscillations are acceptable, and the network performance can still be satisfactory, i.e., the overall system efficiency can still be high, and the packet loss rate and queuing delay can still be well bounded. Therefore, the important issue to investigate is: does the AIMD/RED system always operate in the area close to the desired equilibrium state, and what are the theoretical bounds?

A realistic network normally accommodates flows that undergo multiple bottlenecks. It has been shown that the conditions which guarantee the stability of a single-bottleneck system do not apply to the network system with multiple-bottleneck links anymore. This situation is the main motivation to study the stability properties of the general AIMD/RED system with multiple bottlenecks.

In this thesis, we mainly study the AIMD/RED system and focus on solving all the questions outlined above.

1.2 Related Work and Main Contributions

Internet congestion control is a topic that has drawn the attention of many researchers. Stability problems of TCP or AIMD with RED queue have been investigated in the literature [21, 22, 23, 24, 25, 26]. Some new control mechanisms based on control theory and game theory have been proposed [7]. Instead of proposing a new control mechanism, we focus attention on the stability and performance of the currently dominant AIMD congestion control mechanism over RED queues. In [26], using a fluid model, the stability of single-bottleneck TCP/RED system is proved, neglecting the feedback delay. The stability of TCP/RED with feedback delay has been questioned in [9], which suggested that TCP/RED becomes unstable when delay increases, or more strikingly, when link capacity increases. Furthermore, for the vast-scale Internet, a single bottleneck topology may not be representative. The stability issue with multiple bottlenecks has been investigated in [61], which concluded that TCP/RED may become unstable with multiple bottleneck scenario if the configuration of RED queue is inappropriate.

Our main objective in this thesis is to provide theoretical support for the analysis of AIMD/RED system. Theoretical analysis and simulation results presented in the thesis provide important insights for the in-depth understanding of the AIMD/RED system and can be used as guidelines to set up system parameters in order to maintain network stability and to fully utilize network resources without excessive delay and loss.

In this thesis, the AIMD/RED system, based on the fluid-flow model, is systematically studied. In particular, we concentrate on the system modeling, stability analysis and bounds estimates. We first focus on the stability and fairness analysis of the AIMD/RED system with a single bottleneck. Stability results and fairness conditions are obtained for both homogeneous- and heterogeneous-flow systems with and without feedback delays.

Then, we derive the theoretical estimates for the upper and lower bounds of homogeneous and heterogeneous AIMD/RED systems with feedback delays and further discuss the system performance when it is not asymptotically stable. Last, we develop a general mathematical model for a class of multiple-bottleneck networks and discuss the stability properties of such a system. Our analytical results are validated both numerically and by simulations.

Our theoretical findings in the study of this topic are original and of great practical value for controlling and enhancing system performance and efficiency in terms of bounded delay and packet loss. Our results can also help predict and control the system performance for the Internet with higher data rate links multiplexed with heterogeneous flows.

1.3 Thesis Outline

The rest of this thesis is organized as follows.

Chapter 2 describes in some detail the Internet congestion control problem and summarizes the necessary mathematical background on which the analysis and discussions in this thesis rely.

The stability properties of a class of generalized AIMD/RED system are systemically discussed in Chapter 3. Sufficient conditions for asymptotic stability of both homogeneous- and heterogeneous-flow systems with and without feedback delay are obtained, by using direct Lyapunov and Lyapunov-Razumikhin methods. Also, the relationship between the AIMD parameters and the average window size of competing AIMD flows are derived in this chapter, as well as the TCP-friendly condition.

Chapter 4 focuses on the practical stability of the homogeneous- and heterogeneous-flow AIMD/RED systems with feedback delays, and derives theoretical bounds on the AIMD flow window size and the RED queue length. The system performances are also discussed when AIMD/RED is not asymptotically stable.

Chapter 5 studies the stability properties of the general AIMD/RED system with multiple bottlenecks. A general mathematical model for multi-bottleneck scenarios is first developed and sufficient conditions for the asymptotic stability of multiple-bottleneck systems are obtained for the cases with and without heterogeneous delays.

Concluding remarks and potential research directions for future work are presented in Chapter 6.

1.4 Bibliographic Notes

Most of the research results reported in this thesis have appeared in the research papers and technical reports [27, 28, 29, 30, 31, 32, 33]. Work of Chapter 3 appeared in [27, 28, 29]; Chapter 4 appeared in [30, 31]; Chapter 5 appeared in [32, 33].

Chapter 2

Background

2.1 Internet Congestion Control Overview

The proliferation and universal adoption of the Internet as the information transport platform have escalated it as the key wired network. The explosive growth of the Internet depends on the design of the best-effort service core network. The Internet is a packet switching network. Its intermediate nodes, e.g., routers, forward packets with their best efforts, but with no guarantee. Packets are forwarded on the first in first out (FIFO) strategy, and discarded when buffer overflows. The intermediate nodes know almost nothing and do not maintain any state information about end-to-end sessions. These designs make the core network simple, robust and scalable.

In the Internet, it is the end points, instead of the core network, that take the responsibility of maintaining stability and integrity of the whole system. Since the core network does not explicitly inform the end points of the internal characteristics, e.g., logical topology, background traffic, and available resources, etc., the end points have to take appropriate actions without explicit feedback from the core network. When the best effort service network suffers congestion, the most important signals which end points can capture are packet losses. The end points should appropriately throttle their sending rates to avoid network collapse, i.e., network power, defined as throughput over delay, may dramatically decrease to zero. The first network collapse was seen in the late 1980's. Since then, the dominant Internet transport layer protocol, Transmission Control Protocol (TCP) [1, 2], had been engineered and re-engineered to incorporate the end-to-end flow/congestion control mechanism [3], which is acknowledged as one of the key factors to the overwhelming of the Internet.

Congestion in the Internet can cause high packet loss rates, increased delays, and even break the whole system. Without congestion control, when the offered load is larger than the network capacity, the network power (ratio of throughput to delay) will decrease sharply and the network will be driven to congestion collapse. The main targets of TCP congestion control are to explore and fully utilize the available bandwidth for a connection and to avoid severe congestions in the network.

TCP implements an Additive Increase and Multiplicative Decrease (AIMD) [4] congestion control mechanism. In brief, it additively increase the sending rate to probe the available bandwidth when no congestion occurs and exponentially (multiplicatively) decrease its sending rate in response to congestion signals. With the AIMD congestion control mechanism,TCP is honored for utilizing the bandwidth efficiently, guaranteeing the stability of the networks and maintaining the fairness among co-existing TCP flows, which lead to the explosive growth of the Internet usage in the last decade.

On the other hand, the growth of the Internet is fueled by the development of the Web. The application protocol of text webpage is Hypertext Transfer Protocol (HTTP), which sends data by TCP connection, same as traditional TCP-based application protocols such as File Transfer Protocol (FTP), Simple Mail Transfer Protocol(SMTP), and Telnet Protocol, etc.. These TCP-based applications dominate today's Internet. Briefly speaking, TCP controls the sending rate by a congestion window ($cwnd$). The $cwnd$ of the TCP flow is increased by one packet per round trip time (RTT) when no congestion occurs and halved when a congestion signal is captured by the TCP sender.

2.1.1 Internet Architecture

Before we study the Internet congestion models and algorithms, it would be helpful to know the layered architecture of the Internet in order to understand the framework within which the window flow control protocol is implemented in the Internet. A brief introduction is provided in this subsection. A more detailed description and discussion can be found in [5]. Briefly speaking, the Internet is organized in several layers [6]:

Physical layer

Data link layer

Network layer

Transport layer

Application layer.

The physical layer refers to the collection of protocols that are required to transmit a bit, a 0 or a 1, over a physical medium such as an ethernet cable. Normally, the physical medium takes a waveform as an input and produces a waveform as the output. Therefore, protocols needs to convert 0s and 1s into these waveforms. This function is implemented at the physical layer.

The data link layer consists of the collection of protocols which collect many bits together in the form of a frame and ensures that the frame is transferred from one end of the physical link to the other. In order to guarantee that errors in the frame transmission can be detected and corrected, error correction could also be added at this layer.

The network layer performs the crucial task of routing or delivering a packet from a source to a destination. The protocols at this layer are used to append end-host addresses and other information to data bits to form a packet and further to route packets through the network using these addresses. In the Internet, this layer is also called the IP (Internet Protocol) layer. However, packets passing through the network could be lost or corrupted in the route from the source to the destination. For example, when the source transmission are bigger than the rate at which packets can be processed by the routers, buffers at the routers will overflow. This is a main reason to cause the loss of packet. Thus, although the network layer performs the packet delivery service, the packet delivery may not be reliable.

The transport layer adds reliability to the network layer. The transport layer protocols make sure that lost packets are detected and possibly retransmitted from the source, if necessary, depending upon the application. The transport layer usually turns the unreliable and basic service provided by the network layer into a more powerful one. The predominant transport layer protocol used in today's Internet is the Transmission Control Protocol (TCP). The adaptive window flow control algorithm proposed by Jacobson's is implemented within TCP. TCP provides end-to-end reliable communication and is used for many protocols, including HTTP web browsing, email transfer., etc.There are some other transport layer protocols such as video transmission which can tolerate some amount of packet losses, where packet retransmission may not be required.

Finally, the application layer refers to protocols such as ftp, http, etc. which use the lower layers to transfer files or other forms of data over the Internet. The application layer provides services for an application program to ensure that effective communication with another application program in a network is possible.

The introduction above, which is not intended to be a detailed or accurate description, can be taken as a quick overview of the layered architecture of the Internet. Our target is to point out the layer within which TCP is performed in the Internet and further to indicate that congestion control is implemented within the transport layer protocol TCP. It also shows the fact what are studying in this thesis is part of the collection of protocols that make the Internet function.

2.1.2 TCP Congestion Control

In the 1980's, network congestion was not a concern due to the limited user population, and the original version of TCP did not constitute the congestion control mechanism [1]. Later, with the explosive growth of the Internet, congestion problems became severe owing to the lack of bandwidth. In the mid 1980's, the Internet suffered a series of congestion collapses that the bandwidth suddenly has a factor-of-thousand drop. Not until the late 1980's was a congestion control mechanism developed and widely accepted [3]. Since then TCP congestion control has been modified and engineered to enhance its performance.

Consider a single source accesses a link with the capacity C packets/second. For simplicity, we also assume all packets are of equal size. To ensure that congestion does not occur at this link, the source should transmit at a maximum rate of C packets/second. One way to guarantee it is to use a *window flow control protocol.* A source's window size is the maximum number of unacknowledged packets that the source can send into the network at any time.

The window size started with 1, then the source maintains a counter which has a maximum value of 1. The counter indicates the number of packets that it can send into the network. The counter's value is initially the same as the window size. When the source sends one packet into the network, the counter is reduced by 1. Thus, the counter in this case would become zero after each packet transmission and the source cannot send any more packets into the network till the counter becomes 1 again. To increase the counter, the source waits for the destination to acknowledge the receipt of the packet. This process is accomplished by sending a small packet called the acknowledgement (ack) packet, from the destination back to the source. Once receiving the ack, the counter is increased by 1 and thus the source can send one more packet into the network again. The term round trip time (RTT) is used to refer to the amount of time that elapses between the instant that the source transmits a packet and the instant at which it receives the acknowledgment for the packet. With a window size of 1, since one packet is transmitted during every RTT, the source's data transmission rate is $1/RTT$ packets/sec.

When the window is 2, the counter's value is initially set to 2. Thus, the source can send two packets into the network. For each transmitted packet, the counter is decreased by 1. Thus, after the first two packet transmissions, the counter is decremented to zero. When one of the packets is acknowledged and the ack reaches the source, then the source increments the counter by 1 and can send one more packet into the network. Once the new packet is transmitted, the counter is again decremented back to zero. Thus, after each ack, one packet is sent, and then the source has to wait for the next ack before it can send another packet. If one assumes that the processing speed of the link is very fast, i.e., $1/C \ll RTT$, and that the processing times at the source and destination are negligible, then the source can transmit two packets during every RTT. Thus, the source's transmission rate is $2/RTT$ packets/sec. From the above argument, it should be easy to conclude that, if the window size is W, then the transmission rate can be approximated by W/RTT packets/sec. A precise computation of the rate as a function of the window size is difficult because we need to take processing delays at the source and destination and the queueing delays at the link into account. In common with current literature, we will use the approximate relationship between the window and the transmission rate.

If the link capacity is C and the source's window size W is such that $W/RTT < C$, then *the system will be stable. In other words, all transmitted packets will be eventually processed by the link and reach the intended destination.* However, in a general network, the available capacity cannot be easily determined by a source. The network is also shared by many sources which are sharing the capacities at the different links in the network. Therefore, each source has to adaptively estimate the value of the window size that can be supported by the network. The solution proposed for this by Jacobson [3] is described in the following.

Jacobson's algorithm have been widely implemented in today's TCP. TCP uses a scheme that adjusts its window size depending on the detection of the congestion in the network. The essential idea is that the window size keeps increasing till buffer overflow occurs. The destination detects the overflow by the fact that some of the packets do not reach the destination. Upon the detection of the packets losses, the destination informs the source that will reset the window size to a small value. When there is no packet loss, the window increases rapidly when it is small. After the window size reaches some threshold, it is increased more slowly later by probing the network for bandwidth gradually and trying to stay at this stage as long as possible.

Jacobson's congestion control algorithm operates in two phases [6]:

1. Slow-Start Phase:

Start with a window size of 1.

Increase the window size by 1 for every ack received. This continues till the window size reaches a threshold called the slow-start threshold ($ssthresh$). The initial value of $ssthresh$ is set at the beginning of the TCP connection when the receiver communicates the maximum value of window size that it can handle. The initial value of $ssthresh$ is set to be some fraction (say, half) of the maximum window size. Once the window size reaches $ssthresh$, the slow-start phase ends, and the next phase called the *congestion avoidance* begins. If a packet loss is detected before the window size reaches $ssthresh$, then $ssthresh$ is set to half the current window size, then the current window size is reset to 1, and slow-start begins all over again.

2. Congestion Avoidance Phase:

In the congestion avoidance phase, the window size is increased by $1/cwnd$ for every ack received, where $cwnd$ denotes the current window size. This is roughly equivalent to increasing the window size by 1 after every $cwnd$ $acks$ are received.

When packet loss is detected, the window size is decreased. $ssthresh$ is reset to be half of the current window size, $cwnd$ is reset to one and go back to the slow-start phase.

Remark: Different versions of TCP, such as TCP-Tahoe, TCP-Reno, TCP-SACK, reduce the window size in different ways. However, for modeling purposes, these do not make much of a difference and we will use the algorithm described above for analysis.

In the description of Jacobson's algorithm, how TCP detects packet loss was not discussed. In the early versions of this algorithm, TCP-Tahoe, packet loss was detected only if there was a timeout, i.e., an ack is not received within a certain amount of time. In more recent versions such as TCP-Reno and TCP-NewReno, packet loss is assumed either if there is a timeout or if three duplicate $acks$ are received.

2.1.3 TCP-friendly AIMD Congestion Control

Driven by new commercial demands and technological progress, the Internet is supporting differentiated services, including a large amount of multimedia applications. Although it has been shown that TCP congestion control is very successful for bulk data transfer, its increase-by-one or decrease-by-half strategy produces a highly fluctuating sending rate which is undesirable for many multimedia applications, since most multimedia traffic cannot tolerate its sending rate suddenly cut by half. Since TCP-transported applications are dominant in the Internet, it is crucial to have compatible traffic regulations for non-TCP applications. These regulations, or congestion control should meet the following requirements: 1) different classes of multimedia applications should be able to share the network resources appropriately with ordinary TCP-transported applications. 2) there multimedia applications can coexist and behave properly. We refer to these regulations as TCP-friendly congestion control for non-TCP-transported applications. In addition to the fairness and TCP-friendliness issues[1], any new congestion control scheme

[1]TCP-friendliness is defined as the average throughput of non-TCP-transported applications over a large time scale does not exceed that of any conformant TCP-transported ones under the same circumstance [10].

should also a) have the ability to maintain the network stability by promptly responding to the congestion and be cooperative with other flows in the network; b) utilize the network resources efficiently; c) be capable of providing better quality of service (QoS) and d) be simple and easy to implement, compatible with the legacy, and scalable for incremental deployment.

To overcome the limitations of TCP's saw-teeth flows while meeting all the requirements stated above, a TCP-friendly Additive Increase and Multiplicative Decrease (AIMD) congestion control strategy has been proposed [11] to support heterogeneous services over the Internet. For each round trip time, the AIMD sender either increase its congestion window by α packets if no congestion occurs, or decrease the window to β times its current value when congestion signal is captured. For different traffic, appropriate pair of parameters (α, β) can be chosen according to the traffic characteristics to improve its QoS. The protocol with this congestion control mechanism is called the AIMD(α, β) protocol. TCP is a special case of AIMD with $(\alpha = 1,\ \beta = 0.5)$. Without any modifications to the core networks, the AIMD protocol can be a scalable solution to support differentiated services. [12] also showed that AIMD can be efficient on bandwidth utilization, friendly to ordinary TCP flows, and provide better QoS. By adjusting the pair of (α, β) parameters, different classes of flows can get different weight of bandwidth when they share the link.

2.1.4 Active Queue Management

By itself, TCP/AIMD has no information of network mechanisms contributing to packet loss, which can affect network performance by decreasing the senders' effective transmission and increasing delay due to packet retransmission. In order to detect and control the congestion effectively, TCP/AIMD congestion control mechanism must be paired with a congestion detection scheme. Thus, routers must assume a role in network management by sensing congestion and pre-emptively signaling TCP/AIMD rather than have it to react to unreceived packets.

An Internet router typically maintains a set of queues, one per interface, that hold packets scheduled to go out on that interface. Traditionally, the IP router only maintains a First In First Out (FIFO) queue for each output interface. When the packet arriving rate is larger than the service rate (mainly transmission rate) instantaneously, aggregated packets are buffered in the FIFO queue. When the buffer is full, the following packets will be discarded (in the tail). This is called Drop-Tail queue management. The Drop-Tail queue is known to produce burst packet losses and biased against flows with long $RTTs$, and violates the fairness constraint.

To detect and distribute network congestion indicators fairly to all on-going flows, Active Queue Management (AQM) has been developed to be deployed in the intermediate nodes. Modern routers equipped with AQM can detect congestion even before buffer overflow actually occurs. Random Early Detection (RED) is a well-known AQM scheme [14] and is widely deployed in core networks.

The RED router defines two thresholds. If the queue length is less than the lower threshold, no additional action is taken. If the queue length exceeds the lower threshold a certain level, incoming packets are discarded randomly with some certain dropping probability, which is proportional to the current queue size. Incoming packets are discarded with probability one if the queue length exceeds the upper threshold. The router is not limited to drop packets. It can also mark the incoming packets when the queue length is above the lower threshold, and the packet-marking probability is a function of the queue length. Thus, before the buffer overflows, the congestion signals have already been distributed to on-going flows proportional to their sending rates. The flow with higher sending rate will suffer more packets losses. Therefore, with RED queue management, the link bandwidth can be more fairly distributed to all on-going flows. In addition, since RED helps the end points detect the congestion earlier, the network can recover from congestion quicker and the on-going flows can have better throughput.

RED routers are compatible with in-use FIFO routers, so they can be deployed incrementally. The currently dominant AIMD congestion control mechanism, coupled with the RED queue management that has been widely deployed in the Internet core routers, has been acknowledged as one of the key factors to the overwhelming success of the Internet [40, 41].

2.2 Mathematical Background

Before delving into the modeling and stability analysis of the Internet congestion control problem, we summarize the mathematical background that the analysis and discussions in this thesis rely on. Most of the material in this section are taken from Khalil [51], unless otherwise mentioned.

2.2.1 Basic Definitions and Preliminaries

Consider the following system of differential equations

$$\dot{x}(t) = f(x(t)), \quad x(0) = x_0, \qquad f : D \to R^n \tag{2.1}$$

where D is an open and connected subset of R^n, and f is a locally Lipschitz function mapping D into R^n.

Definition 1 *A point $x = x^*$ is said to be an equilibrium point of system (2.1) if it has the property that whenever the solution $x(t)$ of (2.1) starts at x^*, it remains at x^* for all future time.*

According to this definition, the equilibrium points of (2.1) are then the real roots of the equation $f(x^*) = 0$.

For convenience, we will state all definitions and theorems for the case when the equilibrium point is at the origin $(x^* = 0)$, since any equilibrium point can be shifted to the origin by a change of variables. In the sequel, we will assume that $f(x)$ satisfies $f(0) = 0$.

Definition 2 *The equilibrium point $x^* = 0$ of system (2.1) is said to be*

- *stable if for any $\varepsilon > 0$, there exists a $\delta = \delta(\varepsilon) > 0$ such that $\| x_0 \| < \delta$ implies $\| x(t) \| < \varepsilon, \quad \forall t > 0$;*
- *unstable if it is not stable;*
- *asymptotically stable if it is stable and there exists a constant $\delta > 0$ such that $\| x(t) \| < \delta$ implies $\lim_{t \to \infty} \|x(t)\| = 0$.*

Having defined the stability and asymptotic stability concepts, we use Lyapunov's approach to determining stability. The main idea behind this technique is to determine how a special class of functions behave along the solutions of system (2.1). Let us first define these functions.

Definition 3 *Let D be an open subset of R^n containing $x = 0$. A function $V : D \rightarrow R$ is said to be positive semi-definite on D if it satisfies the following conditions*

(i) $V(0) = 0$;

(ii) $V(x) \geq 0, \forall x \in D - \{0\}$.

It is said to be positive definite on D if it satisfies (i) above and

(ii)* $V(x) > 0, \forall x \in D - \{0\}$.

It is said to be negative definite (semi-definite) on D if $-V$ is positive definite (semi-definite) on D.

Definition 4 *A positive definite function V defined on R^n is said to be radially unbounded (or proper) if the following condition holds:* $\lim_{\|x\| \rightarrow \infty} V(x) \rightarrow \infty$.

In the Lyapunov stability theorems, the focus is on the function V and its time derivative along the trajectories of the dynamical system under consideration. The time derivative of $V(x)$ along the trajectories of system (2.1) is (simply) denoted by $\dot{V}$ and defined as $\dot{V} = \nabla V \cdot f(x)$

Theorem 2.1 *Let $x^* = 0$ be an equilibrium point for system (2.1). Let D be an open subset of R^n containing $x = 0$ and $V : D \rightarrow R$ be a continuously differentiable function defined on D such that*

(i) $V(0) = 0$,

(ii) $V(x) > 0, \ \forall x \in D - \{0\}$

(iii) $\dot{V} \leq 0, \ \forall x \in D - \{0\}$

Then, x^* = 0 is stable. If condition (iii) is replaced by *(iii*)* $\dot{V} < 0,\ \forall x \in D - \{0\}$,

then $x^* = 0$ *is asymptotically stable. Moreover, if* $D = R^n$ *and* V *is radially unbounded, then* $x^* = 0$ *is globally asymptotically stable.*

In the next definition, we define positive definite matrices which play an important role in defining Lyapunov functions.

Definition 5 *[52] A real symmetric* $n \times n$ *matrix is said to be positive definite if and only if it has strictly positive eigenvalues.*

An important class of positive definite functions are the quadratic functions $V(x) = x^T Px$, where P is a positive definite matrix. Let $\lambda_{min}(P)$ and $\lambda_{max}(P)$ denote the minimum and maximum eigenvalues of P, respectively. Then, we have $\lambda_{min}(P) \parallel x \parallel^2 \leq V(x) = x^T Px \leq \lambda_{max}(P) \parallel x \parallel^2$. This inequality is referred to as the *Rayleigh Inequality*.

A special case of system (2.1) is when the vector field function $f(x)$ has the linear form Ax where A is a real $n \times n$ matrix; namely, we have

$$\dot{x}(t) = Ax(t), \quad x(0) = x_0. \tag{2.2}$$

which is called a linear time-invariant (or autonomous) system. The solution of (2.2) is given by $x(t) = e^{At}x_0$.

An efficient technique to investigate the stability properties of system (2.2) is by determining the location of the eigenvalues of the matrix A, as shown in the following theorem.

Theorem 2.2 *The equilibrium point* $x^* = 0$ *of system (2.2) is stable if and only if the eigenvalues of* A $(\lambda_i s)$ *have non-positive real parts and for those with zero real parts and algebraic multiplicity* q_i, $rank(A - \lambda_i I) = n - q_i$, *where* n *represents the dimension of* x. *It is globally asymptotically stable if and only if all eigenvalues of* A *have strictly negative real parts.*

Definition 6 *An* $n \times n$ *matrix is said to be* $Hurwitz$ *(or stable) if all its eigenvalues have negative real part.*

The asymptotic stability property can also be characterized by using Lyapunov's method. Consider the following Lyapunov function candidate $V(x) = x^T P x$, the derivative of $V(x)$ along the trajectories of (2.2) is given by $\dot{V} = \dot{x}^T P x + x^T P \dot{x} = x^T (A^T P + PA) x = -x^T Q x$, where Q is an $n \times n$ matrix given by

$$A^T P + PA = -Q. \tag{2.3}$$

If Q is positive definite, then by Theorem (2.1) the origin is an asymptotically stable equilibrium point. This result is summarized in the next theorems.

Theorem 2.3 *An* $n \times n$ *matrix* A *is* $Hurwitz$ *if and only if, for any given positive definite matrix* Q, *there is a unique positive definite matrix* P *which satisfies (2.3).*

The matrix equation (2.3) is referred to as a Lyapunov equation which is solved for P for a given Q where $P = \int_0^\infty e^{A^T t} Q e^{At} dt.$

Lemma 2.4 *(Schur complement) [52] The following three inequalities are equivalent:*

(1) $\begin{bmatrix} A & B \\ B^T & C \end{bmatrix} \leq 0$;

(2) $A \leq 0$, *and* $C - B^T A^{-1} B \leq 0$;

(3) $C \leq 0$, *and* $A - BC^{-1}B^T \leq 0$,

where A, B, C *are real constant matrices of appropriate dimensions, and* A, C *are symmetric.*

If in a domain about the origin we can find a Lyapunov function whose derivative along the trajectories of the system is negative semi-definite, and if we can establish that no trajectory can stay identically at points where $\dot{V}(x) = 0$, except at the origin, then the origin is asymptotical. This idea follows from LaSalle's invariance principle, which is described as follows.

Theorem 2.5 *Let* $\Omega \subset D$ *be a compact set that is positively invariant with respect to (2.1). Let* $V : D \to R$ *be a continuously differentiable function such that* $\dot{V}(x) \leq 0$ *in* Ω. *Let* E *be the set of all points in* Ω *where* $\dot{V}(x) = 0$. *Let* M *be the largest invariant set in* E. *Then every solution starting in* Ω *approaches* M *as* $t \to \infty$.

Unlike Lyapunov's theorem, Theorem 2.5 does not require the function $V(x)$ to be positive definite.

When our interest is in showing that $x(t) \to 0$ as $t \to \infty$, we need to establish that the largest invariant set in E is the origin. This is done by showing that no solution can stay identically in E, other than the trivial solution $x(t) \equiv 0$.

Theorem 2.6 *[51] Let* $x = 0$ *be an equilibrium point for (2.1). Let* $V : D \to R$ *be a continuously differentiable positive definite function on a domain* D *containing the* *origin $x = 0$, such that $\dot{V}(x) \leq 0$ in D. Let $S = \{x \in D : \dot{V}(x) = 0\}$ and suppose that no solution can stay identically in S, other than the trivial solution $x(t) \equiv 0$. Then, the origin is asymptotically stable.*

2.2.2 Delay Differential Equations

Delay differential equations (DDEs) arise as models for systems where the rate of change of the state depends not only on the current state of the system but also its state at some time(s) in the past (see e.g. [56, 57, 58]).

Ordinary differential equations(ODEs) have played important roles in modeling many physical processes and they will continue to serve as a fundamental tool in future investigations. A drawback of these models is that they are ruled by the principle of causality, that is, the future state of the dynamical system depends only on the present state and not on the past. However, in the more realistic models, some historical values of the state should and have to be taken into account. This leads us to delay differential equations, also known as retarded functional differential equations.

Let $C_\tau = C([-\tau,\ 0],\ R^n)$, with $\tau > 0$, representing a time delay, be the set of continuous functions from $[-\tau,\ 0]$ to R^n. If $\phi \in C_\tau$, the τ-norm of this function is defined by $\|\phi\|_\tau = \sup_{-\tau \leq \theta \leq 0} \|\phi(\theta)\|$, where $\|\cdot\|$ is the Euclidean norm on R^n.

Definition 7 *If x is a function mapping $[t-\tau,\ t]$ into R^n, a new function x_t mapping $[-\tau,\ 0]$ into R^n is defined as follows $x_t(\theta) = x(t+\theta),\ for\ \theta \in [-\tau,\ 0]$.*

Here, $x_t(\theta)$ (or simply x_t) is the segment of the function x, from $t-\tau$ to t, that has been shifted to the interval $[-\tau,\ 0]$. Assume Ω is a subset of $R \times C$, and $f : \Omega \rightarrow R^n$. A general delay differential equation is described as follows

$$\dot{x}(t) = f(t,\ x_t), \tag{2.4}$$

where f depends on both t and x_t. Since x_t is an element of $C([-\tau,\ 0],\ R^n)$, f is called a functional. Unlike the initial state of an ordinary differential equation, the initial state of system (2.4) is defined on the entire interval $[t_0 - \tau,\ t_0]$, not just t_0. Then, an initial condition is given as a continuous function $x_{t_0} = \phi(t)\ for\ t \in [t_0 - \tau,\ t_0]$.

A function x is said to be a solution of the equation (2.4) on $[t_0 - \tau,\ t_0 + A)$ if there are $t_0 \in R$ and $A > 0$ such that $x \in C([t_0 - \tau,\ t_0 + A), R^n)$, $(t,\ x_t) \in \Omega$ and $x(t)$ satisfies the equation (2.4) for $t \in [t_0,\ t_0 + A)$.

Remark: There are several special cases of (2.4). If $\tau = 0$, then (2.4) becomes an ordinary differential equation $\dot{x}(t) = f(t,\ x(t))$, i.e. ODEs are special case of DDEs. If τ takes a finite number of values $\tau_1, \cdots, \tau_k$ and $0 \leq k < \infty$, then (2.4) becomes $\dot{x}(t) = f(t,\ x(t),\ x(t - \tau_1), \cdots, x(t - \tau_k))$.

Theorem 2.7 *(Existence) In (2.4) suppose Ω is an open subset in $R \times C$ and f is continuous on Ω: If $(t_0;\ \phi) \in \Omega$, then there is a solution of (2.4) passing through $(t_0,\ \phi)$.*

We say $f(t; \phi)$ is Lipschitz on ϕ in a compact set K of $R \times C$, if there is a constant $k > 0$ such that, for any $(t,\ \phi_i) \in K,\ i = 1, 2,\ \|f(t,\ \phi_1) - f(t,\ \phi_2)\| \leq k\|\phi_1 - \phi_2\|$.

Theorem 2.8 *(Uniqueness) Suppose Ω is an open subset in $R \times C$, $f : \Omega \rightarrow R^n$ is continuous and $f(t,\ \phi)$ is Lipschitz in ϕ on each compact set in Ω. If $(t_0,\ \phi) \in \Omega$ then there is a unique solution of (2.4) through $(t_0,\ \phi)$.*

Theorem 2.9 *[54] Consider the following delay differential inequality.*

$$\dot{u}(t) \le f(t, u(t), \sup_{\theta \in [t-\tau,\ t]} u(\theta)) \quad t \in [t_0,\ t_0 + a),\ a > 0.$$

Assume that $y(t)$ is a solution of the delay differential equation

$$\dot{y}(t) = f(t, y(t), \sup_{\theta \in [t-\tau,\ t]} y(\theta)) \quad t \in [t_0,\ t_0 + a)$$

such that $y(t) = u(t),\ t \in [t_0 - \tau,\ t_0]$. Then, $u(t) \le y(t)$ for $t \in [t_0,\ t_0 + a)$.

Definition 8 *Suppose $f : R \times C \to R^n$ is continuous and $f(t,\ 0) = 0$ for all t. Then, the solution $x = 0$ of system (2.4) is said to be*

- *stable if, for a given $\varepsilon > 0$, there exists a $\delta = \delta(\varepsilon,\ t_0) > 0$ such that $\|x_{t_0}\|_\tau < \delta$ implies $\|x(t)\| < \varepsilon$ for $\forall t \ge t_0 - \tau$;*
- *unstable if it is not stable;*
- *asymptotically stable if it is stable and there exists a $\delta = \delta(t_0) > 0$ such that $\|x_{t_0}\|_\tau < \delta$ implies $\lim_{t\to\infty} \|x(t)\| = 0$.*

In DDEs the analysis of characteristic equations of linear autonomous delay differential equations is often a difficult task even for equations with two discrete delays or systems with just one discrete delay since those characteristic equations are transcendental. However, this can be overcome by using Lyapunov functionals to obtain sufficient conditions for stability and instability of steady state of DDEs in a way similar to the second method of Lyapunov for ODEs [53, 57].

If $V : R \times C \to R$ is continuous and $x(t_0,\ \phi)$ is the solution of (2.4) through $(t_0,\ \phi)$, then we define

$$\dot{V} = \dot{V}(t,\ \phi) = \lim\sup_{h \to 0^+} \frac{1}{h}[V(t + h,\ x_{t+h}) - V(t,\ \phi)]$$

where $\dot{V}$ is the upper right-hand derivative of $V(t,\ \phi)$ along the solution of (2.4).

Theorem 2.10 *[53] Suppose $f : R \times C \to R^n$ takes $R\times$ (bounded sets of C) into bounded sets of R^n and $\alpha,\ \beta,\ \psi : R^+ \to R^+$ are continuous and nondecreasing functions, $\alpha(s),\ \beta(s)$ are positive for $s > 0$, and $\alpha(0) = \beta(0) = 0$. If there is a continuous function $V : R \times C \to R$ such that,*

$$\alpha(\|\phi(0)\|) \leq V(t,\ \phi) \leq \beta(\|\phi\|_\tau) \quad \textit{and} \quad \dot{V}(t,\ \phi) \leq -\psi(\|\phi(0)\|)$$

then the solution $x = 0$ of (2.4) is uniformly stable. If $\alpha(s) \to \infty$ as $s \to \infty$, then the solution of (2.4) is uniformly bounded. If $\psi(s) > 0$ for $s > 0$, then the solution is uniformly asymptotically stable.

The above theorem tells us that if a Lyapunov functional is monotonically decreasing along the solution of (2.4), then the solution is uniformly asymptotically stable. However, this method may be different since C is much more complicated than R^n and there is no control between $\|x(t)\|$ and $\|x(t+\theta)\|$ for $\theta \in [-\tau,\ 0]$. For this reason another effective method of analyzing stability of DDEs is the application of Razumikhin-type theorems [53, 55, 57]. This technique makes use of functions rather than functionals.

Consider an autonomous DDE defined by

$$\dot{x} = f(x_t), \tag{2.5}$$

and a positive definite and continuously differentiable function $V : R^n \to R$. Then the derivative of V along the solutions of (2.5) is given by

$$\dot{V}(x(t)) = \frac{\partial V(x(t))}{\partial x} f(x_t).$$

To prove $\dot{V}$ is negative definite requires that $x(t)$ somehow dominates $x(t+\theta)$. From the definition of uniform stability, we know that if x_t is initially in a ball $B = B(0, \delta)$ in C, then, for it to escape B, it has to reach the boundary of B at some time t^*: At time t^*, we have $\|x(t^*)\| = \delta$, and $\|x(t^* + \theta)\| < \delta$ for $\theta \in [-\tau,\ 0)$; and we must have $d\|x(t^*)\|/dt \geq 0$. Hence, if we show this is impossible, then we arrive at the stability conclusion. This observation leads to stability results, called Razumikhin type Theorems.

In general, $V : R \times R^n \to R$ is a continuous function, and $\dot{V}(t,\ x(t))$, the derivative of V along the solutions of the DDE (2.4) is defined by

$$\dot{V}(t,\ x(t)) = \lim\sup_{h \to 0^+} \frac{1}{h}[V(t+h,\ x(t+h)) - V(t,\ x(t))],$$

where $x(t) = x(t_0,\ \phi)$ for $t \geq t_0$ is the solution of the DDE (2.4) through $(t_0,\ \phi)$.

Theorem 2.11 *[53] Suppose $f : R \times C \to R^n$ takes $R\times$ (bounded sets of C) into bounded sets of R^n and $\alpha,\ \beta,\ \psi : R^+ \to R^+$ are continuous, nondecreasing functions, satisfying $\alpha(0) = \beta(0) = \psi(0) = 0$, and $\alpha(s),\ \beta(s)$ are positive for $s > 0$. Assume that there is a continuous function $V : R \times R^n \to R$ such that,*

$$\alpha(\|x\|) \leq V(t,\ \phi) \leq \beta(\|x\|) \quad \textit{for} \quad t \in R,\ x \in R^n.$$

Then the solution x = 0 of (2.4) is

(i) uniformly stable if

$$\dot{V}(t,\ x(t)) \leq -\psi(\|x(t)\|) \quad \textit{for} \quad V(t+\theta,\ x(t+\theta)) \leq V(t,\ x(t)),\ \theta \in [-\tau,\ 0];$$

(ii) asymptotically uniformly stable if $\psi(s) > 0$ for $s > 0$ and there is a continuous nonincreasing function $p(s) > s$ for $s > 0$ such that

$$\dot{V}(t,\ x(t)) \leq -\psi(\|x(t)\|) \quad \textit{for} \quad V(t+\theta,\ x(t+\theta)) < p(V(t,\ x(t))),\ \psi \in [-\tau,\ 0].$$

If $\alpha(s) \to \infty$ as $s \to \infty$, then $x = 0$ is globally asymptotically stable.

Chapter 3

Stability Analysis of Single-Bottleneck AIMD/RED Systems

In this chapter, we systematically study the stability of a class of generalized AIMD/RED (Additive Increase and Multiplicative Decrease/Random Early Detection) system. Sufficient conditions are obtained for asymptotic stability of both homogeneous-flow system and heterogeneous-flow system with and without feedback delay by using direct Lyapunov and Lyapunov-Razumikhin method. Our study reveals the relationship between the AIMD parameters and the average window size of competing AIMD flows. Consequently, the TCP (Transmission Control Protocol)-friendly condition is derived. Numerical results with Matlab and simulation results with NS-2 are given to validate the theorems and analytical results. The analysis and the stability conditions derived can be used as a guideline to set up the AIMD/RED system parameters in order to maintain network stability and integrity, and to enhance system performance.

3.1 Introduction

Internet stability depends on the Transmission Control Protocol (TCP), which is voluntarily deployed in the end system based on the Additive Increase and Multiplicative Decrease (AIMD) congestion control mechanism. To support heterogeneous traffic, the general AIMD congestion control uses a pair of parameters (α, β) to set the increase rate and the decrease ratio [10, 11, 12]. On the other hand, the active queue management (AQM) algorithms, such as Random Early Detection or Random Early Discard (RED), have been developed and deployed in the intermediate systems to fairly distribute network congestion signals to all on-going flows. With the RED schemes [14, 15], the packet loss rate of each flow is roughly proportional to the flow sending rate. AIMD and RED both contribute to the overwhelming success of the Internet.

Today's Internet is becoming a more heterogeneous and diverse system: link capacity varies from several Kbps to several Gbps, with six orders of magnitude; transmission bit error rates vary from $< 10^{-9}$ to 10^{-3}, also with about six orders of magnitude; and end-to-end delay varies from several milliseconds to several seconds. A critical and immediate question is whether the AIMD/RED system is a stable, fair, and efficient system, independent of the heterogeneity of the link capacity, end-to-end delay, and network topology. In other words, should we re-design the Internet congestion control mechanism to accommodate future killer applications over the ever-diversified Internet, or can we take an incremental approach of engineering the existing congestion control mechanism and routers' queue management parameters to achieve the same objective?

Stability problems of TCP flows with RED queues have been extensively investigated in [21, 22, 23, 24, 25, 26]. New control mechanisms based on control theory and game theory have also been proposed [7]. Instead of proposing a new control mechanism, we focus on the stability and performance of the dominant AIMD congestion control mechanism with RED queues. In [26], using a fluid model, the global asymptotic stability of TCP/RED is proved, neglecting the feedback delay. The dynamics of TCP/RED with feedback delay has been studied using a frequency domain approach in [9]. Because of the heterogeneity of the Internet, understanding the stability conditions of the general AIMD/RED system with heterogeneous flows and feedback delays is critical for future network planning and design.

In this chapter, we systematically study the stability of the AIMD/RED system, considering heterogeneous flows with different AIMD parameters in both delay-free marking and delayed marking scenarios. The definitions of stability and asymptotic stability follow that in [36]. Consider dynamic systems with time delay of the following form:

$$\frac{dx}{dt} = f(t, x(t), x(t-\tau_1(t)), \cdots, x(t-\tau_m(t)))$$

where $x \in R^n$, $f : I \times R^n \times R^n \times \cdots \times R^n \rightarrow R^n$ is continuous. Let $\tau = \max_{i=1,..,m} \sup_{t \geq t_0} \tau_i(t)$.

The trivial solution of the system is said to be

stable if for every $\epsilon > 0$ and $t_0 \in \mathbb{R}_+$, there exists some $\delta = \delta(t_0, \epsilon) > 0$ such that for any $\xi(t) \in C[[-\tau, 0], R^n]$, $\|\xi\|_\tau < \delta$ implies $\|x(t, t_0, \xi)\| < \epsilon$ for all $t \geq t_0$;

asymptotically stable if the system is stable and for every $t_0 \in \mathbb{R}_+$, there exists some $\eta = \eta(t_0) > 0$ such that $\lim_{t\rightarrow\infty} \|x(t, t_0, \xi)\| = 0$ whenever $\|\xi\|_\tau < \eta$.

Based on the fluid model of the generalized AIMD/RED system, we apply the methods of Lyapunov functional and Lyapunov function with Lyapunov-Razumikhin condition to study the stability properties of the system. Different sufficient conditions are derived for the local asymptotic stability of the system with feedback delays. Since the fluid model captures the ensemble averages of the system parameters, with the sufficient conditions derived, the ensemble averages or the time averages (over a round) of the AIMD/RED system can be locally asymptotically stable, even with heterogeneous feedback and propagation delays, so the AIMD/RED system can be marginally stable. A round is defined as the time interval between two instants at which the sender reduces its window size consecutively. The analysis also reveals the relationship between AIMD parameters and the average window size of competing AIMD flows, and the TCP-friendly condition is also derived. Numerical results are given to validate the analysis. Extensive simulations with NS-2 [60] are performed to study the system performance with realistic protocols and network topologies. The analytical and simulation results can help to better understand the stability and performance of AIMD/RED system, and the theoretical results can be used as a guideline for the setting of system parameters to maintain network stability and enhance system performance.

The remainder of the chapter is organized as follows. Section 3.2 proposes the model of the generalized AIMD/RED system. Section 3.3 studies the stability property of the generalized AIMD/RED system with delay free-marking, and derives the TCP-friendly condition and average queuing delay. The stability and fairness analysis of AIMD/RED system with heterogeneous feedback delays are given in Section 3.4. Numerical results with MATLAB and simulation results with NS-2 are presented in Section 3.5. Related work is briefly introduced in Section 3.6, followed by summary and further discussions in Section 3.7.

3.2 A Fluid-flow Model of AIMD/RED System

A stochastic model of TCP behavior was developed using fluid-flow and stochastic differential equation analysis [22]. Simulation results have demonstrated that this model accurately captures the dynamics of TCP. We extend the fluid-flow model for general AIMD(α, β) congestion control: the window size is increased by α packet per RTT if no packet loss occurs; otherwise, it is reduced to β times its current value.

We first consider the case that all AIMD-controlled flows have the same (α, β) parameter pair and round-trip delay. The AIMD/RED fluid model relates to the *ensemble averages* of key network variables, and it is described by the following coupled, nonlinear differential equations:

$$\frac{dW(t)}{dt} = \frac{\alpha}{R(t)} - \frac{2(1-\beta)}{1+\beta} W(t) \frac{W(t-\tau)}{R(t-\tau)} p(t-\tau),$$

$$\frac{dq(t)}{dt} = \begin{cases} \dfrac{N(t)\cdot W(t)}{R(t)} - C, & q > 0, \\ \\ \{\dfrac{N(t)\cdot W(t)}{R(t)} - C\}^{+}, & q = 0. \end{cases} \tag{3.1}$$

where $\{a\}^{+} = \max\{a, 0\}$, $\alpha > 0$, $\beta \in [0, 1]$, $W \in [0,\ W_{max}]$ is the ensemble average of AIMD window size (packets); $q \in [0,\ q_{max}]$ is the ensemble average of queue length (packets); R is the round-trip time with $R(t) = \frac{q(t)}{C} + T_p$ (secs), where C is the queue capacity (packets/sec) and T_p is the deterministic delay (including propagation, processing, and transmission delay). The delay term τ in $R(\cdot)$, $W(\cdot)$ and $p(\cdot)$ is defined as the average round trip time. N is the number of AIMD flows and p is the probability of a packet being marked (or dropped).

The first differential equation of system (3.1) describes the AIMD(α, β) window control dynamic. Roughly speaking, α/R represents the window's additive increase, while $\frac{2(1-\beta)}{1+\beta}W$ represents the window's multiplicative decrease in response to packet marking (or dropping) probability p. This is because the flow's window size always oscillates between βW_{max} to W_{max}, the average window size over a round is $(1+\beta)W_{max}/2$. Each time, the window size is cut by $(1-\beta)W_{max} = 2(1-\beta)W/(1+\beta)$. The second equation models the bottleneck queue length as simply an accumulated difference between packet arrival rate NW/R and link capacity C. $\{\cdot\}^+$ in the model guarantees queue length is a non-negative number.

With RED, as shown in Fig. 3.1, the packet marking probability is proportional to the average queue length: $p = K_p(q_{act} - \min_{th})$ with $K_p > 0$ and $p \in [0, 1]$. When the actual queue length is less than or equal to the minimum threshold, i.e. $q_{act} \leq \min_{th}$, the marking probability is zero. Therefore, $\frac{dW(t)}{dt} = \frac{\alpha}{R}$, that is, the window size will keep increasing and not converge. In the following, we will discuss the stability property of this model when $q_{act} > \min_{th}$. Without loss of generality, let $q(t) = q_{act}(t) - \min_{th}$. Since the system behaves the same as a Drop-Tail queue once the queue length exceeds the maximum threshold $\max_{th}$, to focus on the behavior of AIMD/RED, we choose $\max_{th}$ to be sufficiently large such that $p_{\max} = 1$.

It should be noted that, (3.1) is a generalized AIMD/RED congestion control model, which includes the model studied in [22, 23, 24, 25, 26, 34]. If we choose $\alpha = 1$, $\beta = 0.5$, (3.1) is equivalent to the traditional TCP/RED model. We will also show in the next section that the stability properties of the specific model in the literature is compatible with the corresponding properties of this generalized model as well.

3.3 Stability and Fairness Analysis with Delay-free marking

3.3.1 Delay-free Homogeneous AIMD/RED system

With the fluid-flow model (3.1), we assume that the traffic load (N AIMD flows) is time-invariant, i.e., $N(t)=N$, and the round-trip time of each flow is a constant, $R(t)=R$. In the case of delay-free marking, i.e., $p = K_p q(t)$, the original delay-free marking model (3.1) can be written as a closed-loop dynamics:

$$\frac{dW(t)}{dt} = \frac{\alpha}{R} - \frac{2(1-\beta)}{1+\beta} W(t) \frac{W(t)}{R} K_p q(t),$$

$$\frac{dq(t)}{dt} = \begin{cases} \dfrac{N \cdot W(t)}{R} - C, & q > 0, \\ \{\dfrac{N \cdot W(t)}{R} - C\}^+, & q = 0. \end{cases} \tag{3.2}$$

For a single-bottleneck system, the equilibrium point $(W_0^*,\ q_0^*)$ for (3.2) is given by

$$W_0^* = \frac{RC}{N}; \qquad q_0^* = \frac{\alpha(1+\beta)N^2}{2(1-\beta)R^2C^2K_p}. \tag{3.3}$$

At equilibrium, the RED queue length is inversely proportional to K_p. Thus, we should choose K_p according to the delay budget.

With the transformed variables $\tilde{W}:=W - W_0^*$, $\tilde{q}:=q - q_0^*$, (3.2) becomes

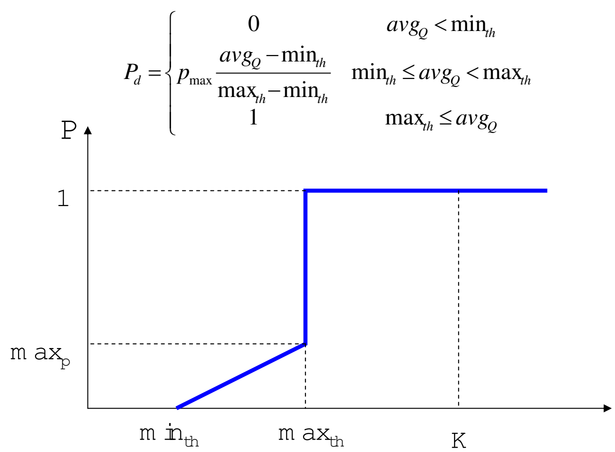

Figure 3.1: RED Marking Scheme

$$
\begin{aligned}
\dot{\tilde{W}}(t) &= -\frac{2(1-\beta)}{1+\beta}\frac{(\tilde{W}(t)+W_0^*)^2}{R}K_p\tilde{q}(t) \\
&\quad -\frac{2(1-\beta)}{1+\beta}\frac{\tilde{W}^2(t)+2\tilde{W}(t)W_0^*}{R}K_p q_0^*, \qquad (3.4) \\
\dot{\tilde{q}}(t) &= \frac{N}{R}\cdot\tilde{W}(t).
\end{aligned}
$$

The equilibrium point of (3.4) is $(\tilde{W}^*,\ \tilde{q}^*)$=(0, 0).

We construct the positive-definite Lyapunov function,

$$
V(\tilde{W},\,\tilde{q}) = \frac{(1+\beta)N^3}{2(1-\beta)R^2C^2}\cdot\tilde{W}^2(t) + \frac{1}{2}K_p\tilde{q}^2(t),
$$

which is used to derive the following theorem.

Theorem 3.1 *The equilibrium point of* (3.2) *is asymptotically stable for all* $K_p > 0$.

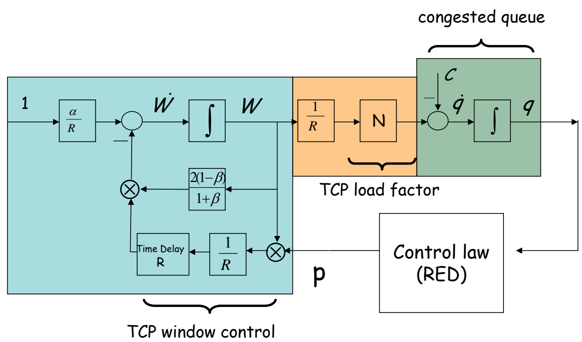

Figure 3.2: Block Diagram of Generalized AIMD/RED System

The proof of Theorem 1 is omitted, and we will prove a more general theorem (Theorem 2) in the next subsection.

From the viewpoint of control theory, the block diagram of the AIMD/RED system is depicted in Fig. 3.2. By a suitable control law, we relate the output q with the input p, which makes the original open loop systems into a closed loop control system to achieve asymptotic stability.

3.3.2 Delay-free Heterogeneous AIMD/RED System

In the previous subsection, we discussed the stability property of the homogeneous-flow system when there is only one type of flows with the parameter pair ($\alpha,\ \beta$). To support heterogeneous multimedia applications, we study the system with heterogeneous-flows, i.e., there are two or more types of flows with the parameter pairs ($\alpha_1,\ \beta_1$), ($\alpha_2,\ \beta_2$), $\cdots$,

(α_m, β_m).

First, we consider the case when there are two different heterogeneous flows: W_I whose RTT is R_1, and W_{II} whose RTT is R_2, with the parameters (α_1, β_1), (α_2, β_2), respectively. The number of W_I flows is N_1, and that of W_{II} flows is N_2. Then the corresponding mathematical model has the following form,

$$\frac{dW_I(t)}{dt} = \frac{\alpha_1}{R_1} - \frac{2(1-\beta_1)}{1+\beta_1} \cdot \frac{W_I^2(t)}{R_1} \cdot K_p q(t),$$

$$\frac{dW_{II}(t)}{dt} = \frac{\alpha_2}{R_2} - \frac{2(1-\beta_2)}{1+\beta_2} \cdot \frac{W_{II}^2(t)^2}{R_2} \cdot K_p q(t),$$

$$\frac{dq(t)}{dt} = \begin{cases} \dfrac{N_1 W_I(t)}{R_1} + \dfrac{N_2 W_{II}(t)}{R_2} - C, & q > 0, \\ \{\dfrac{N_1 W_I(t)}{R_1} + \dfrac{N_2 W_{II}(t)}{R_2} - C\}^+, & q = 0. \end{cases} \tag{3.5}$$

The equilibrium points (W_I^*, W_{II}^*, q_0^*) of (3.5) can be obtained as

$$W_I^* = \frac{R_1 R_2 C}{R_2 N_1 + (\frac{\alpha_2(1-\beta_1)(1+\beta_2)}{\alpha_1(1+\beta_1)(1-\beta_2)})^{1/2} \cdot R_1 N_2};$$

$$W_{II}^* = \frac{R_1 R_2 C}{(\frac{\alpha_1(1+\beta_1)(1-\beta_2)}{\alpha_2(1-\beta_1)(1+\beta_2)})^{1/2} \cdot R_2 N_1 + R_1 N_2};$$

$$q_0^* = \frac{\alpha_1(1+\beta_1)[R_2 N_1 + (\frac{\alpha_2(1-\beta_1)(1+\beta_2)}{\alpha_1(1+\beta_1)(1-\beta_2)})^{1/2} R_1 N_2]^2}{2 R_1^2 R_2^2 C^2 K_p (1-\beta_1)}. \tag{3.6}$$

With the transformed variables $\tilde{W}_I(t) := W_I(t) - W_I^*, \quad \tilde{W}_{II}(t) := W_{II}(t) - W_{II}^*$ and $\tilde{q}(t) := q(t) - q_0^*$, (3.5) becomes

$$\begin{aligned}
\dot{\tilde{W}}_I(t) = & -\frac{2(1-\beta_1)}{1+\beta_1}\frac{(\tilde{W}_I(t)+W_I^*)^2}{R_1}K_p\tilde{q}(t) \\
& -\frac{2(1-\beta_1)}{1+\beta_1}\frac{\tilde{W}_I^2(t)+2W_I^*\tilde{W}_I(t)}{R_1}K_p q_0^*, \\
\dot{\tilde{W}}_{II}(t) = & -\frac{2(1-\beta_2)}{1+\beta_2}\frac{(\tilde{W}_{II}(t)+W_{II}^*)^2}{R_2}K_p\tilde{q}(t) \\
& -\frac{2(1-\beta_2)}{1+\beta_2}\frac{\tilde{W}_{II}^2(t)+2W_{II}^*\tilde{W}_{II}(t)}{R_2}K_p q_0^*, \\
\dot{\tilde{q}}(t) = & \frac{N_1\cdot\tilde{W}_I(t)}{R_1}+\frac{N_2\cdot\tilde{W}_{II}(t)}{R_2}.
\end{aligned} \tag{3.7}$$

The equilibrium point of (3.7) is then ($\tilde{W}_I^*,\ \tilde{W}_{II}^*,\ \tilde{q}_0^*$)=$(0, 0, 0)$.

With (3.7), choose the following positive-definite Lyapunov function,

$$\begin{aligned}
& V(\tilde{W}_I(t),\ \tilde{W}_{II}(t),\ \tilde{q}(t)) \\
& = \frac{(1+\beta_1)N_1}{2(1-\beta_1)W_I^{*2}}\cdot\tilde{W}_I^2(t)+\frac{(1+\beta_2)N_2}{2(1-\beta_2)W_{II}^{*2}}\cdot\tilde{W}_{II}^2(t) \\
& \quad +K_p\tilde{q}^2(t).
\end{aligned}$$

Then,

$$
\begin{aligned}
\dot{V} &= \frac{(1+\beta_1)N_1}{(1-\beta_1)W_I^{*2}}\tilde{W}_I(t)\dot{\tilde{W}}_I(t) \\
&\quad + \frac{(1+\beta_2)N_2}{(1-\beta_2)W_{II}^{*2}}\tilde{W}_{II}(t)\dot{\tilde{W}}_{II}(t) + 2K_p\tilde{q}(t)\dot{\tilde{q}}(t) \\
&= -\frac{2N_1K_p}{W_I^{*2}R_1}\tilde{W}_I^2(t)(\tilde{W}_I(t)+2W_I^*)(\tilde{q}(t)+q_0^*) \\
&\quad -\frac{2N_2K_p}{W_{II}^{*2}R_2}\tilde{W}_{II}^2(t)(\tilde{W}_{II}(t)+2W_{II}^*)(\tilde{q}(t)+q_0^*) \\
&\leq 0.
\end{aligned}
$$

From the physics constraint point of view, the positive-definite Lyapunov function is the total energy function of the system, i.e., the sum of kinetic and potential energy. Here $\dot{V} \leq 0$, since $\tilde{W}_I(t) + 2W_I^* > 0$, $\tilde{W}_{II}(t) + 2W_{II}^* > 0$ and $\tilde{q}(t) + q_0^* \geq 0$, which means the energy of the system is non-increasing. Thus, we prove that the equilibrium point is stable. To conclude asymptotic stability, we first consider the set of states where $\dot{V} = 0$,

$$
\begin{aligned}
\mathcal{M}: &= \{(\tilde{W}_I,\, \tilde{W}_{II},\, \tilde{q}) : \dot{V} = 0\} \\
&= \{(\tilde{W}_I,\, \tilde{W}_{II},\, \tilde{q}) : \tilde{W}_I{=}\tilde{W}_{II}{=}0 \text{ or } \tilde{q}{=}-q_0^*\}.
\end{aligned}
$$

By LaSalle's Invariance Principle [36], trajectories of (3.7) converge to the largest invariant set contained in $\mathcal{M}$. We will then prove that the only invariant set contained in $\mathcal{M}$ is the equilibrium point ($0,\, 0,\, 0$). If $(\tilde{W}_I(t),\, \tilde{W}_{II}(t),\, \tilde{q}(t))$ is equal to $(0,\, 0,\, \tilde{q}(t))$ or $(\tilde{W}_I(t),\, \tilde{W}_{II}(t),\, -q_0^*)$, by using (3.7), we can conclude that $(\tilde{W}_I(t^+),\, \tilde{W}_{II}(t^+),\, \tilde{q}(t^+))$ is not in $\mathcal{M}$, which implies that no trajectory can stay in $\mathcal{M}$, other than the point ($0,\, 0,\, 0$). Therefore, asymptotic stability is obtained, which we summarize as follows:

Theorem 3.2 *For any $K_p > 0$, the equilibrium point of (3.7) is asymptotically stable for any positive pairs $(\alpha_1,\ \beta_1)$, $(\alpha_2,\ \beta_2)$ and any positive R_1, R_2.*

We can also extend our results to the case when more than two heterogeneous flows exist in the same system. Suppose that there are M different heterogeneous flows ($\alpha_1,\ \beta_1$), ($\alpha_2,\ \beta_2$), $\cdots$, ($\alpha_m,\ \beta_m$) sharing the resources, with the number $N_1,\ N_2, \cdots,\ N_m$, and different $RTTs$ $R_1,\ R_2, \cdots,\ R_m$ respectively, then those flows can be mathematically modeled as,

$$\frac{dW_I(t)}{dt} = \frac{\alpha_1}{R_1} - \frac{2(1-\beta_1)}{1+\beta_1} \cdot \frac{W_I(t)^2}{R_1} \cdot K_p q(t),$$

$$\frac{dW_{II}(t)}{dt} = \frac{\alpha_2}{R_2} - \frac{2(1-\beta_2)}{1+\beta_2} \cdot \frac{W_{II}(t)^2}{R_2} \cdot K_p q(t),$$

$$\cdots\cdots\cdots\cdots$$

$$\frac{dW_M(t)}{dt} = \frac{\alpha_m}{R_m} - \frac{2(1-\beta_m)}{1+\beta_m} \cdot \frac{W_M(t)^2}{R_m} \cdot K_p q(t),$$

$$\frac{dq(t)}{dt} = \begin{cases} \sum_{i=1}^{m} \frac{N_i W_i(t)}{R_i} - C, & q > 0, \\ \\ \{\sum_{i=1}^{m} \frac{N_i W_i(t)}{R_i} - C\}^+, & q = 0. \end{cases} \tag{3.8}$$

With (3.8), we choose a positive-definite Lyapunov function as

$$V(\tilde{W}_I(t),\, \tilde{W}_{II}(t), \cdots, \tilde{W}_M(t),\, \tilde{q}(t))$$

$$= \frac{(1+\beta_1)N_1}{2(1-\beta_1)W_I^{*2}} \cdot \tilde{W}_I^2(t) + \frac{(1+\beta_2)N_1}{2(1-\beta_2)W_{II}^{*2}} \cdot \tilde{W}_{II}^2(t)$$

$$+ \cdots + \frac{(1+\beta_m)N_m}{2(1-\beta_m)W_M^{*2}} \cdot \tilde{W}_M^2(t) + K_p\tilde{q}^2(t),$$

where $\tilde{W}_i(t),\ i{=}1, 2, \cdots, m$, and $\tilde{q}(t)$ have the same meaning as in (3.7). Then,

$$\dot{V} = \frac{(1+\beta_1)N_1}{(1-\beta_1)W_I^{*2}}\tilde{W}_I\dot{\tilde{W}}_I + \frac{(1+\beta_2)N_2}{(1-\beta_2)W_{II}^{*2}}\tilde{W}_{II}\dot{\tilde{W}}_{II}$$

$$+ \cdots + \frac{(1+\beta_m)N_M}{(1-\beta_m)W_M^{*2}}\tilde{W}_M\dot{\tilde{W}}_M + 2K_p\tilde{q}\dot{\tilde{q}}$$

$$= -\frac{2N_1K_p}{W_I^{*2}R_1}\tilde{W}_I^2(\tilde{W}_I + 2W_I^*)(\tilde{q} + q_0^*) - \cdots$$

$$-\frac{2N_mK_p}{W_M^{*2}R_m}\tilde{W}_M^2(\tilde{W}_M + 2W_M^*)(\tilde{q} + q_0^*)$$

$$\leq 0.$$

We can obtain its asymptotic stability by applying LaSalle's Invariance Principle, and thus have the following theorem,

Theorem 3.3 *For any $K_p{>}0$, the equilibrium point of system(3.8) is asymptotically stable for any positive pairs $(\alpha_1,\ \beta_1)$, $(\alpha_2,\ \beta_2)$, $\cdots$, $(\alpha_m,\ \beta_m)$ and any positive $R_1,\ R_2,\ \cdots,\ R_m$.*

3.3.3 TCP-friendliness and Differentiated Services

For two competing AIMD flows, from (3.6), we can also get the relationship between W_I^* and W_{II}^* as follow:

$$\frac{W_I^*}{W_{II}^*} = [\frac{\alpha_1(1+\beta_1)(1-\beta_2)}{\alpha_2(1-\beta_1)(1+\beta_2)}]^{1/2}. \tag{3.9}$$

This means that the ratio of W_I^* and W_{II}^* depends only on the choices of $(\alpha_1,\, \beta_1)$ and $(\alpha_2,\, \beta_2)$, and regardless of the traffic loads in the network and their initial states. Therefore, by choosing suitable $(\alpha_1,\, \beta_1)$ and $(\alpha_2,\, \beta_2)$, we can guarantee the fair share of bottleneck bandwidth for each flow. Consequently, for AIMD$(\alpha,\, \beta)$ flows to be TCP-friendly, i.e., co-existing TCP and AIMD flows obtain the same share of bottleneck bandwidth, the necessary and sufficient condition is

$$\alpha = \frac{3(1-\beta)}{1+\beta}. \tag{3.10}$$

A large value of β can be chosen for applications that cannot tolerate drastic changes of the throughput, and α can be set according to the TCP-friendly condition.

In the Internet, different types of multimedia services are provided with different resource requirements. To provide differentiate services, we can assign different traffic a different weight. Eq. (3.9) indicates that we can easily adjust the AIMD parameters of the end systems to provide differentiated services according to different QoS requirements. For instance, let the throughput of an AIMD$(\alpha_1,\, \beta_1)$ flow be k times that of an AIMD$(\alpha_2,\, \beta_2)$ flow, the AIMD parameter pairs should satisfy

$$\frac{\alpha_1}{\alpha_2} = \frac{k^2(1-\beta_1)(1+\beta_2)}{(1+\beta_1)(1-\beta_2)}. \tag{3.11}$$

3.3.4 Numerical Results

The traces of average window size and queue length of 100 TCP ($\alpha = 1$, $\beta = 0.5$) flows and 100 AIMD(0.2, 0.875) flows are given in Figs. 3.3 and 3.4, respectively. The parameters used are $C = 100,000$ packet/sec, $R = 100$ ms, $K_p = 0.0001$, and $\min_{th} = 200$ packets. For the TCP-friendliness, let 100 TCP flows and 24 AIMD(0.2, 0.875) flows share the bottleneck, and the numeric results with Matlab are shown in Fig. 3.5. It can be seen that when the flows in the network possess the same (α, β) parameter pair, the ensemble averages of window size and the bottleneck queue length converge to some certain values, i.e., the equilibrium points we derived in the previous analysis. When TCP and AIMD(0.2, 0.875) flows co-exist, they will fairly share the link capacity in steady state, since (0.2, 0.875) satisfies the TCP-friendly condition (3.10). Thus, the numeric results validate the theorems.

Furthermore, from Figs. 3.3 and 3.4, with a smaller value of α and a larger value of β, it takes longer time for the system to converge to the steady state, and the link utilization during the transient stage is low; however, in steady state, the oscillation amplitudes of the instantaneous window size and queue length are smaller. In other words, with a smaller value of α and a larger value of β, the queuing delay jitter is smaller, and the link utilization in steady state is higher, which are desired for supporting time-sensitive multimedia applications.

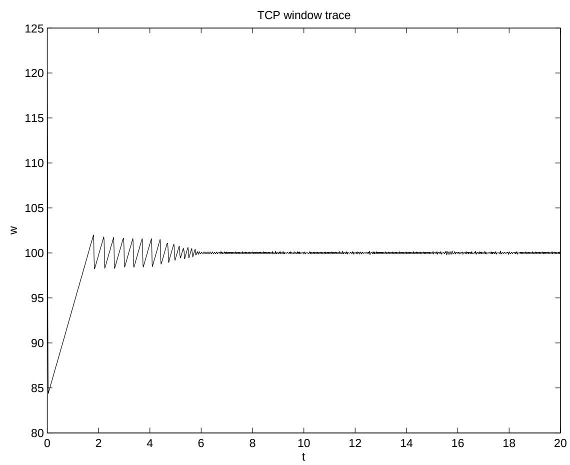

(a) TCP window trace

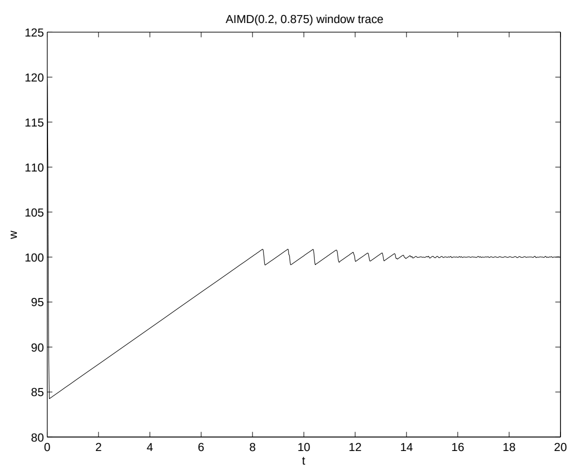

(b) AIMD(0.2, 0.875) window trace

Figure 3.3: Window Trace

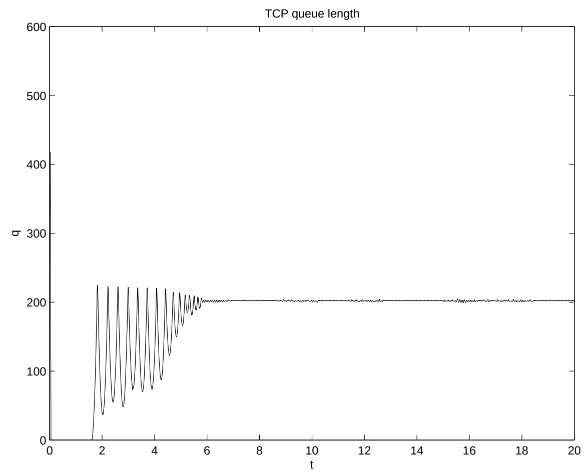

(a) TCP queue length

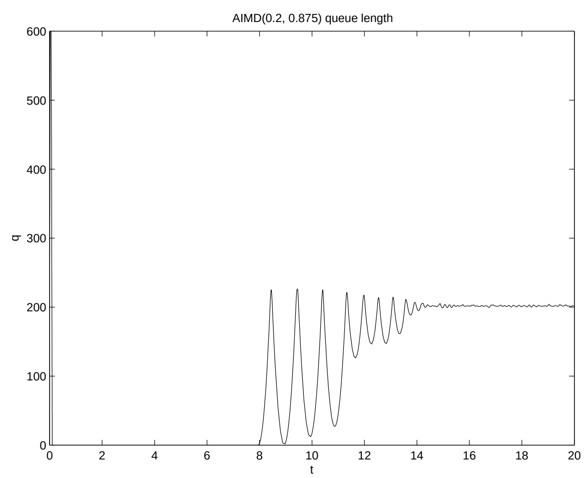

(b) AIMD(0.2, 0.875) queue length

Figure 3.4: Queue Length

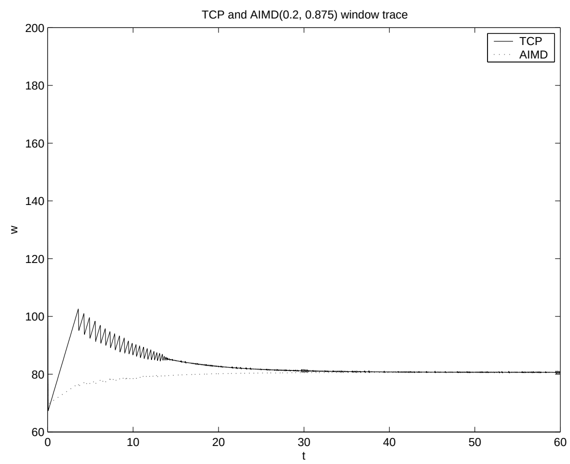

(a) TCP and AIMD(0.2, 0.875) window trace

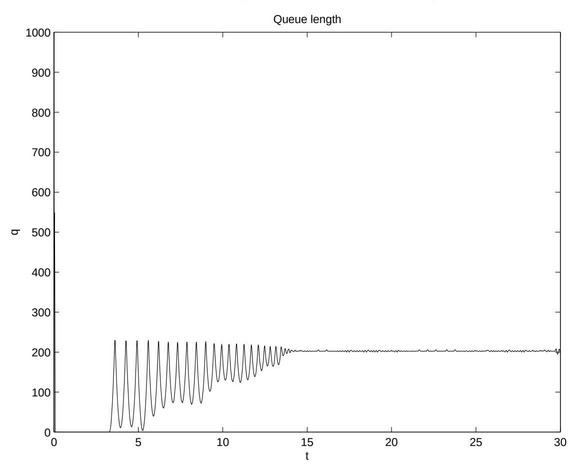

(b) Queue length

Figure 3.5: TCP-friendliness

3.4 Stability and Fairness Analysis with Heterogeneous Feedback Delays

In this section, we study the stability properties of the AIMD/RED system with feedback delay, using the method of Lyapunov functional and Lyapunov function with Lyapunov-Razumikhin condition, to establish different sufficient conditions for the stability of the AIMD/RED system with heterogeneous flows and feedback delays.

3.4.1 Homogeneous Delayed AIMD/RED System

For AIMD/RED system with feedback delay, i.e., $p(t-\tau) = K_p q(t-\tau)$, we can obtain the equilibrium point $(W_0^*,\, q_0^*)$ of the system (3.1) as

$$W_0^* = \frac{R^* C}{N}; \qquad q_0^* = \frac{\alpha(1+\beta)N^2}{2(1-\beta)R^{*2}C^2K_p}. \tag{3.12}$$

where $R^* = \frac{q_0^*}{C} + T_p$. Due to the highly nonlinear nature and the effect of delays in the system, no suitable Lyapunov function could be constructed to prove global asymptotic stability of the equilibrium. Without loss of generality, we fix the time-delay argument $t-\tau$ in the system to $t-R^*$. Then, the system (3.1) can be linearized as

$$\begin{aligned}\dot{\tilde{W}}(t) = & -\frac{\alpha N}{R^{*2}C}\tilde{W}(t) - \frac{\alpha N}{R^{*2}C}\tilde{W}(t-R^*) - \frac{\alpha}{R^{*2}C}\tilde{q}(t) \\ & - \left(\frac{2(1-\beta)}{1+\beta}\frac{K_p C^2 R^*}{N^2} - \frac{\alpha}{R^{*2}C}\right)\tilde{q}(t-R^*), \\ \dot{\tilde{q}}(t) = & \frac{N}{R^*}\tilde{W}(t) - \frac{1}{R^*}\tilde{q}(t).\end{aligned} \tag{3.13}$$

where $\tilde{W}{:=}W - W_0^*,\ \tilde{q}{:=}q - q_0^*$.

System (3.13) can be written in the form of

$$\dot{x}(t) = Ax(t) + Bx(t - R^*), \tag{3.14}$$

with $x = (\tilde{W}(t),\ \tilde{q}(t))^T$, $A = \begin{bmatrix} \frac{-\alpha N}{R^{*2}C} & \frac{-\alpha}{R^{*2}C} \\ \frac{N}{R^*} & -\frac{1}{R^*} \end{bmatrix}$ and $B = \begin{bmatrix} \frac{-\alpha N}{R^{*2}C} & \frac{-2(1-\beta)}{1+\beta}\frac{K_pC^2R^*}{N^2} + \frac{\alpha}{R^{*2}C} \\ 0 & 0 \end{bmatrix}$.
The norm of matrix is defined by $\|A\| = \sqrt{\lambda_{\max}(A^TA)}$, i.e., the square root of the maximum eigenvalue of A^TA.

It can be checked that A is a Hurwitz matrix, which implies that for any positive definite matrix Q, there exists certain positive definite matrix P, such that $A^TP + PA = -Q$.

Theorem 3.4 *Let $M{=}\sqrt{\lambda_{\max}(P)/\lambda_{\min}(P)}$, if there exist positive definite P and Q satisfying $A^TP + PA{=}-Q$ such that matrix $Q - 2M\,\|PB\|\,I$ is positive definite, then the equilibrium point of (3.2) is locally asymptotically stable.*

Proof: With (3.13) and (3.14), we choose Lyapunov function $V(x) = x^TPx$. Then

$$\begin{aligned} \dot{V} &= \dot{x}^TPx + x^TP\dot{x} \\ &= x^T(t)(A^TP + PA)x(t) + 2x^T(t - R^*)B^TPx(t). \end{aligned}$$

Applying Lyapunov-Razumikhin condition, we assume $\mu{>}1$ such that

$$V(\xi) \leq \mu^2V(t),\ \text{for } t - R^* \leq \xi \leq t,$$

which implies that $\|x(\xi)\|{\leq}M{\cdot}\mu{\cdot}\|x(t)\|$, where $M{=}\sqrt{\frac{\lambda_{\max}(P)}{\lambda_{\min}(P)}}$.

Thus,

$$\begin{aligned}\dot{V} &\leq -x^T(t)Qx(t) + 2\|x(t-R^*)\|\,\|PB\|\,\|x(t)\| \\ &\leq -x^T(t)[Q - 2\mu\, M\,\|PB\|\, I]x(t).\end{aligned}$$

Since $Q - 2M\,\|PB\|\,I$ is positive definite, there exists $\mu > 1$ such that $\dot{V} < 0$. The local asymptotic stability of system (3.2) is then obtained. □

Lyapunov-Razumikhin condition is used in Theorem 3.4 to deal with the delayed terms in $\dot{V}$. Lyapunov functional is another method that can be applied when studying the stability of delayed systems. In the following, we apply the method of Lyapunov functional to give a different sufficient condition for the local asymptotic stability of system (3.2).

Theorem 3.5 *If there exist positive definite P and Q satisfying $A^TP + PA = -Q$ and positive definite H such that matrix $\begin{bmatrix} Q-H & -PB \\ -B^TP & H \end{bmatrix}$ is positive definite, the equilibrium point of (3.2) is locally asymptotically stable.*

Proof: With (3.13) and (3.14), we choose Lyapunov functional $V(x) = x^TPx + \int_{t-R^*}^{t} x^T(s)Hx(s)ds$, then

$$\begin{aligned}\dot{V} &= x^T(t)(A^TP+PA)x(t)+2x^T(t-R^*)B^TPx(t)\\ &\quad +x^T(t)Hx(t)-x^T(t-R^*)Hx(t-R^*)\\ &= -x^T(t)(Q-H)x(t)+2x^T(t-R^*)B^TPx(t)\\ &\quad -x^T(t-R^*)Hx(t-R^*)\\ &= -(x^T(t),x^T(t-R^*))\cdot\begin{bmatrix} Q-H & -PB\\ -B^TP & H\end{bmatrix}\cdot\begin{bmatrix} x(t)\\ x(t-R^*)\end{bmatrix}.\end{aligned}$$

Thus, system (3.2) is locally asymptotically stable if $\begin{bmatrix} Q-H & -PB\\ -B^TP & H\end{bmatrix}$ is positive definite. □

The two theorems provide sufficient conditions of local asymptotic stability for the AIMD/RED system. We give a numerical example for Theorem 3.5: Let $N{=}10$, $C{=}3000$ $(packets/sec)$, $T_p{=}0.02(sec)$, $K_p{=}0.0005$ with $\alpha{=}1$, $\beta{=}0.5$.

We choose $Q{=}\begin{bmatrix} 39.0410 & 2.2648\\ 2.2648 & 6.4539\end{bmatrix}$ and $H{=}\frac{1}{2}Q$. Note that Q and H are positive definite. we get $P{=}\begin{bmatrix} 19.0990 & 0.2793\\ 0.2793 & 0.0599\end{bmatrix}$ with Matlab, and the eigenvalues of the matrix $\begin{bmatrix} Q-H & -PB\\ -B^TP & H\end{bmatrix}$ are all positive: 0.1780, 3.2305, 3.4105, 38.6758; therefore, $\begin{bmatrix} Q-H & -PB\\ -B^TP & H\end{bmatrix}$ is positive definite. Thus, the condition of Theorem 3.5 holds and the system is locally asymptotically stable. Simulation results using the same parameters will be given in Sec. 3.5.

Theorems 3.4 and 3.5 give different sufficient asymptotic stability conditions, which allow us to use any of them at our convenience. Again, the asymptotic stability is for the average values of window size and queue length. Given that the average window size converges to W_0^*, the maximum instantaneous window size is bounded to $2W_0^*/(1+\beta)$, so the AIMD window size can be marginally stable with known bounds. Similarly, the instantaneous queue length is bounded.

So far, we have mathematically derived the local stability conditions of AIMD/RED system. For local asymptotic stability, once the system enters the stability region or region-of-attraction, the system will converge to the equilibrium asymptotically. Obviously, the equilibrium point belongs to the stability region. We conjecture that, with both the slow-start and the AIMD algorithms of the TCP/AIMD protocols, the system will eventually evolve to the stability region and equilibrium, and thus global asymptotic stability can be achieved. Simulations in Sec. 3.5 also demonstrate this tendency. Global asymptotic stability conditions for AIMD/RED systems are still under investigation.

3.4.2 Heterogeneous Delayed AIMD/RED System

In the previous subsection, we discuss the stability issue of homogeneous flows with the same AIMD ($\alpha,\ \beta$) pair and the same round-trip delay. With the emergence of more and more heterogeneous traffics in the Internet, understanding the stability properties of the AIMD/RED system with heterogeneous flows is critical for future network planning and design. In this section, we first consider two classes of flows with parameters ($\alpha_1,\ \beta_1$), ($\alpha_2,\ \beta_2$), traffic loads $N_1,\ N_2$ and RTTs $R_1,\ R_2$, respectively, as depicted in Fig. 3.6.

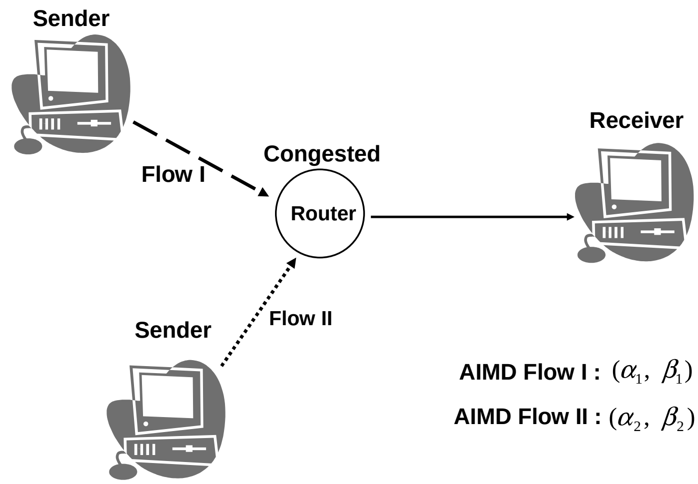

Figure 3.6: Heterogeneous AIMD/RED System

The model and results in this part can be generalized to any number of flows with heterogeneous AIMD parameters and feedback delays.

Taking all the time delays into consideration, the AIMD/RED system shared by two classes of flows can be modeled as

$$\frac{dW_I(t)}{dt}=\frac{\alpha_1}{R_1(t)}-\frac{2(1-\beta_1)}{1+\beta_1}\frac{W_I(t)W_I(t-\tau_1)}{R_1(t-\tau_1)}K_p q(t-\tau_1),$$

$$\frac{dW_{II}(t)}{dt}=\frac{\alpha_2}{R_2(t)}-\frac{2(1-\beta_2)}{1+\beta_2}\frac{W_{II}(t)W_{II}(t-\tau_2)}{R_2(t-\tau_2)}K_p q(t-\tau_2),$$

$$\frac{dq(t)}{dt}=\begin{cases}\dfrac{N_1W_I(t)}{R_1(t)}+\dfrac{N_2W_{II}(t)}{R_2(t)}-C, & q>0,\\[2ex] \{\dfrac{N_1W_I(t)}{R_1(t)}+\dfrac{N_2W_{II}(t)}{R_2(t)}-C\}^+, & q=0.\end{cases} \tag{3.15}$$

with τ_1 and τ_2 as the average of round trip time $R_1(t)$ and $R_2(t)$, respectively .

Then, the delayed linearized system about the equilibrium point is

$$\begin{aligned}
\dot{\tilde{W}}_I(t) =& -\frac{\alpha_1(N_1R_2^*G+N_2R_1^*)}{GCR_1^*R_2^*}(\tilde{W}_I(t)-\tilde{W}_I(t-R_1^*)) \\
& -\frac{2(1-\beta_1)}{1+\beta_1}\frac{K_pG^2C^2R_1^*R_2^{*2}}{(N_1R_2^*G+N_2R_1^*)^2}\tilde{q}(t-R_1^*) \\
& -\frac{\alpha_1\tilde{q}(t)}{R_1^{*2}C}+\frac{\alpha_1}{CR_1^{*2}}\tilde{q}(t-R_1^*), \\
\dot{\tilde{W}}_{II}(t) =& -\frac{\alpha_2(N_1R_2^*G+N_2R_1^*)}{CR_1^*R_2^*}(\tilde{W}_{II}(t)-\tilde{W}_{II}(t-R_2^*)) \\
& -\frac{2(1-\beta_2)}{1+\beta_2}\frac{K_pC^2R_1^{*2}R_2}{(N_1R_2^*G+N_2R_1^*)^2}\tilde{q}(t-R_2^*) \\
& -\frac{\alpha_2\tilde{q}(t)}{R_2^{*2}C}+\frac{\alpha_2}{CR_2^{*2}}\tilde{q}(t-R_2^*), \\
\dot{\tilde{q}}(t) =& \frac{N_1}{R_1^*}\tilde{W}_I(t)+\frac{N_2}{R_2^*}\tilde{W}_{II}(t)-\frac{GN_1R_2^*}{R_1^*(N_1R_2^*G+N_2R_1^*)}\tilde{q}(t) \\
& -\frac{N_2R_1^*}{R_2^*(N_1R_2^*G+N_2R_1^*)}\tilde{q}(t).
\end{aligned} \tag{3.16}$$

where $\tilde{W}_I := W - W_I^*,\ \tilde{W}_{II} := W - W_{II}^*,\ \tilde{q} := q - q_0^*$.

$(W_I^*, W_{II}^*, q_0^*)=(\frac{GCR_1^*R_2^*}{N_1R_2^*G+N_2R_1^*}, \frac{CR_1^*R_2^*}{N_1R_2^*G+N_2R_1^*}, \frac{\alpha_1(1+\beta_1)}{2(1-\beta_1)W_I^{*2}K_p})$ is the equilibrium point of system (3.15). Similar to Sec. 3.4.1, we also set τ_1 and τ_2 to be R_1^* and R_2^*, respectively, where $R_1^* = \frac{q_0^*}{C} + T_{p1},\ R_2^* = \frac{q_0^*}{C}+T_{p2}$, and $G=(\frac{\alpha_1(1+\beta_1)(1-\beta_2)}{\alpha_2(1-\beta_1)(1+\beta_2)})^{1/2}$.

System (3.16) can be rewritten as

$$\dot{x}(t) = Ax(t) + B_1 x(t - R_1^*) + B_2 x(t - R_2^*), \tag{3.17}$$

with $x = (\tilde{W}_I(t), \tilde{W}_{II}(t), \tilde{q}(t))^T$,

$$A = \begin{bmatrix} a_{11} & 0 & \frac{-\alpha_1}{R_1^{*2}C} \\ 0 & a_{22} & \frac{-\alpha_2}{R_2^{*2}C} \\ \frac{N_1}{R_1^*} & \frac{N_2}{R_2^*} & a_{33} \end{bmatrix}, B_1 = \begin{bmatrix} b1_{11} & 0 & b1_{13} \\ 0 & 0 & 0 \\ 0 & 0 & 0 \end{bmatrix} \text{ and } B_2 = \begin{bmatrix} 0 & 0 & 0 \\ 0 & b2_{22} & b2_{23} \\ 0 & 0 & 0 \end{bmatrix}.$$

where $a_{11} = -\dfrac{\alpha_1(N_1R_2^*G + N_2R_1^*)}{GCR_1^*R_2^*}$, $a_{22} = -\dfrac{\alpha_2(N_1R_2^*G + N_2R_1^*)}{CR_1^*R_2^*}$,

$a_{33} = -\dfrac{GN_1R_2^{*2} + N_2R_1^{*2}}{R_1^*R_2^*(N_1R_2^*G + N_2R_1^*)}$, $b1_{11} = -\dfrac{\alpha_1(N_1R_2^*G + N_2R_1^*)}{GCR_1^*R_2^*}$,

$b1_{13} = -\dfrac{2(1-\beta_1)}{1+\beta_1}\dfrac{K_pG^2C^2R_1^*R_2^{*2}}{(N_1R_2^*G + N_2R_1^*)^2} + \dfrac{\alpha_1}{CR_1^{*2}}$,

$b2_{22} = -\dfrac{\alpha_2(N_1R_2^*G + N_2R_1^*)}{CR_1^*R_2^*}$, $b2_{23} = -\dfrac{2(1-\beta_2)}{1+\beta_2}\dfrac{K_pC^2R_1^{*2}R_2}{(N_1R_2^*G + N_2R_1^*)^2} + \dfrac{\alpha_2}{CR_2^{*2}}$.

Also, we can check that A is a Hurwitz matrix. Let $M = \sqrt{\lambda_{\max}(P)/\lambda_{\min}(P)}$, we have the following theorem.

Theorem 3.6 *If there exist positive definite P and Q satisfying $A^TP + PA = -Q$ such that matrix $Q - 2M\,(\|PB_1\| + \|PB_2\|)I$ is positive definite, then the equilibrium point of (3.15) is locally asymptotically stable.*

Proof: With (3.16) and (3.17), we choose Lyapunov function $V(x) = x^TPx$, then

$$\begin{aligned} \dot{V} &= x^T(t)(A^TP + PA)x(t) + 2x^T(t - R_1^*)B_1^TPx(t) \\ &+ 2x^T(t - R_2^*)B_2^TPx(t). \end{aligned}$$

Let $R^* = \max\{R_1^*,\, R_2^*\}$. Applying the Lyapunov-Razumikhin condition, we assume $\mu{>}1$ such that

$$V(\xi) \leq \mu^2 V(t), \qquad t - R^* \leq \xi \leq t,$$

which implies that $\|x(\xi)\| \leq M{\cdot}\mu{\cdot}\|x(t)\|$.

Thus,

$$\begin{aligned}
\dot{V} &\leq -x^T(t)Qx(t){+}2\|x(t-R^*)\|\,\|PB_1\|\,\|x(t)\| \\
&\quad +2\|x(t-R^*)\|\,\|PB_2\|\,\|x(t)\| \\
&\leq -x^T(t)[Q - 2\mu\, M\,(\|PB_1\| + \|PB_2\|)I]x(t).
\end{aligned}$$

Therefore, there exists $\mu{>}1$ such that $\dot{V}{<}0$ under the condition of the Theorem. The local asymptotic stability of system (3.15) is then obtained. □

We can also apply the method of Lyapunov functional to obtain a different sufficient condition for the local asymptotic stability of system (3.15).

Theorem 3.7 *If there exist positive definite P and Q satisfying $A^T P + PA = -Q$ and positive definite H such that matrix* $\begin{bmatrix} Q-2H & -PB_1 & -PB_2 \\ -B_1^T P & H & 0 \\ -B_2^T P & 0 & H \end{bmatrix}$ *is positive definite, the equilibrium point of* (3.15) *is locally asymptotically stable.*

Proof: With (3.16) and (3.17), we choose Lyapunov functional

$$V(x){=}x^T Px{+}\int_{t-R_1^*}^{t} x^T(s)Hx(s)ds{+}\int_{t-R_2^*}^{t} x^T(s)Hx(s)ds,$$

then

$$\begin{aligned}
\dot{V} &= x^T(t)(A^TP + PA)x(t) + 2x^T(t-R_1^*)B_1^TPx(t) \\
&\quad +2x^T(t-R_2^*)B_2^TPx(t) + 2x^T(t)Hx(t) \\
&\quad -x^T(t-R_1^*)Hx(t-R_1^*) - x^T(t-R_2^*)Hx(t-R_2^*) \\
&= -x^T(t)(Q-2H)x(t) + 2x^T(t-R_1^*)B_1^TPx(t) \\
&\quad +2x^T(t-R_2^*)B_2^TPx(t) - x^T(t-R_1^*)Hx(t-R_1^*) \\
&\quad -x^T(t-R_2^*)Hx(t-R_2^*) \\
&= -(x^T(t), x^T(t-R_1^*), x^T(t-R_2^*))\cdot \\
&\quad \begin{bmatrix} Q-2H & -PB_1 & -PB_2 \\ -B_1^TP & H & 0 \\ -B_2^TP & 0 & H \end{bmatrix} \cdot \begin{bmatrix} x(t) \\ x(t-R_1^*) \\ x(t-R_2^*) \end{bmatrix}.
\end{aligned}$$

Denote $D = \begin{bmatrix} Q-2H & -PB_1 & -PB_2 \\ -B_1^TP & H & 0 \\ -B_2^TP & 0 & H \end{bmatrix}$. Thus, system (3.15) is locally asymptotically stable if D is positive definite.

The two theorems provide sufficient conditions of local asymptotic stability for the

AIMD/RED system with heterogeneous delays. We now give a numerical example for Theorem 3.7: let N_1=N_2=10, K_p=0.0001, C=12000$(packets/sec)$. Choose $(\alpha_1,\ \beta_1) = (1,\ 0.5)$ with T_{p1}=0.01(sec), and $(\alpha_2,\ \beta_2) = (0.2,\ 0.875)$ with T_{p2}=0.008(sec), respectively. Let $Q=\begin{bmatrix} 107.8925 & 66.0119 & 49.7801 \\ 66.0119 & 62.8475 & 38.7408 \\ 49.7801 & 38.7408 & 52.1792 \end{bmatrix}$ and $H=\frac{1}{4}Q$. Note that Q and H are positive definite. We obtain matrix $P=\begin{bmatrix} 13.8052 & 6.9367 & -0.3094 \\ 6.9367 & 11.6831 & -0.1195 \\ -0.3094 & -0.1195 & 0.1443 \end{bmatrix}$ with Matlab, and the eigenvalues of the matrix $D = \begin{bmatrix} Q-2H & -PB_1 & -PB_2 \\ -B_1^TP & H & 0 \\ -B_2^TP & 0 & H \end{bmatrix}$ are all positive: 2.4997, 3.4597, 3.8422, 5.5610, 7.9974, 13.6734, 46.2107, 46.2592, 93.4159; therefore, D is positive definite. Thus, the condition of Theorem 3.7 holds and the system is locally asymptotically stable. Simulation results using the same parameters will be give in Sec. 3.5.

While choosing parameters in the numerical example, we have also found that link capacity C and feedback delays cannot be too large, so that the matrix D can be positive definite. This observation is also consistent with [9], which suggested that TCP/RED will become unstable when delay increases, or more strikingly, when link capacity increases.

Similarly, we can obtain the local stability of the AIMD/RED system when it is shared by more than two classes of heterogeneous flows as well. The proof is omitted here.

3.4.3 TCP-friendliness

According to the equilibrium point of the system, $W_I^*/W_{II}^* = G$ is a function of the AIMD parameter pairs, and it is independent of the delays. In other words, for two AIMD flows, as long as their AIMD parameters satisfy the condition that $G = 1$, their average window sizes are the same and their flow throughputs inversely proportional to their RTTs. To be TCP-friendly, the necessary and sufficient condition is still $\alpha = 3(1-\beta)/(1+\beta)$, the same as the condition (3.10) derived in the delay free systems in Sec. 3.3.3.

3.5 Performance Evaluation

Matlab is used to obtain the system evolution trajectory of the fluid model in order to verify the asymptotic stability proved in Sec. 3.4. Network simulator, NS-2, is used to evaluate the performance of the AIMD/RED systems.

3.5.1 Numerical Results

The traces of window size and queue length of 10 TCP flows and 10 AIMD(0.2, 0.875) flows in a RED-enabled link with feedback delays are given in Figs. 3.7 and 3.8, respectively. The parameters used are the same as those in the numerical example of Theorem 3.5, i.e., C=3000 packet/sec, K_p=0.0005, $RTT = 0.02$ sec, and $\min_{th} = 200$ packets. For heterogeneous-flow case, let 10 TCP flows and 10 AIMD(0.2, 0.875) flows share the bottleneck with C=12000 packet/sec, K_p=0.0001, and RTTs of the TCP and AIMD flow are 0.01 sec and 0.008 sec, respectively. These parameters are the same as those

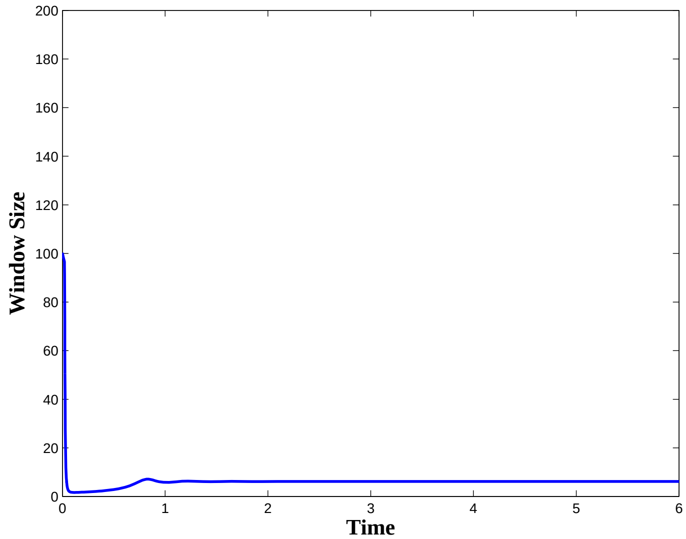

(a) Window trace

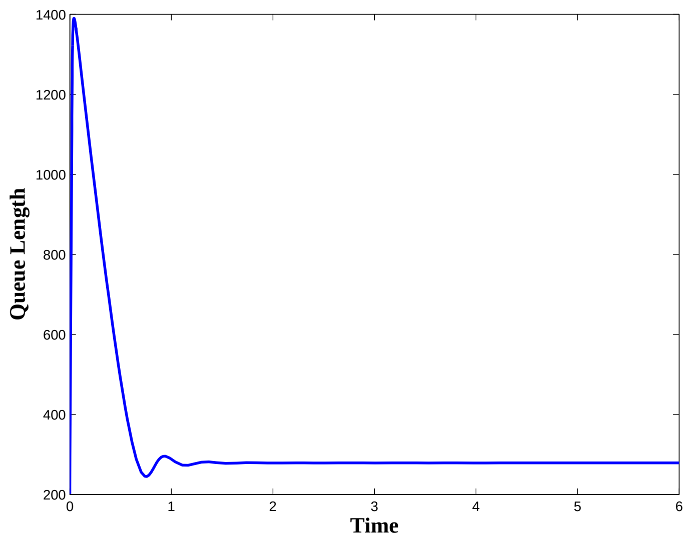

(b) Queue length

Figure 3.7: TCP flows

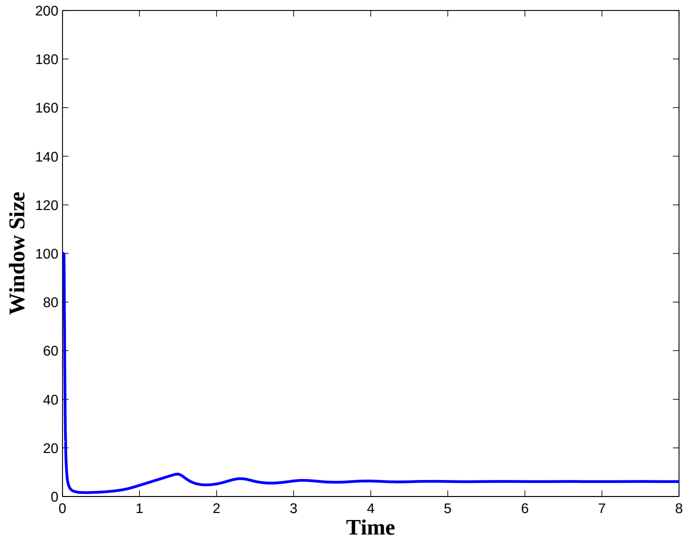

(a) Window trace

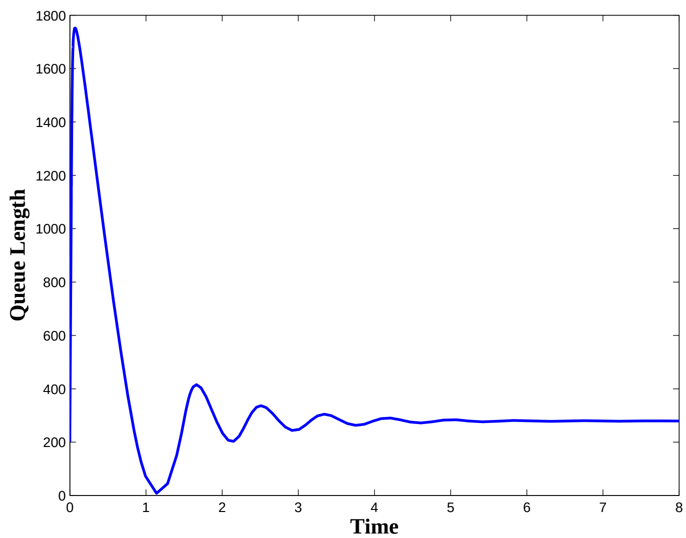

(b) Queue length

Figure 3.8: AIMD(0.2, 0.875) flows

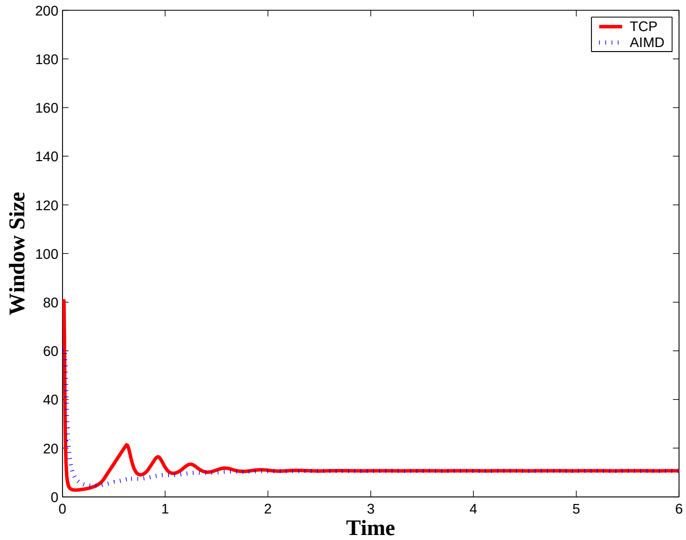

(a) Window trace

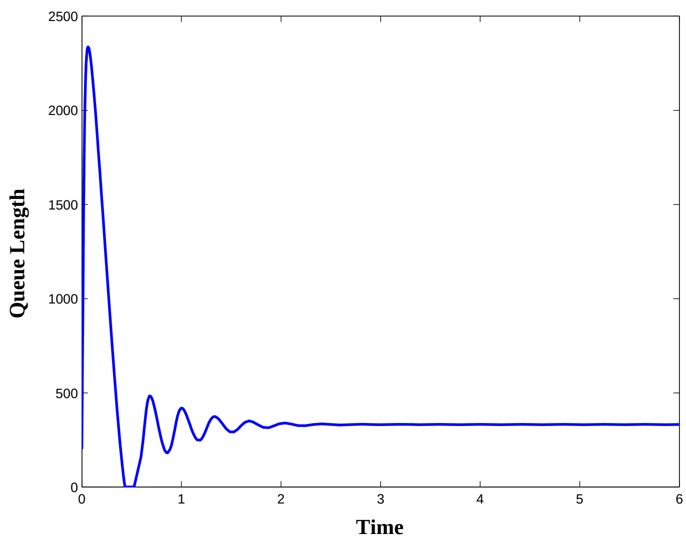

(b) Queue length

Figure 3.9: TCP vs. AIMD(0.2, 0.875) flows

in the numerical example of Theorem 3.7. To show the local asymptotic stability of the system, we choose the value of the initial condition close to the equilibrium point. As shown in the figures, all systems are asymptotically stable, and the numerical results validate the theorems proved in this chapter. Since the parameter pair (0.2, 0.875) satisfies the TCP-friendly condition derived, the average window sizes of the competing TCP and AIMD (0.2, 0.875) flows should be the same, which is verified by the numerical results shown in Fig. 3.9.

3.5.2 Simulation Results

We use network simulator (NS-2) to further study the performance of the AIMD/RED system with realistic protocols and network topologies. Both single bottleneck and multiple bottleneck topologies are used in the simulations. The following parameters are used unless otherwise explicitly stated. The routers adjacent to the bottleneck link are RED-capable: all packets can be queued when the average queue length is less than 200 packets, and the packets will be discarded with probability K_p times the current average queue length minus 200. The packet size of all flows is $1,250$ bytes. The bottleneck link capacity is 1 Gbps, equivalent to $100,000$ packet/sec.

We first let 100 TCP flows and 100 AIMD(0.2, 0.875) flows with homogeneous delays share a single bottleneck, respectively. Their window traces and instantaneous queue lengths are given in Figs. 3.10, 3.11, 3.12, and 3.13, with different values of RTT and K_p. All figures show that the flow window sizes and queue lengths are periodically oscillating in steady state, and their time averages over a round are converging to certain values, i.e., their time averages are asymptotically stable.

As shown in Figs. 3.10 and 3.11, a small value of K_p can reduce the oscillation

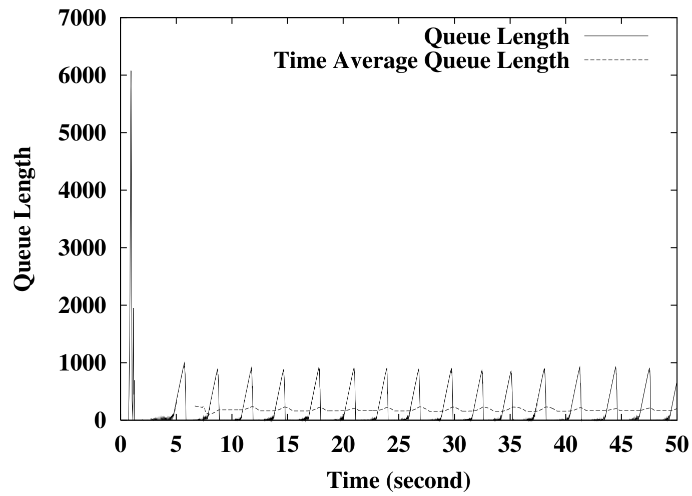

(a) Queue length

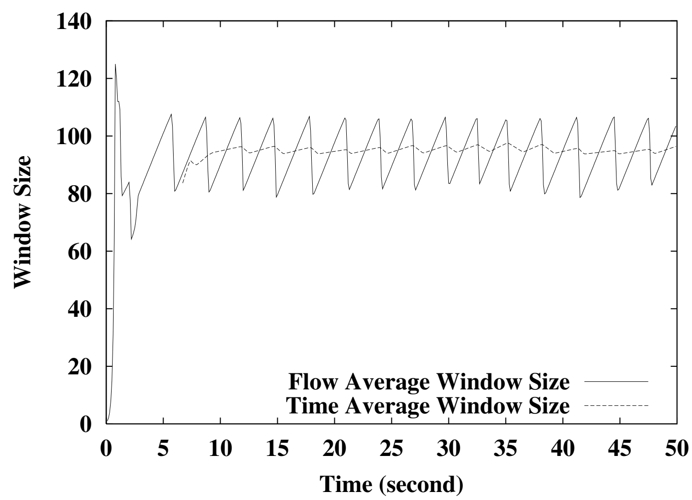

(b) Window trace

Figure 3.10: TCP, $K_p = 0.0001$, $R = 100$ms

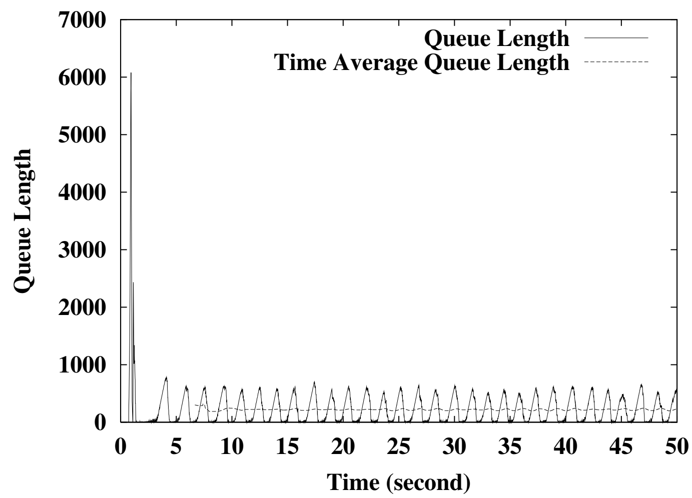

(a) Queue length

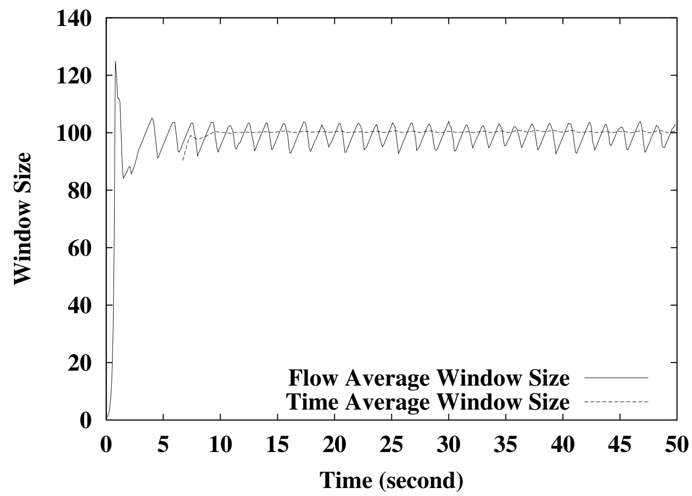

(b) Window trace

Figure 3.11: TCP, $K_p = 0.00002$, $R = 100$ms

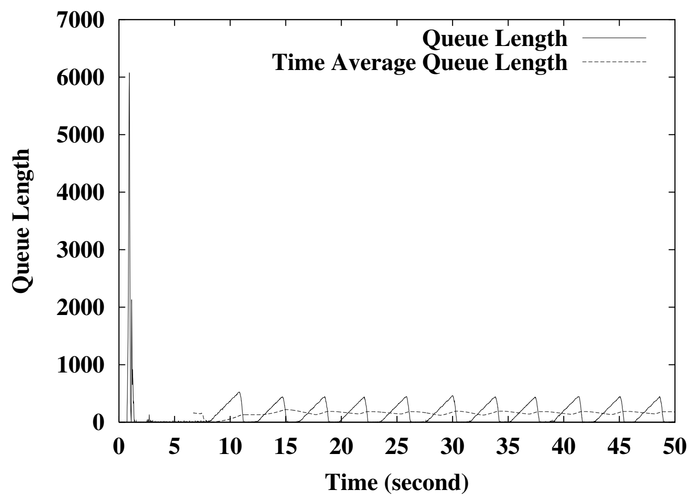

(a) Queue length

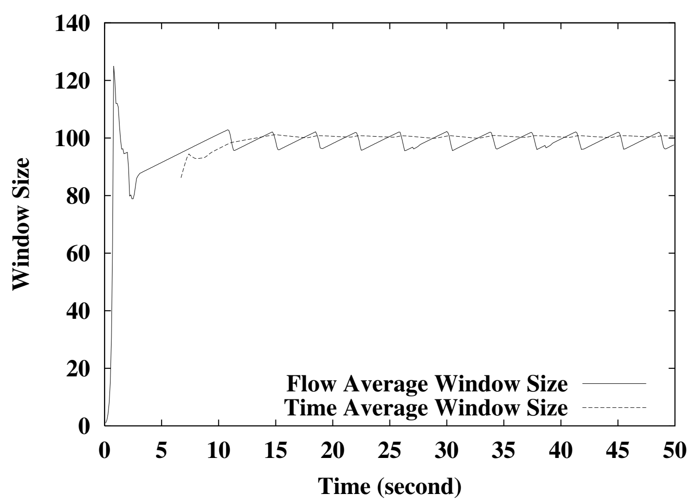

(b) Window trace

Figure 3.12: AIMD$(0.2, 0.875)$, $K_p = 0.0001$, $R = 100$ms

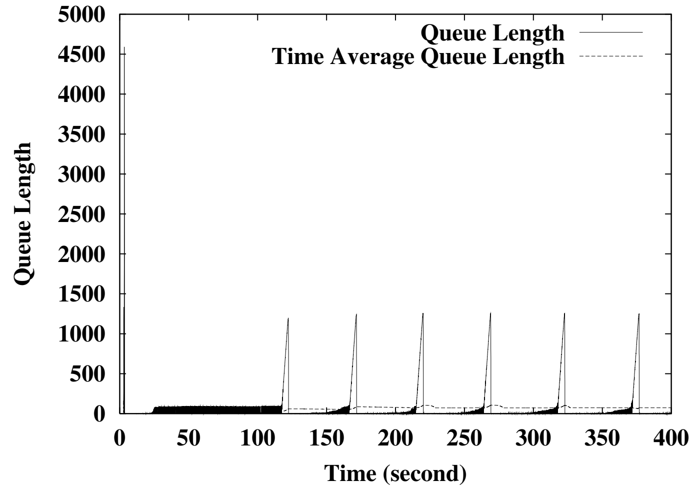

(a) Queue length

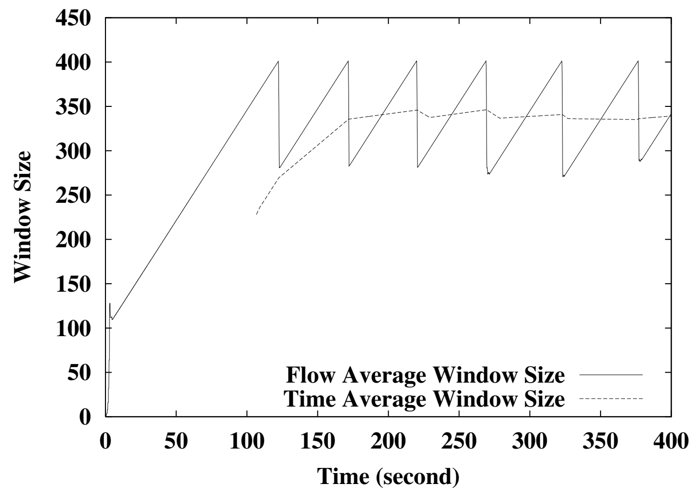

(b) Window trace

Figure 3.13: TCP, $K_p = 0.0001$, $R = 400$ms

amplitude in the steady state, and thus improve the link utilization and reduce delay jitter in the steady state, at the cost of taking longer for the system to reach the steady state. The network utilization in transient states is low, so a slow convergence speed is not desired. Comparing Figs. 3.10 and 3.12, it is noticed that the system with AIMD (0.2, 0.875) flows has smaller oscillation amplitude in the steady state because the AIMD flows have a smaller value of α and a larger value of β than that of TCP flows. Another observation from Figs. 3.10 and 3.13 is that the larger the RTT, the slower the system converges to the steady state and the larger the variation of the queue length in the steady state.

To study the system performance with heterogeneous flows, let 24 AIMD($0.2, 0.875$) flows compete with 100 TCP flows, and their RTTs are randomly chosen between 0.09 sec to 0.1 sec. The traces of their average window size and queue length are given in Fig. 3.14. It is shown that, when heterogeneous TCP and AIMD(0.2, 0.875) flows share the network, the network converges to the steady state quickly and the queue oscillation in the steady state is small. In other words, when heterogeneous traffic shares the network, the system performance is even better than that with only TCP flows (high oscillation amplitude in the steady state) or homogeneous AIMD (0.2, 0.875) flows (slow convergence speed). Another observation from Fig. 3.14 is that the average window sizes of the TCP flows and the AIMD (0.2, 0.875) flows are close to each other, therefore validating the TCP-friendly condition derived in Sec. 3.3.

A realistic network will accommodate flows with heterogeneous round-trip delays, and some flows may undergo multiple bottlenecks. The topology used for a multiple-bottleneck scenario is shown in Fig. 3.15; 100 group I flows compete with 50 group II TCP flows in link r_0r_1 and with 50 group III TCP flows in link r_1r_2. The round-trip times of the flows are randomly chosen from 50 ms to 400 ms. There are 50 TCP flows

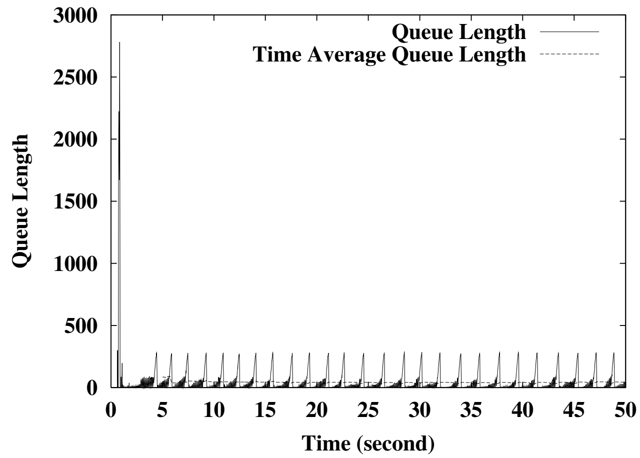

(a) Queue length

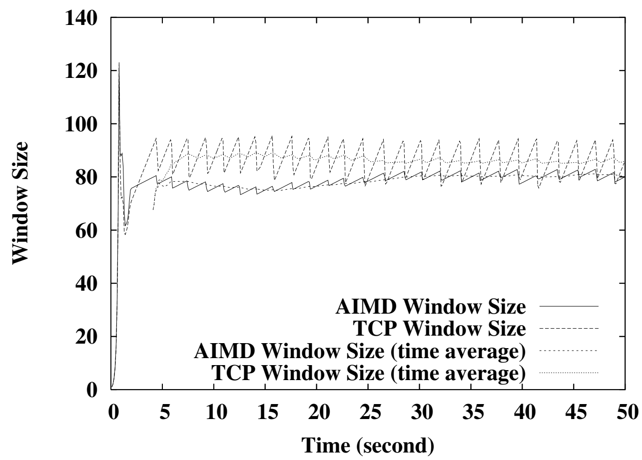

(b) Window trace

Figure 3.14: TCP and AIMD($0.2, 0.875$) flows

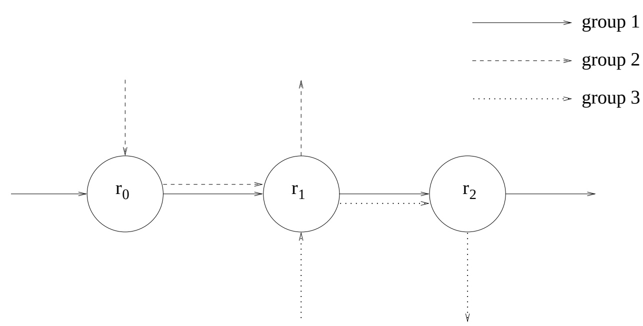

Figure 3.15: Queue length, multiple-bottleneck topology

and 50 AIMD(0.2, 0.875) flows in group I. The trace of queue length at r_0 is shown in Fig. 3.16. Although the instantaneous queue length oscillates over time, the time average does not change significantly. The stability conditions for multiple-bottleneck AIMD/RED systems are discussed in Chapter 5.

3.6 Related Work

Congestion control mechanisms and AQM schemes for the Internet have been extensively studied, aiming to achieve quick convergence to efficiency, stability, fair bandwidth sharing, and low packet loss rate.

Internet stability properties and fairness issues in the presence of feedback delay have received much attention recently. The original work of proposing the congestion controller using utility optimization has been done [16]. Since then, lots of work have been conducted for the TCP/Random Exponential Marking (REM) system. For example, for the case of a single node and a single source in the TCP/REM system, the design of congestion controllers and the stability problems with delays are studied in [7, 17, 18], and

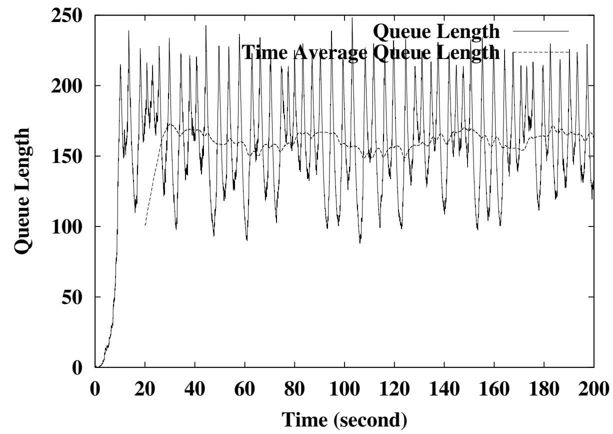

Figure 3.16: Multiple-bottleneck, heterogeneous round-trip delays

the sufficient conditions for global stability are given as well. Recently, a discrete congestion control system has been proposed in [19] to maintain both stability and fairness under heterogeneous delayed feedback. The boundedness and stability for the TCP/REM system are discussed in [20].

In the design of congestion controllers, one of the important criteria is asymptotic stability, i.e., the capability of the network to avoid oscillations in the steady-state and to properly respond to other external perturbations. AQM schemes recently discussed include RED, REM, Proportional-Integral (PI) control and Loss Ratio-based RED (LRED). For TCP/RED system, the sufficient conditions for global stability in the absence of feedback delay are given in [26]; the conditions for the stability of TCP/RED system in the frequency domain are given in [9] by Nyquist stability criterion. The design and analysis of the PI controller for RED routers are discussed in [23]. Newly proposed AQM scheme, LRED in [35], measures the latest packet loss ratio, and uses it as a complement to queue length for adaptively adjusting the packet drop probability. To the best of our knowledge, the stability properties of AIMD/RED systems in the presence of heterogeneous AIMD and TCP flows with heterogeneous feedback delays have not been studied and they are the main focus of this chapter.

3.7 Summary and Future Discussions

In this chapter, we have studied the stability of AIMD/RED systems with and without the consideration of feedback delays. Delay-free systems have been proved asymptotically stable. Sufficient conditions have been obtained for the asymptotic stability of both homogeneous-flow and heterogeneous-flow systems with feedback delays, which provide insight and guidelines for the design of a stable system. TCP-friendliness issue has also been discussed for multiple flows with different AIMD parameters and different $RTTs$. Numerical results have been given to validate the analytical results, and extensive simulations with NS-2 have been conducted to study the system performance with realistic protocols and network topologies. The study will be useful to re-design and re-engineer TCP congestion control for supporting heterogeneous multimedia application in more diversified Internet in the future.

There are many interesting open issues require further research. First, for RED queues, the packet drop probability depends on the queue length only. With the model presented in the chapter, the average queue length in the steady state can be derived, which can be used to give a rough estimation of the packet loss rate. However, the packet loss rate depends on the queue length distribution, which is unknown from the model. Second, the robustness of the system with disturbance from short-lived TCP connections and UDP connections is an important open issue. Third, a single bottleneck topology is used in this chapter. In a follow-up work, we will discuss the stability analysis to systems with multiple bottlenecks in Chapter 5. Finally, since multicast applications may use a large portion of Internet bandwidth in the future, how to design and analyze flow/congestion control mechanisms for multicast applications is a very challenging issue beckon for more research.

Chapter 4

Bounds of AIMD/RED Systems with Time Delays

The Additive Increase and Multiplicative Decrease (AIMD) congestion control algorithm of TCP (Transmission Control Protocol) deployed in the end systems and the Random Early Detection (RED) queue management scheme deployed in the intermediate systems contribute to Internet stability and integrity. Previous research based on the fluid-flow model analysis indicated that with the consideration of time delays, the TCP/RED system may not be asymptotically stable when the time delays or the link capacity becomes large [9]. However, as long as the system operates near its desired equilibrium, small oscillations are acceptable, and the network performance (in terms of efficiency, loss rate, and delay) is still satisfactory. Deriving the bounds of these oscillations for the AIMD/RED system with time delays is non-trivial. In this chapter, we study the practical stability of the homogeneous-flow and heterogeneous-flow AIMD/RED system with feedback delays, and obtain theoretical bounds of the AIMD flow window size and the RED queue length, as functions of number of flows, link capacity, RED queue parameters, and AIMD parameters. Numerical results with Matlab and simulation results with NS-2 are given to validate the correctness and demonstrate the tightness of the derived bounds. The analytical and simulation results provide important insights on which system parameters contribute to higher oscillations of the system and how to set system parameters to ensure system efficiency with bounded delay and loss. Our results can also help to predict and control the system performance for Internet with higher data rate links multiplexed with more flows with different parameters.

4.1 Introduction

Internet stability has been an active research topic since its first congestion collapse was observed. With a fluid-flow model of the system, it has been proved that, without feedback delay, the AIMD congestion control mechanism, coupled with the RED queue management, can ensure the asymptotic stability of the system [29]. However, with a non-negligible feedback delay, the AIMD/RED system may not be asymptotically stable when the delay becomes large and/or when the link capacity becomes large [9]. On the other hand, the Internet is a very dynamic system, and can tolerate some transient congestion events. In fact, TCP controlled flows aggressively probe for available bandwidth in the network, and create transient congestions. From a practical point of view, a concrete system is considered stable if the deviation of the motion from the equilibrium remains within certain bounds determined by the physical situation. The desired state of a system may be mathematically unstable and yet the system oscillates close enough to this state for its performance to be acceptable. To deal with such situations, the notion of *practical stability* is more useful.

With large time delays or link capacities, the AIMD/RED system as a whole may not be asymptotically stable [9]. However, it can be practically stable as long as the end systems do not overshoot the available bandwidth too severely. In this case, the overall system efficiency can still be high, and the packet loss rate and queuing delay can still be well bounded, i.e., its performance is still acceptable. Therefore, the critical issue to investigate is: does the AIMD/RED system always operate in the area close to the desired equilibrium state, and what are the theoretical bounds? To answer these questions, studying system practical stability and bounds is the key, which is also the focus of this chapter.

With clearly defined bounds, a system is considered practically stable. The bounds can be used as a guideline to set up the AIMD/RED system parameters to enhance system performance. Using the fluid-flow model of the AIMD/RED system with homogeneous and heterogeneous flows, instead of applying the Lyapunov-like method, we derive upper and lower bounds of congestion window size and queue length by directly studying the inherent properties of the AIMD/RED system. The derived theoretical bounds provide important insights on which system parameters contribute to high oscillations of the system and how to choose system parameters to ensure system efficiency with bounded delay and loss. The theorems given in this chapter can also help to predict the system performance for the future Internet with higher capacity and more flows with different flow parameters.

The remainder of the chapter is organized as follows. Fluid-flow models of homogeneous and heterogeneous AIMD/RED systems are reviewed in Sec. 4.2 and Sec. 4.3, respectively; upper and lower bounds of the homogeneous and heterogeneous AIMD/RED systems with feedback delays are also obtained. In Sec. 4.4, numerical results with Matlab and simulation results using NS-2 are presented to validate the derived bounds, and the impacts of different system parameters on the system performance are also discussed. Sec. 4.5 briefly introduces the related work, followed by the summary in Sec. 4.6.

4.2 Bounds and Practical Stability of Homogeneous AIMD/RED System

4.2.1 A Fluid-flow Model of Homogeneous AIMD/RED System

For all AIMD-controlled flows with the same (α, β) parameter pair and round-trip delay, the AIMD/RED fluid model relates to the *ensemble averages* of key network variables [22, 23] and is described by the coupled, nonlinear differential equations (3.1)

The equilibrium point $(W^*,\ q^*)$ for (3.1) is given by

$$W^* = \frac{R{\cdot}C}{N}; \qquad q^* = \frac{\alpha(1+\beta)N^2}{2(1-\beta)R^2C^2K_p}.$$

Remark 1. At the equilibrium, the total arrival rate equals the total link capacity, so the link bandwidth can be fully utilized. In other words, the equilibrium point is also the most desired operating point of the system. If the window size is larger than W^*, the queue will build up which results in a longer queueing delay; if the window size is less than W^*, the network load is smaller than its capacity, so the network resources are not fully utilized.

4.2.2 Upper Bound on Window Size

It has been demonstrated in [9] that an AIMD/RED system becomes (asymptotically) unstable with the increase of round trip delays of the system. Using the fluid-flow model, sufficient conditions for the asymptotic stability of AIMD/RED systems with feedback delays have been derived in [27]. In this section, we show that even though the system may become (asymptotically) unstable because of the effects of time delay, its window size and queue length are still bounded, and the upper bound of window size is close to the equilibrium.

We study the delayed homogeneous AIMD system with RED defined by (3.1) and derive the upper and lower bounds of the system. We set $\min_{th} = 0$ in RED and assume that the traffic load (i.e., the number of AIMD flows) is time-invariant, i.e., $N(t) = N$. With ever-increasing link capacity and appropriate congestion control mechanism, variation of queuing delays becomes small relative to propagation delays. In fact, recent work [48] reveals that the variable nature of RTT due to queueing delay variation helps to stabilize the TCP/RED system. Therefore, we ignore the effect of the delay jitter on the round-trip time and derive the bounds of AIMD/RED system assuming RTT to be constant. Simulation results with NS-2 in Sec. 4.4 shows that the obtained bounds estimates is still applicable when RTT is actually time-varying.

Notice that the AIMD/RED system defined by (3.1)are described by delayed differential equations, with initial conditions given by $1 \leq W(t) \leq W^*$ and $0 \leq q(t) \leq q^*$ on the interval $t \in [-R, 0]$. According to (3.1), it is also reasonable that we let $\dot{W}(t) \leq \frac{\alpha}{R}$ for $t \in [-R, 0]$.

Theorem 4.1 *Let $U_B > 0$ be the largest real root of*

$$U_B \cdot (U_B - \alpha) \cdot (U_B - \frac{R{\cdot}C}{N} - \alpha)^2 = \frac{\alpha^2(1+\beta)}{(1-\beta)NK_p},$$

then $W(t) \le U_B$ for $t \ge 0$.

Proof: With (3.1), we note that $\dot{W} \le \frac{\alpha}{R}$ for $t \ge 0$, since $W(t) \ge 1$ and $q(t) \ge 0$. For $\tau > 0$, taking integration on both sides from $t-\tau$ to t gives

$$W(t) - W(t-\tau) \le \frac{\alpha}{R} \cdot \tau \quad \text{for} \quad t \ge 0. \tag{4.1}$$

We show that the U_B (> 0) in the theorem is an upper bound of $W(t)$ for $t \ge 0$, i.e., if $W(t) = U_B$ for some $t = t_1 \ge 0$, then $\dot{W}(t_1) \le 0$.

With (4.1) and $W(t_1) = U_B$, and taking $\tau = R$ and $t = t_1$, we have

$$W(t_1 - R) \ge U_B - \alpha. \tag{4.2}$$

Notice that $W(t_1 - \tau) \ge U_B - a{\cdot}\alpha$ when $\tau \in [R,\ aR]$ for any real number $a > 1$.

Consider

$$\dot{q}(t) = \begin{cases} \frac{N \cdot W(t)}{R} - C, & q > 0, \\ \{\frac{N \cdot W(t)}{R} - C\}^+, & q = 0. \end{cases}$$

Taking integration on both sides from $t_1 - aR$ to $t_1 - R$, we have

$$\begin{aligned} \int_{t_1-aR}^{t_1-R} \dot{q}(s)ds &\ge \frac{N}{R}\int_{t_1-aR}^{t_1-R} W(s)ds - (a-1)R{\cdot}C \\ &\ge N \cdot (a-1) \cdot (U_B - a{\cdot}\alpha) - (a-1)RC \end{aligned}$$

which implies

$$q(t_1 - R) \ge [N \cdot (U_B - a{\cdot}\alpha) - R{\cdot}C] \cdot (a-1) \tag{4.3}$$

since $q(t) \geq 0$.

Taking $f(a) = (a-1) \cdot [N \cdot (U_B - a{\cdot}\alpha) - R{\cdot}C]$ and computing the maximum value of $f(a)$ by letting $f'(a) = 0$ gives $a = (N{\cdot}U_B + R{\cdot}C + N{\cdot}\alpha)/(2\alpha N)$ and

$$f(a) = N(U_B - R{\cdot}C/N - \alpha)^2/(2\alpha). \tag{4.4}$$

Therefore, it follows from (4.2), (4.3) and (4.4) that, $\dot{W}(t_1) \leq 0$ since U_B satisfies

$$\frac{N \cdot U_B \cdot (U_B - \alpha) \cdot (U_B - R{\cdot}C/N - \alpha)^2}{2\alpha} = \frac{\alpha(1+\beta)}{2(1-\beta)K_p}, \tag{4.5}$$

which implies $W(t) \leq U_B$ for $t \geq 0$. □

If all AIMD flows are TCP-friendly, i.e., the average throughput of non-TCP-transported flows over a large time scale does not exceed that of any conformant TCP-transported ones under the same circumstance [47], the (α, β) pair should satisfies the TCP-friendly condition $\alpha = 3(1-\beta)/(1+\beta)$ derived in [12, 29]. Thus, the above equality (4.5) becomes

$$U_B \cdot (U_B - \alpha) \cdot (U_B - R{\cdot}C/N - \alpha)^2 = \frac{3\alpha}{NK_p}. \tag{4.6}$$

By the continuity property of $U_B \cdot (U_B - \alpha) \cdot (U_B - R{\cdot}C/N - \alpha)^2$ and the fact that the RHS of (4.5) is always greater than zero, we can conclude that the largest root of (4.5) must be greater than $R{\cdot}C/N + \alpha$, where $R{\cdot}C/N$ is the equilibrium value of the window size for AIMD/RED system. Therefore, the oscillation of the window size from its equilibrium value will increase with the increment of α and the decrement of K_p. In addition, the upper bound U_B itself will increase with the increment of $R{\cdot}C$, α and the decrement of N, K_p.

It is also noted that the upper bound derived in Theorem 4.1 is a global one for the time t, i.e., the window size $W(t)$ will not go above U_B for any $t > t_1$. If we assume, instead, that there exists $t_1' > t_1$ and $\Delta W > 0$, such that $W(t_1') = U_B + \Delta W$, then there must be some $\tau' \in (0,\ t_1' - t_1)$ such that $W(t_1' - \tau') = U_B$ and $\dot{W}(t_1' - \tau') > 0$. However, similar to the proof of Theorem 4.1, we have $\dot{W}(t_1' - \tau') \leq 0$, which is a contradiction. Therefore, the window size is upper bounded by U_B for any $t \geq 0$.

4.2.3 Lower Bound on Window Size and Upper Bound on Queue Length

In the previous subsection, we proved that the AIMD window size $W(t)$ is bounded from above, and an upper bound, U_B, is defined by (4.5). In this subsection, we show that the window size is also bounded from below while the queue length is upper bounded.

Theorem 4.2 *Define* $A := \frac{\alpha}{R} - \frac{2(1-\beta)}{1+\beta}\frac{{U_B}^2}{R}$ *and let* $L_{B1} > 0$ *be the root of*

$$L_{B1} \cdot (L_{B1} - AR) = \frac{\alpha(1+\beta)}{2(1-\beta)},$$

then $W(t) \geq L_{B1}$ *for* $t \geq 0$*.*

Proof: From Theorem 4.1, $W(t) \leq U_B$ for $t \geq 0$, which implies

$$\dot{W}(t) \geq \frac{\alpha}{R} - \frac{2(1-\beta)}{1+\beta}\frac{{U_B}^2}{R} =: A$$

It can be seen from the definition of U_B that $A < 0$. We show that $L_{B1} > 0$ is the lower bound of $W(t)$ for $t \geq 0$, i.e., if $W(t) = L_{B1}$ at time $t = t_2 \geq 0$, then $\dot{W}(t_2) \geq 0$.

Taking integration on both sides from $t_2 - R$ to t_2 gives $W(t_2 - R) \leq W(t_2) - AR = L_{B1} - AR$.

Since dropping/marking probability $p(t) = K_p \cdot q(t) \leq 1$ for all t, then $\dot{W}(t_2) \geq \frac{\alpha}{R} - \frac{2(1-\beta)}{1+\beta}\frac{L_{B1} \cdot (L_{B1} - AR)}{R}$. Therefore, $\dot{W}(t_2) \geq 0$ since L_{B1} satisfies

$$L_{B1} \cdot (L_{B1} - AR) = \frac{\alpha(1+\beta)}{2(1-\beta)}, \tag{4.7}$$

which implies $W(t) \geq L_{B1}$ for $t \geq 0$. □

Notice that L_{B1} in Theorem 4.2 is the lower bound of $W(t)$ for all $t \geq 0$, which is a global one. By similar analysis to the upper bound of window size U_B, it is easy to check that the window size $W(t)$ will not go below L_{B1} for any $t > t_2$. However, the value of L_{B1} is actually very small since $\alpha(1+\beta)/(2(1-\beta))$ is fairly small compared to $-AR$. Therefore, the global lower bound does not provide much information about the performance of AIMD/RED systems.

Since window size oscillates around its equilibrium in the steady state, the amplitude of the oscillation is more important than the global lower bound. Next, We will show the local lower bound of the window size after the first time it reaches the peak value at moment t_1. This local lower bound is more useful for understanding the performance of AIMD/RED systems.

Theorem 4.3 *Define T_1 and U_Q as*

$$T_1 = \frac{U_B - \frac{R \cdot C}{N}}{\frac{2(1-\beta)}{1+\beta} \cdot \frac{C \cdot K_p}{N} \cdot [\frac{R \cdot C}{N}\Delta q + \Delta W(q_0^* + \Delta q)]},$$

$$U_Q = \inf_{\substack{\Delta q > 0, \\ \Delta W \in [0, U_B - \frac{R \cdot C}{N}]}} \{(q_0^* + \Delta q) + (\frac{N}{R} \cdot U_B - C) \cdot (T_1 + R)\},$$

where U_B is defined in Theorem 4.1. Let $L_{B2} > 0$ satisfy

$$L_{B2} \cdot (L_{B2} + \frac{2(1-\beta)}{1+\beta} {U_B}^2 \cdot K_p \cdot U_Q - \alpha) \cdot K_p \cdot U_Q = \frac{\alpha(1+\beta)}{2(1-\beta)},$$

then $q(t) \leq U_Q$ *for* $t \geq 0$ *and* $W(t) \geq L_{B2}$ *for* $t \geq t_1$.

Proof: We first derive the upper bound of $q(t)$ for $t \geq 0$. At moment $t = t_1$, $W(t)$ reaches its peak value. To get a loose upper bound of $q(t)$, we introduce the comparison theorem [51]. Instead of following system (3.1), we consider its comparison system: $\dot{q}(t) = U_B/R - C$, and $W(t) \equiv U_B$ for $t \in [t_1, t_1']$. Notice that the solutions of the comparison system are larger than those of the original system, so the bounds derived in the following are also the bounds for system (3.1).

Assume that $W(t)$ does not decrease for some time after t_1, and thus $q(t)$ increases at the rate $\frac{N}{R}U_B - C$. Moment t_1' is chosen such that $q(t_1') = q^* + \Delta q$ with $\Delta q > 0$, then $W(t)$ decreases from t_1' while $q(t)$ keeps increasing till moment t_2 such that $\dot{q}(t_2) = 0$ (i.e., $W(t_2) = R{\cdot}C/N$). Therefore, $q(t_2)$ is the local maximum value of $q(t)$. It should be noticed that this estimate of $q(t)$ might be greater than the real maximum value of $q(t)$ since $W(t)$ may not stay at its peak value after t_1, and $q(t)$ will still increase after t_1, but with the rate less than $\frac{N}{R}U_B - C$.

From above analysis, for $t \in [t_1', \ t2]$, $\dot{q}(t) \leq \frac{N}{R} \cdot U_B - C$. Thus,

$$\int_{t_1'}^{t_2} \dot{q}(s)ds \leq (\frac{N}{R} \cdot U_B - C) \cdot (t_2 - t_1'),$$

which implies

$$\begin{aligned} q(t_2) &\leq q(t_1') + (\frac{N}{R} \cdot U_B - C) \cdot (t_2 - t_1') \\ &= (q_0^* + \Delta q) + (\frac{N}{R} \cdot U_B - C) \cdot (t_2 - t_1'). \end{aligned} \tag{4.8}$$

To estimate the length of the interval $[t_1',\ t_2]$, for $t \in [t_1' + R,\ t_2]$, it follows from the analysis above that

$$\begin{aligned} W(t) &\geq W(t_2) = \frac{R{\cdot}C}{N}, \\ q(t-R) &\geq q(t_1') = q_0^* + \Delta q, \\ W(t-R) &\geq W(t_2 - R) = \frac{R{\cdot}C}{N} + \Delta W, \end{aligned}$$

for some $\Delta q > 0$ and $\Delta W \in (0,\ U_B - \frac{R\cdot C}{N})$.

Thus,

$$\dot{W}(t) \leq -\frac{2(1-\beta)}{1+\beta} \cdot \frac{C{\cdot}K_p}{N} \cdot [\Delta W(q_0^* + \Delta q) + \frac{R{\cdot}C}{N}\Delta q] \tag{4.9}$$

for $t \in [t_1' + R,\ t_2]$.

On the other hand,

$$\int_{t_1'+R}^{t_2} \dot{W}(s)ds = W(t_2) - W(t_1' + R) \geq \frac{R{\cdot}C}{N} - U_B. \tag{4.10}$$

It follows from (4.9) and (4.10) that,

$$\begin{aligned} \frac{R{\cdot}C}{N} - U_B \leq -& \frac{2(1-\beta)}{1+\beta} \cdot \frac{C{\cdot}K_p}{N} \cdot (t_2 - t_1' - R) \\ & \cdot [\Delta W\,(q_0^* + \Delta q) + \frac{R{\cdot}C}{N}\,\Delta q], \end{aligned}$$

i.e.,

$$t_2 - t_1' - R \leq \frac{U_B - \frac{R{\cdot}C}{N}}{\frac{2(1-\beta)}{1+\beta} \cdot \frac{C{\cdot}K_p}{N} \cdot [\frac{R{\cdot}C}{N}\Delta q + \Delta W(q_0^* + \Delta q)]}.$$

With the definition of T_1 in the theorem, we have $t_2 - t_1' \leq T_1 + R$. Therefore, it follows from (4.8) that

$$q(t) \leq \inf_{\substack{\Delta q > 0, \\ \Delta W \in [0,\, U_B - \frac{R\cdot C}{N}]}} \{(q_0^* + \Delta q) + (\frac{N}{R} \cdot U_B - C) \cdot (T_1 + R)\}, \tag{4.11}$$

i.e., $q(t) \leq U_Q$ for $t \geq 0$, which indicates that U_Q is the upper bound of the RED queue length. Since the packet loss in a RED queue is proportional to the queue length, the derived queue length upper bound also reflects the upper bound of packet loss rate.

We finally show that $L_{B2} > 0$ is a lower bound of $W(t)$ for $t \geq t_1$, i.e., if $W(t) = L_{B2}$ at time $t = t_3 > t_1$, then $\dot{W}(t_3) \geq 0$.

With (4.5) and (4.11),

$$\dot{W}(t) \geq \frac{\alpha}{R} - \frac{2(1-\beta)}{1+\beta} \cdot \frac{{U_B}^2}{R} \cdot K_p \cdot U_Q \tag{4.12}$$

for $t \geq 0$, we have

$$\int_{t_3-R}^{t_3} \dot{W}(s)ds \geq \alpha - \frac{2(1-\beta)}{1+\beta} \cdot {U_B}^2 \cdot K_p \cdot U_Q,$$

i.e.,

$$W(t_3 - R) \leq L_{B2} + \frac{2(1-\beta)}{1+\beta} \cdot {U_B}^2 \cdot K_p \cdot U_Q - \alpha. \tag{4.13}$$

It follows from (4.13) that,

$$\dot{W}(t_3) \geq \frac{\alpha}{R} - \frac{2(1-\beta)}{1+\beta} \cdot \frac{L_{B2} \cdot U_W}{R} \cdot K_p \cdot U_Q$$

with $U_W := L_{B2} + \frac{2(1-\beta)}{1+\beta} \cdot {U_B}^2 \cdot K_p \cdot U_Q - \alpha$.

Thus, $\dot{W}(t_3) \geq 0$ if L_{B2} is chosen to satisfy

$$L_{B2} \cdot U_W \cdot K_p \cdot U_Q = \frac{\alpha(1+\beta)}{2(1-\beta)}, \tag{4.14}$$

and thus L_{B2} is the lower bound of $W(t)$ for $t \geq t_1$.

Therefore, the heterogeneous AIMD/RED system is practically stable with the bounds derived in Theorems 4.1 and 4.3. □

4.3 Bounds and Practical Stability of Heterogeneous AIMD/RED System

4.3.1 A Fluid-flow Model of Heterogeneous AIMD/RED System

In this section, we study the AIMD/RED system with heterogeneous flows, considering time delays. With the emergence of more and more heterogeneous traffics in the Internet, understanding the stability properties and bounds of the AIMD/RED system with heterogeneous flows is critical for future network planning and design.

We consider the case when there are two classes of flows with parameters ($\alpha_1,\ \beta_1$), ($\alpha_2,\ \beta_2$), time-invariant traffic loads $N_1,\ N_2$, respectively. We assume that all the flows have the same round-trip time (since variation of queuing delays becomes negligible compared to the round-trip delays, the effect of the delay jitter on the round-trip time is ignored and the round-trip time of each flow assumed to be a constant, $R(t) = \tau = R$). The model in this section can be extended to any certain number of flows in multiple classes with heterogeneous AIMD parameters and feedback delays.

Taking time delays into consideration, a heterogeneous AIMD/RED system shared by two classes of flows can be modeled as

$$\frac{dW_I(t)}{dt} = \frac{\alpha_1}{R} - \frac{2(1-\beta_1)}{1+\beta_1}\frac{W_I(t)W_I(t-R)}{R}K_p q(t-R),$$

$$\frac{dW_{II}(t)}{dt} = \frac{\alpha_2}{R} - \frac{2(1-\beta_2)}{1+\beta_2}\frac{W_{II}(t)W_{II}(t-R)}{R}K_p q(t-R),$$

$$\frac{dq(t)}{dt} = \begin{cases} \dfrac{N_1 W_I(t)}{R(t)} + \dfrac{N_2 W_{II}(t)}{R(t)} - C, & q > 0, \\ \\ \{\dfrac{N_1 W_I(t)}{R(t)} + \dfrac{N_2 W_{II}(t)}{R(t)} - C\}^+, & q = 0. \end{cases} \tag{4.15}$$

It is shown in [26] that $W_i(t)W_i(t{-}R)$ in (4.15) can be approximated by $W_i^2(t)$ for $i = I,\ II$ when the window size is much larger than one. We apply this approximation in following analysis for the convenience of computation.

For the heterogeneous system (4.15), the equilibrium point (W_I^*, W_{II}^*, q_0^*) is given by

$$W_I^*{=}\frac{GCR}{N_1G{+}N_2}, W_{II}^*{=}\frac{CR}{N_1G{+}N_2}, q_0^*{=}\frac{\alpha_1(1{+}\beta_1)}{2(1{-}\beta_1)W_I^{*2}K_p},$$

where $G{=}\sqrt{\frac{\alpha_1(1+\beta_1)(1-\beta_2)}{\alpha_2(1-\beta_1)(1+\beta_2)}}$.

The physical significance of studying the stability properties of the equilibrium point of AIMD/RED system is because the equilibrium point is the most desired operating point of the system. At the equilibrium, the total window size is $N_1W_I^* + N_2W_{II}^*$ and the total arrival rate equals the total link capacity, thus the link bandwidth is fully utilized.

In (4.15), we take $\bar{W}(t) = N_1{\cdot}W_I(t) + N_2{\cdot}W_{II}(t)$, $M_1 = \frac{(1-\beta_1)}{1+\beta_1}$, $M_2 = \frac{(1-\beta_2)}{1+\beta_2}$, $r_1 = M_1/N_1$, and $r_2 = M_2/N_2$, then

$$\begin{aligned} \dot{\bar{W}} &= (N_1\alpha_1 + N_2\alpha_2)/R \\ &- 2[r_1{\cdot}(N_1W_I)^2(t){+}r_2{\cdot}(N_2W_{II})^2(t)] \cdot K_p q(t-R)/R. \end{aligned} \tag{4.16}$$

Note that $W_i(t) \geq 0$ for $i = I,\ II$. Take $r_{min} = \min(r_1,\ r_2)$, and $r_{max} = \max(r_1,\ r_2)$, the following inequality can be obtained:

$$-2r_{max}\frac{\bar{W}^2(t)}{R} \leq \frac{\dot{\bar{W}}(t) - \frac{N_!\alpha_1+N_2\alpha_2}{R}}{K_p q(t{-}R)} \leq -r_{min}\frac{\bar{W}^2(t)}{R}. \tag{4.17}$$

Also, we have

$$\dot{q}(t) = \begin{cases} \bar{W}(t)/R - C, & q > 0, \\ \{\bar{W}(t)/R - C\}^+, & q = 0. \end{cases} \tag{4.18}$$

Thus, with the new variable pair $(\bar{W}(t),\ q(t))$, the original heterogeneous AIMD/RED system (4.15) can be rewritten by (4.16) and (4.18). We will study the properties of $(\bar{W}(t),\ q(t))$ in the following to show the practical stability and derive the bounds of the system.

Remark 2. Our focus in the analysis below is $\bar{W}(t)$, the total window size at t. This is because $\bar{W}(t)$ indicates the entire throughput of the heterogeneous AIMD/RED system, which is more useful than the throughput of each individual flow.

4.3.2 Upper Bound on Window Size

The bounds estimates of heterogeneous AIMD/RED system are given in the following.

Theorem 4.4 *Let $\bar{U}_B > 0$ be the largest real root of*

$$\bar{U}_B^2 \cdot [\bar{U}_B - R{\cdot}C - (N_1\alpha_1 + N_2\alpha_2)]^2 = \frac{4(N_1\alpha_1 + N_2\alpha_2)^2}{r_{min} \cdot K_p}, \tag{4.19}$$

then $\bar{W}(t) \leq \bar{U}_B$ for $t \geq 0$.

Proof: With (4.16), $\dot{\bar{W}}(t) \leq (N_1\alpha_1 + N_2\alpha_2)/R$ for $t \geq 0$. For $\tau > 0$, take integration on both sides from $t - \tau$ to t:

$$\bar{W}(t) - \bar{W}(t-\tau) \leq (N_1\alpha_1 + N_2\alpha_2) \cdot \tau / R. \tag{4.20}$$

We show that $\bar{U}_B > 0$ in the theorem is an upper bound of $\bar{W}(t)$ for $t \geq 0$, i.e., if $\bar{W}(t) = \bar{U}_B$ for some $t = \bar{t}_1 \geq 0$, then $\dot{\bar{W}}(\bar{t}_1) \leq 0$.

Integrating on both sides of (4.18) from $\bar{t}_1 - a \cdot R$ to $\bar{t}_1 - R$ for $a > 1$ gives

$$\int_{\bar{t}_1 - aR}^{\bar{t}_1 - R} \dot{q}(s) ds \quad \geq \quad \frac{1}{R} \int_{\bar{t}_1 - aR}^{\bar{t}_1 - R} \bar{W}(s) ds - (a-1) R \cdot C.$$

Note that (4.20) implies $\bar{W}(\bar{t}_1 - \tau) \geq \bar{U}_B - a \cdot (N_1\alpha_1 + N_2\alpha_2)$ when $\tau \in [R,\ aR]$. Thus,

$$q(\bar{t}_1 - R) \geq [\bar{U}_B - a \cdot (N_1\alpha_1 + N_2\alpha_2)] \cdot (a-1) - R \cdot C \cdot (a-1), \tag{4.21}$$

since $q(t) \geq 0$.

Taking $f(a) = (a-1) \cdot [\bar{U}_B - a \cdot (N_1\alpha_1 + N_2\alpha_2) - R \cdot C]$ and computing the maximum value of $f(a)$ by letting $f'(a) = 0$ gives

$$f(a) = [\bar{U}_B - R \cdot C - (N_1\alpha_1 + N_2\alpha_2)]^2 / [4(N_1\alpha_1 + N_2\alpha_2)], \tag{4.22}$$

with $a = [\bar{U}_B - R \cdot C + (N_1\alpha_1 + N_2\alpha_2)]/[2(N_1\alpha_1 + N_2\alpha_2)]$ and $f''(a) < 0$.

Therefore, it follows from (4.17), (4.21) and (4.22) that, $\dot{\bar{W}}(\bar{t}_1) \leq 0$ if $\bar{U}_B$ satisfies

$$\bar{U}_B^2 \cdot [\bar{U}_B - R \cdot C - (N_1\alpha_1 + N_2\alpha_2)]^2 = \frac{4(N_1\alpha_1 + N_2\alpha_2)^2}{r_{min} \cdot K_p}, \tag{4.23}$$

which implies $\bar{W}(t) \leq \bar{U}_B$ for $t \geq 0$.

It is also noted that the upper bound derived in here is global for the time t, i.e., the window size $\bar{W}(t)$ will not go above $\bar{U}_B$ for any $t > \bar{t}_1$. If we assume, instead, that there exists $\bar{t}_1' > \bar{t}_1$ and $\Delta W > 0$, such that $\bar{W}(\bar{t}_1') = \bar{U}_B + \Delta W$, there must be some $\tau' \in (0,\ \bar{t}_1' - \bar{t}_1)$ such that $\bar{W}(\bar{t}_1' - \tau') = \bar{U}_B$ and $\dot{\bar{W}}(\bar{t}_1' - \tau') > 0$. However, similar to the proof of Theorem 4.4, we have $\dot{\bar{W}}(\bar{t}_1' - \tau') \leq 0$, which is a contradiction. Therefore, the window size is upper bounded by $\bar{U}_B$ for all $t \geq 0$.

By the continuity property of $\bar{U}_B^2 \cdot [\bar{U}_B - R \cdot C - (N_1\alpha_1 + N_2\alpha_2)]^2$ and the fact that the RHS of (4.19) is always greater than zero, we can conclude that there exists at least one real root for (4.19) and the largest root must be greater than $R{\cdot}C{+}(N_1\alpha_1{+}N_2\alpha_2)$. Therefore, the upper bound $\bar{U}_B$ itself will increase with the increment of $R{\cdot}C$ and $(N_1\alpha_1 + N_2\alpha_2)$. In addition, the oscillation of the window size from its equilibrium value will increase with the increment of $N_1\alpha_1 + N_2\alpha_2$ and the decrement of K_p.

4.3.3 Lower Bound on Window Size and Upper Bound on Queue Length

We have showed that the AIMD window size $\bar{W}(t)$ is bounded by $\bar{U}_B$, which is defined by (4.19). In this subsection, we prove that the window size is lower bounded while the queue length is upper bounded.

Theorem 4.5 *Let* $\bar{L}_{B1} := (\frac{N_1\alpha_1+N_2\alpha_2}{2\cdot r_{max}})^{1/2}$*, then* $\bar{W}(t) \geq \bar{L}_{B1}$ *for* $t \geq 0$.

Proof: Showing that $\bar{L}_{B1} > 0$ is the lower bound of $\bar{W}(t)$ for $t \geq 0$, we should prove that if $\bar{W}(t) = \bar{L}_{B1}$ at time $t = \bar{t}_2 \geq 0$, then $\dot{\bar{W}}(\bar{t}_2) \geq 0$.

Since the dropping/marking probability $p(t) = K_p \cdot q \leq 1$ for all t, then

$$\begin{aligned}\dot{\bar{W}}(\bar{t}_2) &\geq \frac{N_1\alpha_1 + N_2\alpha_2}{R} - 2\cdot r_{max}\frac{\bar{W}^2(t)}{R}K_p q(t-R) \\ &\geq \frac{N_1\alpha_1 + N_2\alpha_2}{R} - 2\cdot r_{max}\frac{\bar{W}^2(t)}{R}.\end{aligned}$$

Therefore, $\dot{\bar{W}}(\bar{t}_2) \geq 0$ when $\bar{W}(t) = \bar{L}_{B1}$ with $\bar{L}_{B1}$ defined in the theorem, which implies $\bar{W}(t) \geq \bar{L}_{B1}$ for $t \geq 0$.

Notice that $\bar{L}B1$ in Theorem 4.5 is the lower bound of $\bar{W}(t)$ for all $t \geq 0$, which is a global bound. To show this, similar analysis to the upper bound of window size $\bar{U}_B$ can be applied to check that the window size $\bar{W}(t)$ will not go below $\bar{L}_{B1}$ for any $t > \bar{t}_2$. □

Note that $\bar{L}_{B1}$ in Theorem 4.5 is a global bound, but it does not provide much information about the system performance. This is because the value of $\bar{L}_{B1}$ is actually very small caused by the loose approximation of $K_p \cdot q$ and the fact that $(\alpha_i,\, \beta_i)$ pair are all small real numbers for $i{=}1,\ 2$. We next derive the upper bound of queue length and local lower bound of the window size after the first time it reaches the peak value at $\bar{t}_1$. The local lower bound is more useful for understanding the performance of the AIMD/RED system since window size oscillates around its equilibrium in the steady state, the amplitude of the oscillation is more important than the global lower bound.

Theorem 4.6 *Define $\bar{T}_1$ and $\bar{U}_Q$ as*

$$\bar{T}_1 := \frac{\bar{U}_B - R{\cdot}C}{r_{min} \cdot RC^2 \cdot K_p \cdot (q_0^*{+}\Delta q) - \dfrac{N_1\alpha_1 + N_2\alpha_2}{R}},$$

$$\bar{U}_Q{:=} \inf_{\Delta q > 0}\{(q_0^* + \Delta q) + (\frac{\bar{U}_B}{R} - C) \cdot (\bar{T}_1 + R)\},$$

where $\bar{U}_B$ is defined in Theorem 4.4. Let $\bar{L}_{B2} > 0$ satisfy

$$\bar{L}_{B2}^2 \cdot K_p \cdot \bar{U}_Q = \frac{N_1\alpha_1 + N_2\alpha_2}{2r_{max}}, \tag{4.24}$$

then $q(t) \leq \bar{U}_Q$ for $t \geq 0$ and $\bar{W}(t) \geq \bar{L}_{B2}$ for $t \geq \bar{t}_1$.

Proof: We first derive the upper bound of $q(t)$ for $t \geq 0$. Suppose that $\bar{W}(t)$ reaches its peak value at moment $t = \bar{t}_1$. To get a loose upper bound of $q(t)$, we introduce the comparison theorem [51]. Instead of following system (4.16) and (4.18), we consider its comparison system: $\dot{q}(t) = \bar{U}_B/R - C$, and $\bar{W}(t) \equiv \bar{U}_B$ for $t{\in}[\bar{t}_1,\, \bar{t}_1']$. Notice that the solutions of the comparison system are larger than those of the original system, so the bounds derived in the following are also the bounds for system (4.16) and (4.18).

Assume that $\bar{W}(t)$ does not decrease for some time after $\bar{t}_1$, and thus $q(t)$ increases at the rate of $\bar{U}_B/R - C$. $\bar{t}_1'$ is chosen such that $q(\bar{t}_1') = q^* + \Delta q$ with $\Delta q > 0$, then $\bar{W}(t)$ decreases from $\bar{t}_1'$ while $q(t)$ keeps increasing till $\bar{t}_2$ such that $\dot{q}(\bar{t}_2) = 0$ ($\bar{W}(\bar{t}_2) = RC$) with $\bar{t}_2 \geq \bar{t}_1' + R$. Therefore, $q(\bar{t}_2)$ is the local maximum value of $q(t)$. It should be noticed that this estimate of $q(t)$ might be greater than the real maximum value of $q(t)$ since $\bar{W}(t)$ may not stay at its peak value after $\bar{t}_1$, and $q(t)$ will still increase after $\bar{t}_1$, but with the rate less than $\bar{U}_B/R - C$.

From the above analysis, for $t \in [\bar{t}_1',\ t2]$, $\dot{q}(t) \leq \dfrac{\bar{U}_B}{R} - C$, which implies

$$\begin{aligned} q(\bar{t}_2) &\leq q(\bar{t}_1') + (\frac{\bar{U}_B}{R} - C) \cdot (\bar{t}_2 - \bar{t}_1') \\ &= (q_0^* + \Delta q) + (\frac{\bar{U}_B}{R} - C) \cdot (\bar{t}_2 - \bar{t}_1'). \end{aligned} \tag{4.25}$$

To estimate the length of the interval $[\bar{t}_1',\ \bar{t}_2]$, for $t \in [\bar{t}_1' + R,\ \bar{t}_2]$, it follows from the analysis above that

$$\begin{aligned} \bar{W}(t) &\geq \bar{W}(\bar{t}_2) = RC, \\ q(t-R) &\geq q(\bar{t}_1') = q_0^* + \Delta q, \end{aligned}$$

for some $\Delta q > 0$.

Thus,

$$\dot{\bar{W}}(t) \leq \frac{N_1\alpha_1 + N_2\alpha_2}{R} - r_{min} \cdot \frac{(RC)^2}{R} \cdot K_p \cdot (q_0^* + \Delta q), \tag{4.26}$$

for $t \in [\bar{t}_1' + R,\ \bar{t}_2]$.

On the other hand,

$$\int_{\bar{t}_1'+R}^{\bar{t}_2} \dot{\bar{W}}(s)ds = \bar{W}(\bar{t}_2) - \bar{W}(\bar{t}_1' + R) \geq RC - \bar{U}_B. \tag{4.27}$$

It follows from (4.26) and (4.27) that,

$$\begin{aligned} RC-\bar{U}_B &\leq [(N_1\alpha_1 + N_2\alpha_2)/R - r_{min}\cdot RC^2\cdot K_p\cdot(q_0^*+\Delta q)] \\ &\quad \cdot(\bar{t}_2 - \bar{t}_1' - R), \end{aligned}$$

i.e.,

$$\bar{t}_2-\bar{t}_1'-R \leq \frac{\bar{U}_B - RC}{r_{min}RC^2K_p(q_0^*+\Delta q) - (N_1\alpha_1 + N_2\alpha_2)/R}.$$

With the definition of $\bar{T}_1$ in the theorem, we have $\bar{t}_2 - \bar{t}_1' \leq \bar{T}_1 + R$. Therefore, it follows from (4.25) that

$$q(t) \leq \inf_{\Delta q>0}\{(q_0^* + \Delta q) + (\frac{\bar{U}_B}{R} - C)\cdot(\bar{T}_1 + R)\}, \tag{4.28}$$

i.e., $q(t) \leq \bar{U}_Q$ for $t \geq 0$, which indicates that $\bar{U}_Q$ is the upper bound of the RED queue length. Since the packet loss in a RED queue is proportional to the queue length, the derived queue length upper bound also reflects the maximum packet loss rate.

We finally show that $\bar{L}_{B2} > 0$ is a lower bound of $\bar{W}(t)$ for $t \geq \bar{t}_1$, i.e., if $\bar{W}(t) = \bar{L}_{B2}$ at time $t = \bar{t}_3 > \bar{t}_1$, then $\dot{\bar{W}}(\bar{t}_3) \geq 0$.

With (4.17) and (4.28),

$$\dot{\bar{W}}(\bar{t}_3) \geq \frac{N_1\alpha_1 + N_2\alpha_2}{R} - 2r_{max}\cdot\frac{\bar{L}_{B2}^2}{R}\cdot K_p\cdot\bar{U}_Q.$$

Thus, $\dot{\bar{W}}(\bar{t}_3) \geq 0$ if $\bar{L}_{B2}$ is chosen to satisfy (4.24). Therefore, $\bar{L}_{B2}$ is the lower bound of $\bar{W}(t)$ for $t \geq \bar{t}_1$. □

Therefore, the heterogeneous AIMD/RED system is practically stable with the bounds derived in Theorems 4.4 and 4.6.

*Remark 3.*The approach applied in this section can also be extended to obtain the theoretical bounds for the AIMD/RED system when it is shared by more than two classes of flows. Details are omitted here due to space limit.

(α, β)	(9/5, 1/4)		(1, 1/2)		(3/7, 3/4)		(1/5, 7/8)		(3/31, 15/16)	
	Num	**Ana**	**Num**	**Ana**	**Num**	**Ana**	**Num**	**Ana**	**Num**	**Ana**
$W_{\max}$	12.22	12.44	11.33	11.50	10.65	10.76	10.36	10.43	10.21	10.26
$W_{\min}$	1.06	0.06	3.23	0.26	6.87	1.28	8.68	2.90	9.42	3.58
$Q_{\max}$	24.70	39.20	17.30	26.50	10.95	17.70	7.70	12.80	5.88	10.10

Table 4.1: Bounds with different (α, β)

4.4 Performance Evaluation

In this section, numerical results with Matlab and simulation results with NS-2 [60] are given to validate the theorems and evaluate how the system performance is affected by different parameters.

4.4.1 AIMD Parameter Pairs of Homogeneous Flows

First, we investigate how the AIMD parameter pair (α, β) affects the bounds of window size and queue length. Let N, R, C and K_p be constants: $N = 10, R = 0.1$ sec, $C = 1000$ packet/sec and $K_p = 0.01$. The AIMD (α, β) pairs are chosen to be TCP-friendly, varying from $(9/5, 1/4)$ to $(3/31, 15/16)$, and the results are given in Table 4.1 and Fig. 4.1. It can be seen that for the upper and lower bounds of the window size and the upper bound of the queue length, the numerical results are all within the bounds given by Theorem 4.1 and Theorem 4.3, which verifies the correctness of the Theorems. In addition, the upper bound of the window size given by the Theorem is very tight. The

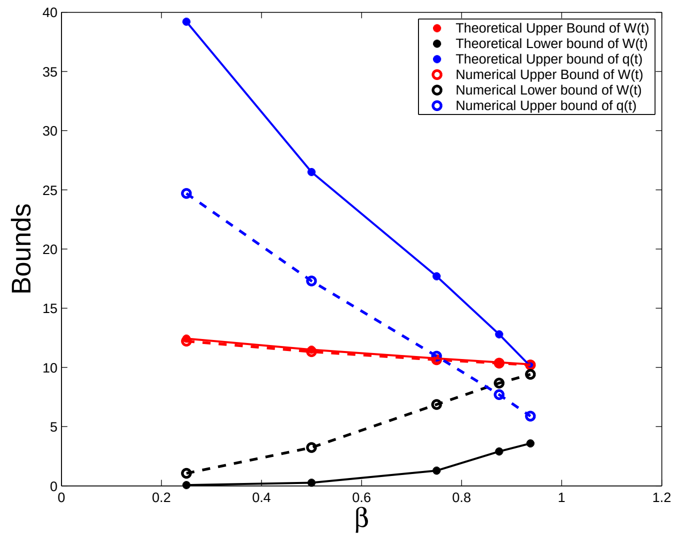

Figure 4.1: Bounds of window size and queue length with different $(\alpha,\ \beta)$

one for queue length is a loose bound as mentioned in the proof of Theorem 4.3. The theoretical lower bound of window size is also a loose bound because of the approximation of $\dot{W}(t)$. How to find a tight lower bound for window size will be a future research issue.

Another observation is that the differences between numerical and theoretical results is getting smaller as $(\alpha,\ \beta)$ pair varies from ($9/5, 1/4$) to ($3/31, 15/16$), which shows that the theoretical results become tighter when the value of β gets larger.

In ideal cases, the window size should converge to $R{\cdot}C/N$, which is 10 packets per RTT in the above cases. The results in Table 4.1 and Fig. 4.1 show that with a smaller value of α and a larger value of β, the AIMD flows have less oscillation amplitude around the optimal operation point, so they can utilize network resources more efficiently with less delay and loss in steady state. This is because, with a smaller value of α, the AIMD flows overshoot the available bandwidth in a slower pace; with a larger value of β, the

AIMD flows will not decrease drastically for any single packet loss. Also, as shown in Fig. 4.1, the upper bound of the queue length becomes smaller w.r.t. β; thus, the average queueing delay (and thus loss rate) becomes smaller in steady state.

Fig. 4.3 shows the traces of TCP flows with AIMD parameter pair of $(1, 1/2)$ and those of AIMD($1/5, 7/8$) flows. Here, N=10, C=10000 packet/sec, R=0.05 sec and K_p=0.005. For NS-2 simulations, we set $Q_{\min}$ of the RED queue to be 20 packets. Therefore, the upper bound of window size of each flow should be enlarged by $Q_{\min}/N = 2$ packets, and the upper bound of the queue length should be enlarged by $Q_{\min} = 20$ packets. We compare the theoretical bounds with both the average window size among all flows and its time average of window size over a round. Both the numerical results with Matlab and simulation results with NS-2 show that although the window variation of AIMD($1/5, 7/8$) in steady state is smaller, it takes longer time for AIMD($1/5, 7/8$) flows to converge to the steady state. The oscillations of the average window size and queue length with Matlab are bigger than those with NS-2, because $RTTs$ are set as constants in the Matlab results (which is the same as the assumptions of bounds estimates theorems in the chapter), while $RTTs$ are time varying in NS-2. This difference in the system oscillations is consistent with the conclusions in [48] which reveals that the variable nature of RTT helps to stabilize the AIMD/RED system. Simulation results also demonstrate the tightness of the upper bound of window size. Another interesting observation is that although the upper bound of queue length is not tight comparing to the time average of queue length, it is close to the maximum instantaneous queue length in steady state. The average window size in the NS-2 simulation results are slightly larger than the numerical results, because the numerical results simulations with Malab ignore the queuing delay in $RTTs$, which slightly underestimates the window size.

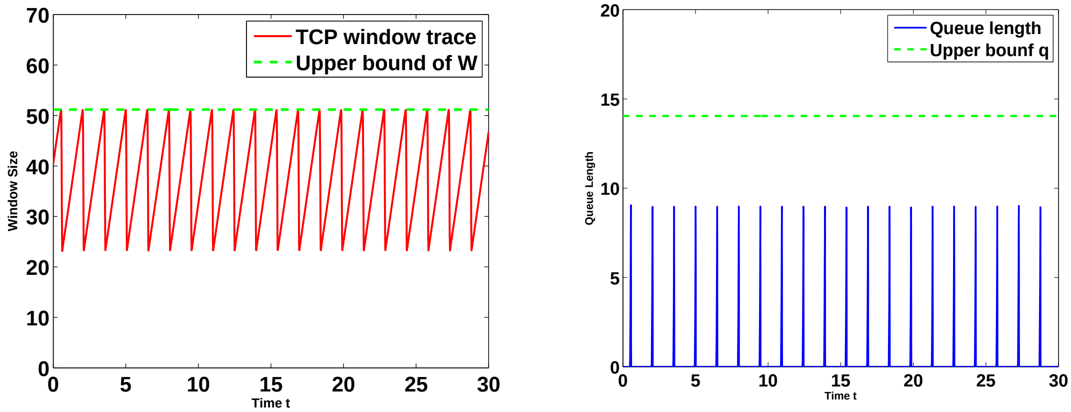

TCP flows (Matlab)

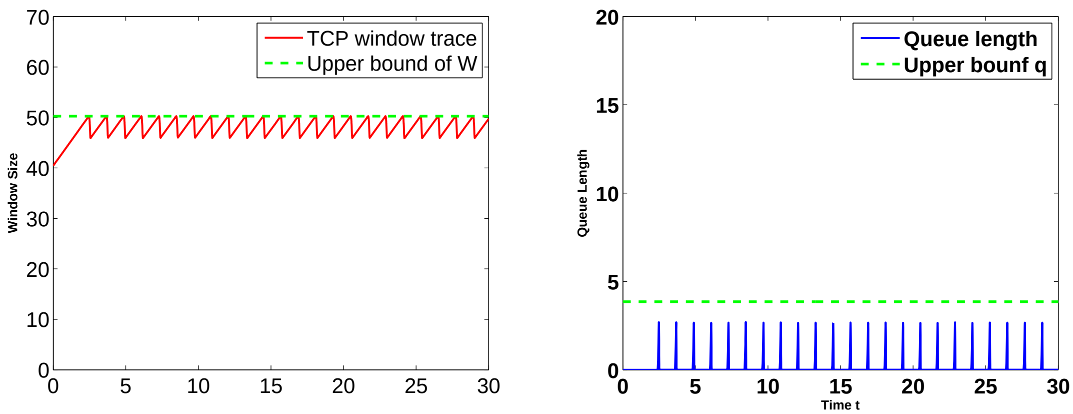

small AIMD$(1/5, 7/8)$ flows (Matlab)

Figure 4.2: Bounds of window size and queue length,

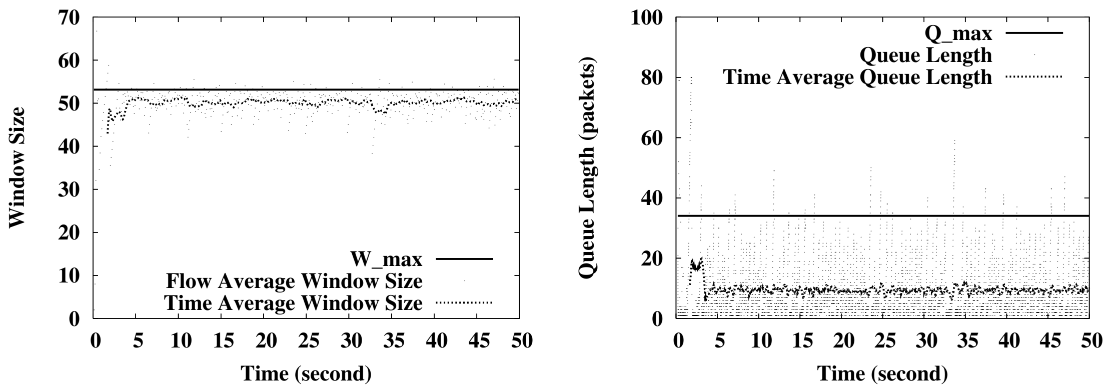

TCP flows (NS-2)

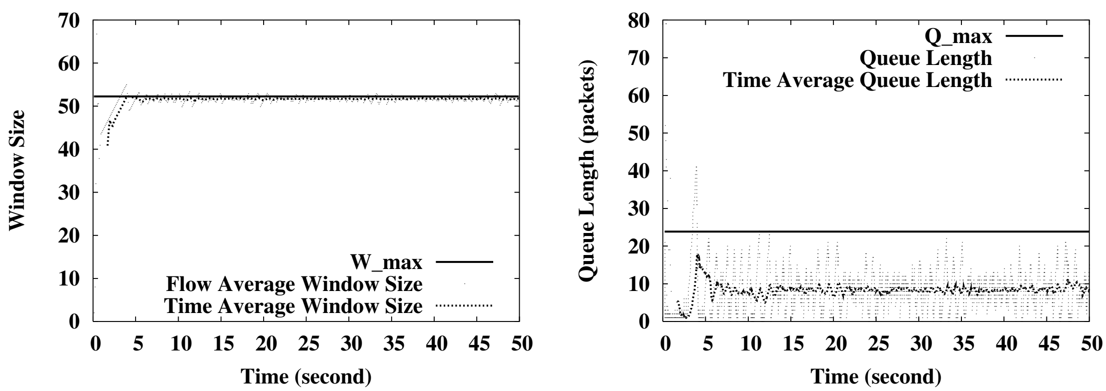

AIMD($1/5$, $7/8$) flows (NS-2)

Figure 4.3: Bounds of window size and queue length,

4.4.2 Impact of System Parameters: Homogeneous Flows

In the following, we study how the parameters N, R, C and K_p affect the bounds of window size and queue length. We choose (α, β) pair to be $(1, 1/2)$ and $(1/5, 7/8)$, and obtain the results with different network parameters as shown in Tables 4.2 and 4.3.

Round-trip delay and link capacity

First, comparing rows 1 and 2 in both tables. By enlarging the delay from 0.02 sec to 0.05 sec (by 2.5 times), the upper bound of window sizes only increases by 1.54 times and 1.86 times for TCP and AIMD($1/5, /, 7/8$), respectively, which means a larger delay reduces the relative oscillation amplitude of window size. In addition, the upper bound of queue length is decreasing. Similar trend can be found if comparing rows 4 and 5 in both tables. This is a surprising result. From [9], a longer delay may drive the system from stable to unstable. We can explain it as follows. A larger delay means that the window size increasing speed (in terms of packet per second) during the additive increase period is smaller, and the AIMD flows will overshoot the network capacity in a slower pace; thus, the upper bound of window size is closer to the optimal operating point, and the maximum queue length is smaller. Similar results are found if we compare rows 4 and 6 in both tables. By enlarging the link capacity by 10 times, the upper bound of window size is increased by 7.5 and 8.9 times, for TCP and AIMD ($1/5, /, 7/8$), respectively. Although enlarging the link capacity may drive the system from stable to unstable [9], the oscillating amplitude of window size (relative to the equilibrium W^*) and queue length will actually decrease. The window and queue traces of 10 TCP flows in a link with 1000 packet/sec and $10,000$ packet/sec are depicted in Fig. 4.5. The conclusion is that larger values of delay and link capacity will actually reduce the oscillating amplitude

No.	N	R	C	K_p	(W^*, q^*)	U_B		L_{B2}		U_Q	
						Num	**Ana**	**Num**	**Ana**	**Num**	**Ana**
1	10	0.02	1000	0.01	(2, 37.5)	4.04	4.41	1.52	0.09	51.25	147.50
2	10	0.05	1000	0.01	(5, 6)	6.60	6.80	2.13	0.32	28.15	43.30
3	20	0.05	2000	0.005	(5, 12)	6.60	6.80	2.12	0.38	56.34	78.0
4	10	0.05	1000	0.005	(5, 12)	6.82	7.10	2.78	0.66	39.10	54.60
5	10	0.4	1000	0.005	(40, 3/16)	41.30	42.02	14.14	0.11	9.85	23.2
6	10	0.05	10,000	0.005	(50, 3/25)	51.09	51.15	23.22	0.18	8.35	14.05
7	20	0.05	20,000	0.005	(50, 3/25)	51.00	51.20	8.91	0.068	14.89	23.12
8	100	0.05	10,000	0.005	(5, 12)	6.28	6.41	0.72	0.04	153.16	241.6
9	1000	0.1	1,000,000	0.001	(100, 3/20)	101.00	101.02	0.026	0.0002	576.95	1024.15
10	10000	0.1	1,000,000	0.001	(10, 15)	11.04	11.05	0.02	$1.6*10^{-4}$	6731.3	10785.0
11	10000	0.1	1,000,000	0.005	(10, 3)	11.017	11.023	0.005	$6.9*10^{-6}$	5941.6.5	10349.4
12	10000	0.1	1,000,000	0.01	(10, 3/2)	11.011	11.016	0.002	$1.8*10^{-6}$	5713.5	10247.9

Table 4.2: AIMD/RED system bounds with $(\alpha,\ \beta)$=$(1,\ 1/2)$

No.	N	R	C	K_p	(W^*, q^*)	U_B		L_{B2}		U_Q	
						Num	**Ana**	**Num**	**Ana**	**Num**	**Ana**
1	10	0.02	1000	0.01	(2, 37.5)	2.81	3.03	1.76	0.59	55.39	135.50
2	10	0.05	1000	0.01	(5, 6)	5.50	5.63	4.19	1.77	17.64	31.20
3	20	0.05	2000	0.005	(5, 12)	5.51	5.65	4.19	1.65	35.3	65.2
4	10	0.05	1000	0.005	(5, 12)	5.62	5.80	4.27	2.10	29.13	48.70
5	10	0.4	1000	0.005	(40, 3/16)	40.25	40.29	36.79	5.38	3.10	5.21
6	10	0.05	10,000	0.005	(50, 3/25)	50.23	50.26	45.93	6.31	2.48	3.85
7	20	0.05	20,000	0.005	(50, 3/25)	50.23	50.26	43.99	3.24	4.28	7.10
8	100	0.05	10,000	0.005	(5, 12)	5.34	5.46	3.76	1.39	66.59	83.8
9	1000	0.1	1,000,000	0.001	(100, 3/20)	100.20	100.21	39.26	0.025	127.34	211.15
10	10000	0.1	1,000,000	0.001	(10, 15)	10.22	10.23	2.02	0.02	1666.5	2361.4
11	10000	0.1	1,000,000	0.005	(10, 3)	10.208	10.211	0.07	0.00097	1354.8	2158.8
12	10000	0.1	1,000,000	0.01	(10, 3/2)	10.205	10.207	0.015	0.00024	1265.7	2111.5

Table 4.3: AIMD/RED system bounds with $(\alpha,\ \beta)$=$(1/5,\ 7/8)$

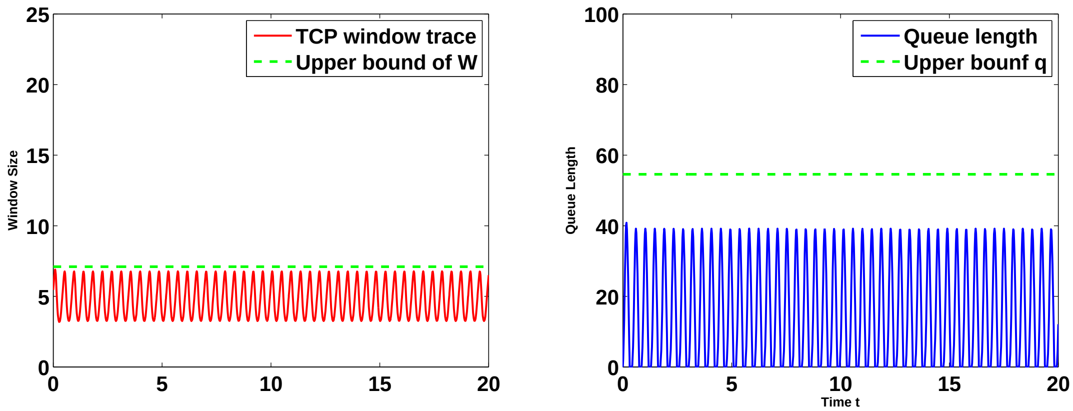

$C = 1000$ packet/sec (Matlab)

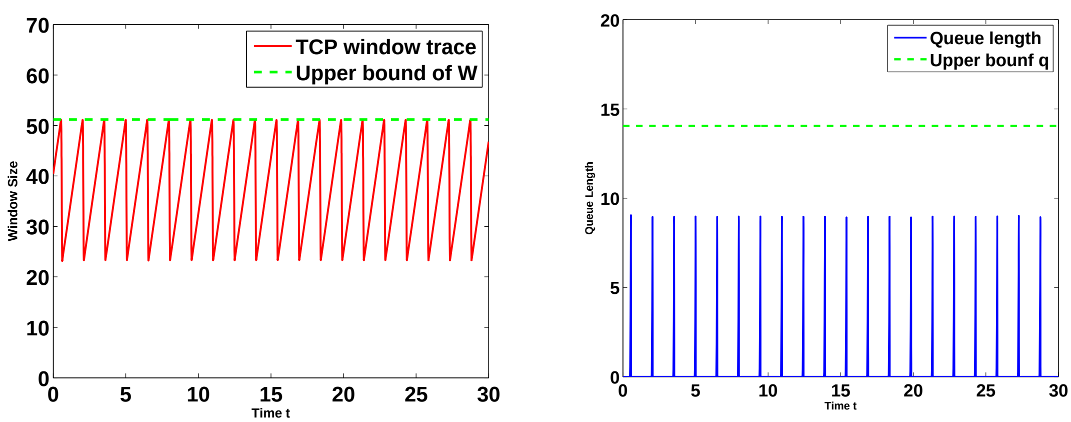

$C = 10,000$ packet/sec (Matlab)

Figure 4.4: Bounds of TCP window size and queue length with different C

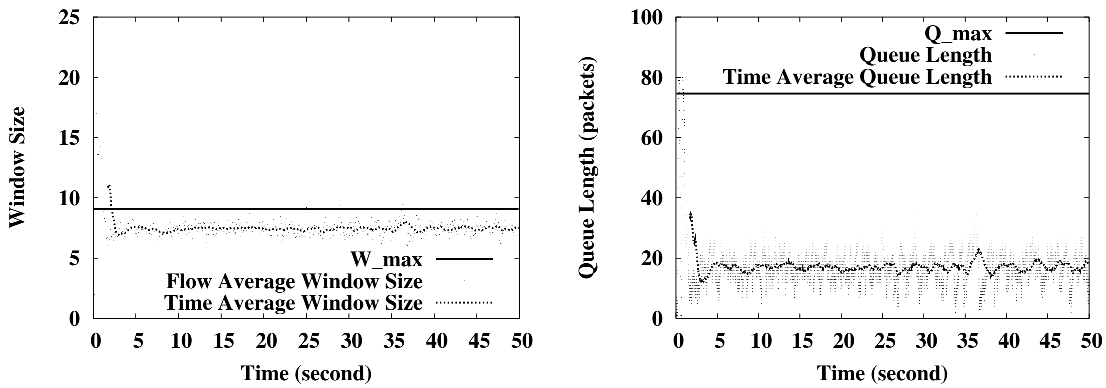

$C = 1000$ packet/sec (NS-2)

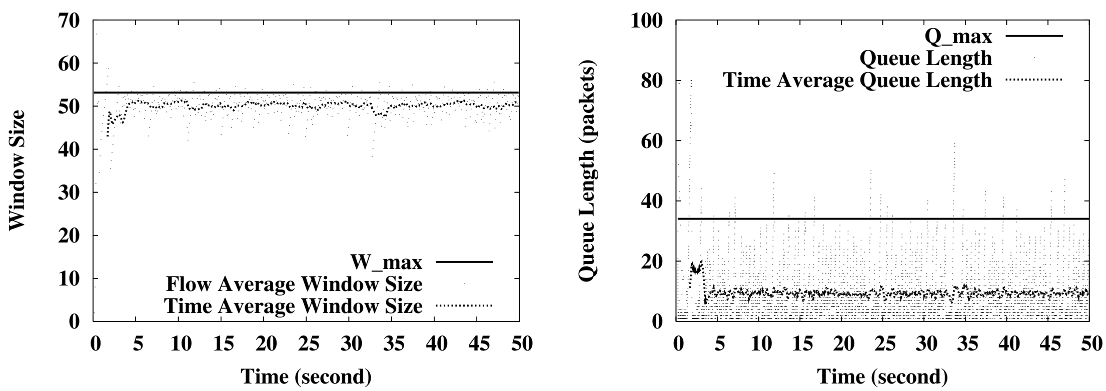

$C = 10,000$ packet/sec(NS-2)

Figure 4.5: Bounds of TCP window size and queue length with different C

of window size and queue length, and significantly reduce the maximum queueing delay.

Number of flows

Comparing rows 3 and 4, or rows 6 and 7 in Tables 4.2 and 4.3, we conclude that if we increase the number of flows and the link capacity proportionally, the bounds of window size are almost un-affected. With twice the flows multiplexed in a twice capacity link, the upper bound of queue length increases less than twice. Therefore, the queuing delay bound is slightly reduced because of the multiplexing gain.

Comparing rows 6 and 8 in Tables 4.2 and 4.3, if we increase the number of flows in the same link, the $N \cdot U_B$ becomes larger. In other words, the oscillation of window size will increase significantly if the number of flows in a link increases, and the queueing delay will also increase significantly. This can be understood as N AIMD(α, β) flows will increase their windows by $N\alpha$ packets per RTT, and the larger the increasing rate during Additive Increase stage, the more significantly the flows will overshoot the link capacity. This suggests that we should limit the number of TCP/AIMD connections in a link or promote to use more conservative AIMD parameter pairs to ensure that the queueing delay (and also the loss rate) is less than certain threshold.

Marking/Dropping parameter K_p

Comparing rows 2 and 4 in Tables 4.2 and 4.3, for a smaller value of K_p, the RED parameter will result in a larger bounds of both window size and queue length.

The last four rows of Tables 4.2 and 4.3 are the upper bounds of the TCP/AIMD window size and queueing delay in a highly multiplexed, high bandwidth (tens of Gbps), and long delay (0.1 sec RTT) link. It can be seen for TCP flows, the queuing delay can be bounded to 10.785 ms if the K_p is chosen to be 0.001. The delay bound can be slightly reduced to 10.349 ms and 10.248 ms if K_p is increased to 0.005 and 0.01, respectively. The results show that although K_p can be adjusted to control the queueing delay in the system, the impact is limited for high bandwidth cases. Limiting the number of flows or using more conservative AIMD pairs are more effective in reducing queueing delay. For instance, if the number of flows is reduced to 100 or 1000, the queueing delay bound can be reduced to 0.241 ms or 1.079 ms, respectively. If using an AIMD parameter pair of ($1/5$, $7/8$), the queueing delay for 10000 flows with $K_p = 0.001$ can be bounded to 2.361 ms only.

4.4.3 Impact of System Parameters: Heterogeneous Flows

Considering that the Internet might contain mixed traffic with different AIMD parameters, we further study the performance of the AIMD/RED system with heterogeneous flows. Parameters are firstly chosen as C=$10,000$ packet/sec, K_p=0.005, and $R = 0.05$ sec for 5 TCP flows competing with 5 AIMD($1/5$, $7/8$) flows. For comparison, we also choose C=20000 packet/sec, K_p=0.005, and $R = 0.05$ sec for 10 TCP flows and 10 AIMD($1/5$, $7/8$) flows.

For the case of 5 TCP flows competing with 5 AIMD($1/5$, $7/8$) flows, the upper bound of $N_1W_I + N_2W_{II}$ is 508.9 packets, the lower bound $\bar{L}_{B2}$ is 28.28 packets, and the upper bound of the queue length is 10.2 packets. For the case of 10 TCP flows competing with 10 AIMD($1/5$, $7/8$) flows, the upper bound of $N_1W_I + N_2W_{II}$ is 1016.1 packets, the lower bound $\bar{L}_{B2}$ is 55.80 packets, and the upper bound of queue length is 19.6 packets. In the NS-2 simulations, since the RED threshold $\min_{th}$ is set to 20 packets, the upper

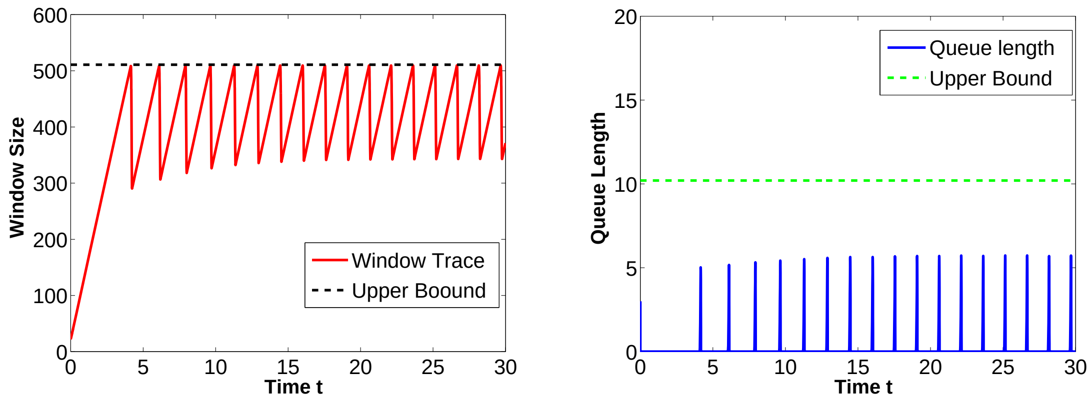

5 TCP vs. 5 AIMD flows, C=$10,000$ pac/sec (Matlab)

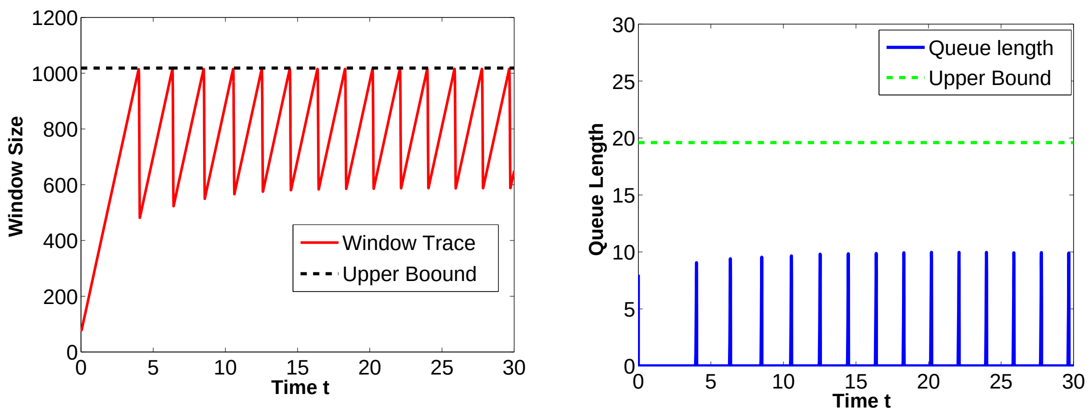

10 TCP vs. 10 AIMD flows, C=$20,000$ pac/sec (Matlab)

Figure 4.6: Bounds of Heterogeneous flows, K_p=0.005, $R = 0.05$ sec

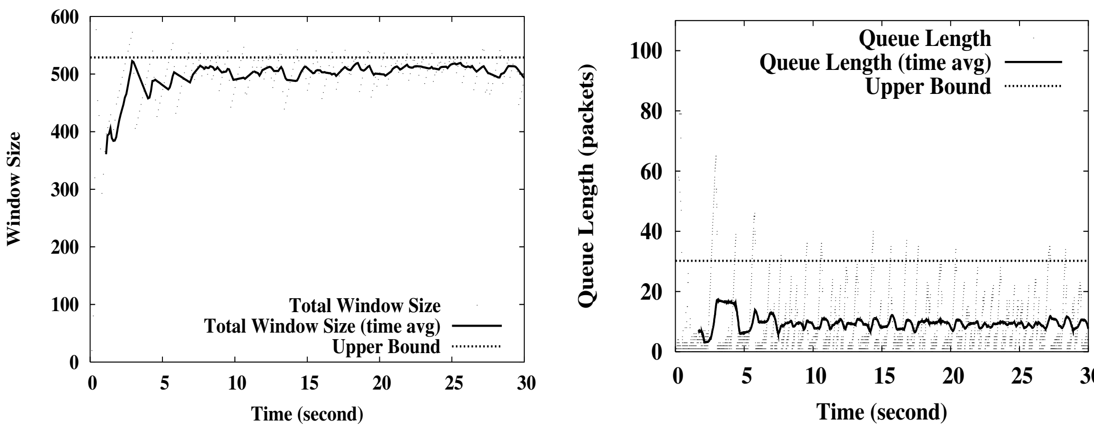

5 TCP vs. 5 AIMD flows, C=$10,000$ pac/sec (NS-2)

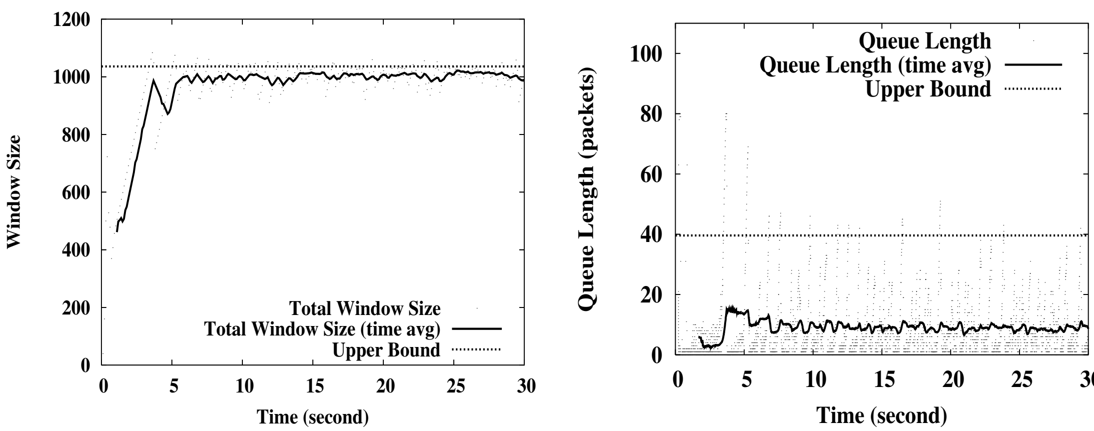

10 TCP vs. 10 AIMD flows, C=$20,000$ pac/sec (NS-2)

Figure 4.7: Bounds of Heterogeneous flows, K_p=0.005, $R = 0.05$ sec

bounds of total window size and queue length are enlarged by 20 packets accordingly. For the simulation results, we compare the theoretical bounds with both the total window size of all flows and its time average over a round. The correctness of our theoretical bounds and the tightness of the upper bound of window size are demonstrated by the numerical and simulation results, as shown in Fig. 4.7. The average window sizes in the NS-2 simulation results are slightly larger than the numerical results. This is because the numerical simulations with Matlab ignore the queuing delays in RTT, which may under-estimates the window size. It is also observed from Fig. 4.7 that, if the number of flows and the link capacity are increased proportionally, the upper bound of per-flow window size is closer to its optimal value. With both the number of flows and the link capacity being doubled, the upper bound of the queue length is less than twice of the previous bound. Therefore, the queuing delay bound is slightly reduced because of the multiplexing gain. An interesting conclusion is that although the increase of link capacity may cause an AIMD/RED system to become asymptotically unstable [9], the system queuing delay has lower bound and the upper bound of flows window size is closer to the optimal operating point. This result demonstrates the importance of studying practical stability and bounds of the AIMD/RED system.

Fig. 4.9 shows the window trace and queue length when 20 TCP flows share the bottleneck with 40 AIMD($1/5$, $7/8$) flows with K_p=0.005 and K_p=0.001, respectively. For the case of K_p=0.005, the upper bound of $N_1W_I + N_2W_{II}$ is 3034.4 packets and the upper bounds of queue length is 43.1 packets; while for the case of K_p=0.001, the upper bound of $N_1W_I + N_2W_{II}$ is 3042.4 packets and the upper bounds of queue length is 60.7 packets. It can be seen that a smaller value of K_p results in a slightly larger bounds on both window size and queue length. This observation is consistent with our analysis in subsection. However, in the case of higher bandwidth, the impact of K_p is less. Similar results are shoed with homogeneous AIMD flows.

4.5 Related Work

Control Problems arising in the Internet congestion have received wide attention recently [7, 9, 23, 26]. For delay-free marking scheme, the fluid-model of the AIMD/RED system has been proved to be asymptotically stable [29] by applying the method of Lyapunov function. It is well known [9] that the system may become asymptotically unstable in the presence of time delays. In [27], sufficient conditions for the asymptotic stability of AIMD/RED system with feedback delays are given in terms of linear matrix inequalities. However, simulation results show that even though the system is not asymptotically stable, it oscillates around the steady state periodically. Motivated by this phenomenon, we present performance bounds of the AIMD/RED system in this chapter and demonstrate that the delayed AIMD/RED system is bounded from above and below.

Different from many previous work [7, 9, 23, 26, 27] on the sufficient conditions for the asymptotic stability of AIMD/RED or other network control systems, in this chapter, we study the practical stability of the AIMD/RED system, and derive its theoretical bounds in both homogeneous-flow and heterogeneous-flow cases, i.e., flows' congestion window size and intermediate systems' queue length, given the number of flows sharing the link, their AIMD parameter pairs and round-trip times, link capacity, and RED queue parameters. Since the bounds are closely related to system performance, our results provide important insights for in-depth understanding of the whole system.

The boundedness issue has been studied in [43, 44, 45] without giving the bounds

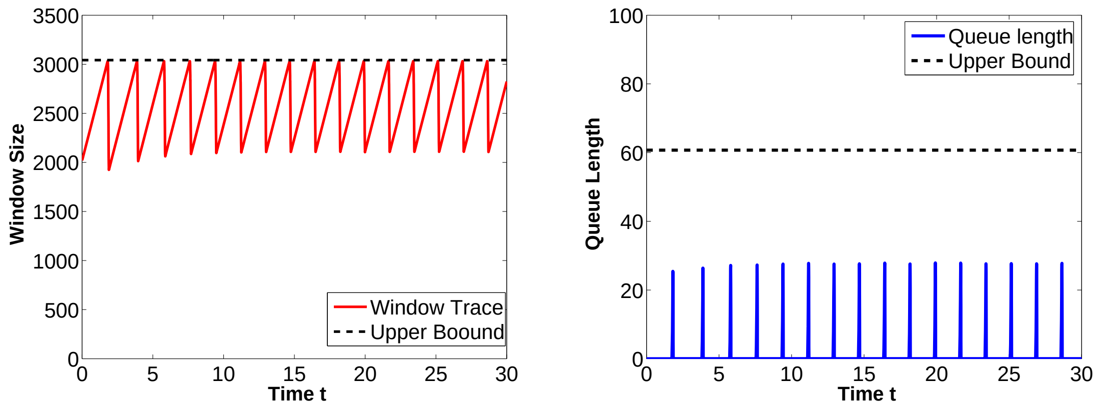

20 TCP vs. 40 AIMD flows, $K_p = 0.001$ (Matlab)

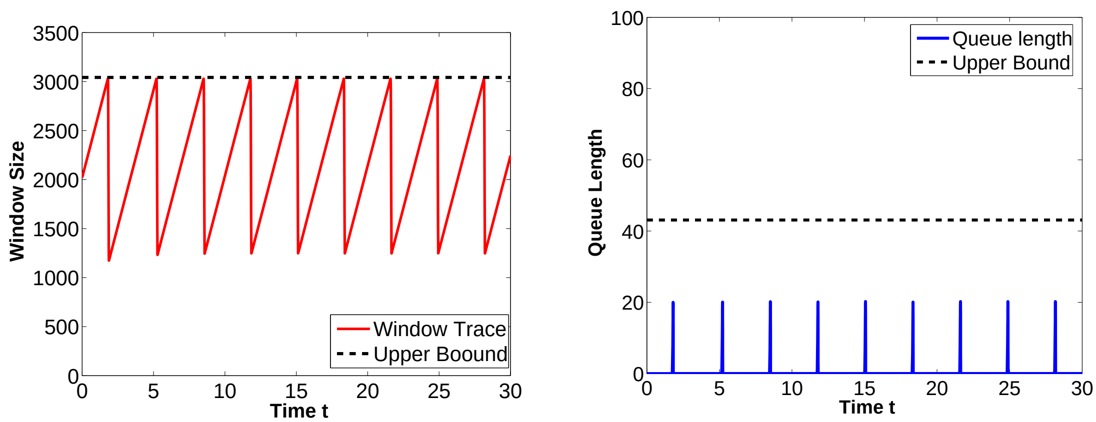

20 TCP vs. 40 AIMD flows, $K_p = 0.005$ (Matlab)

Figure 4.8: Bounds of Heterogeneous flows, C=$60,000$ packet/sec, $R = 0.05$ sec

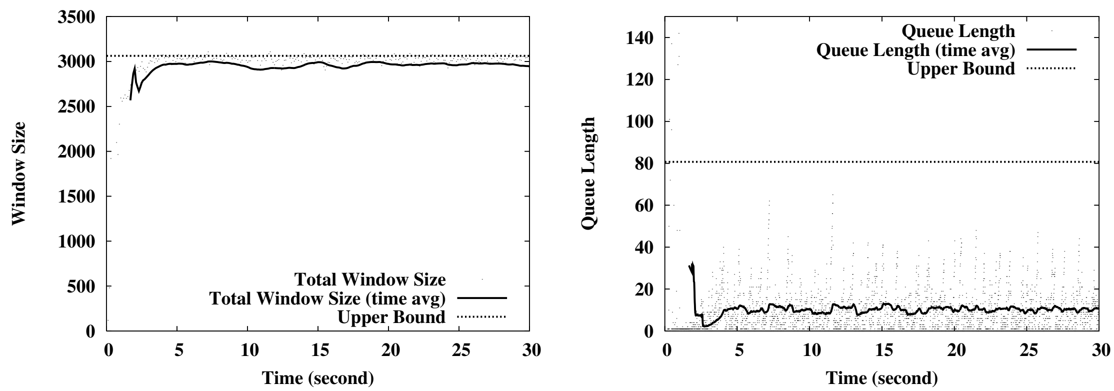

20 TCP vs. 40 AIMD flows, $K_p = 0.001$ (NS-2)

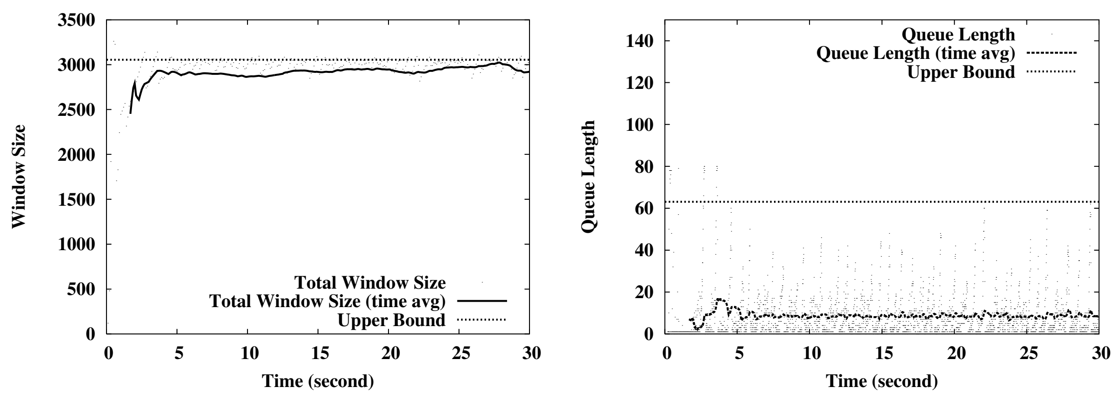

20 TCP vs. 40 AIMD flows, $K_p = 0.005$ (NS-2)

Figure 4.9: Bounds of Heterogeneous flows, $C{=}60,000$ packet/sec, $R = 0.05$ sec

estimates, by applying Lyapunov-like method for some TCP-like congestion control algorithms. [46] justified the use of deterministic model for Internet congestion control and [42] gave the upper bound on the transmission rate for two kinds of TCP-like traffic. However, to the best of our knowledge, the theoretical upper and lower bounds of window size and queue length of AIMD/RED system with homogeneous and heterogeneous flows considering feedback delays have not been reported in the literature.

4.6 Summary

In this chapter, we have studied the practical stability of the AIMD/RED system by deriving theoretical bounds of window size and queue length of the AIMD/RED system for both homogeneous and heterogeneous cases. The theoretical results obtained in the chapter can provide important insights and guidelines for setting up parameters for the AIMD/RED system in order to maintain network stability and to fully utilize network resources without excessive delay and loss. The simulation results given in the chapter can also help to predict and control the system performance for the Internet with higher data rate links multiplexed with more flows with different parameters. Our main findings are 1) larger values of delay and link capacity will actually reduce the oscillating amplitude of window size and queue length from their equilibrium in steady state; 2) although AIMD flows can adapt their sending rates according to available bandwidth, larger number of flows leads to longer queueing delay in the AIMD/RED system. Thus, we should limit the number of AIMD connections in a link or promote to use more conservative AIMD parameters to bound the queueing delay and loss; and 3) if we proportionally increase the link capacity and number of TCP/AIMD flows, the queueing delay will be slightly reduced, so the multiplexing gain slightly increases. Thus, AIMD/RED should be suitable in the Internet with higher bandwidth and heterogeneous flows.

There are many interesting research issues worth further investigation: a) how to deploy effective admission control for TCP/AIMD flows to bound delay and loss; b) how to adapt AIMD parameter pair to ensure that the system can converge to the equilibrium quick enough and to control the queueing delay and loss in the network; and c) how to extend the work to heterogeneous flows with different $RTTs$ and multiple bottleneck links cases.

Chapter 5

Stability Analysis of Multiple-Bottleneck Networks

A TCP/RED system with multiple-bottleneck links could be unstable even if its system parameters are set the same as those in a stable single-bottleneck system. In this chapter, we study the stability of the general AIMD /RED system with multiple bottlenecks. We develop a general mathematical approach to analyze network stability for both delay-free AIMD/RED systems and those with feedback delays. We derive sufficient conditions for the asymptotic stability of multiple-bottleneck systems with heterogeneous delays by appealing to Lyapunov stability theory with Lyapunov-Razumikhin conditions, and these conditions can be easily assessed by using LMI (Linear Matrix Inequality) Toolbox. Numerical results with Matlab and simulation results with NS-2 are given to validate the analytical results.

5.1 Introduction

For the vast-scale Internet, the single bottleneck topology may no longer be representative and a flow may traverse multiple links with non-negligible packet losses. In [61], it is shown that a multiple-bottleneck network may be unstable even if the same system parameters are used as those in a single bottleneck, stable network. In fact, the congestion signals from multiple links sharing by different flows may lead to chaotic behaviors. Clearly, the results from single bottleneck networks can not be directly applied to multiple-bottleneck networks. In a nutshell, the stability property of multiple-bottleneck networks remains an important open issue beckoning for further investigation.

In this chapter, after developing a general mathematical model of multiple-bottleneck AIMD/RED system, we study the stability properties of the system, considering heterogeneous flows with different feedback delays. The main contributions of the chapter are summarized as follows. First, the fluid model of a general multiple-bottleneck AIMD/RED system without feedback delay is proved to be *globally asymptotically stable*, independent of the number of flows in each bottleneck, flow parameter pairs (α, β), and their round-trip delays, etc. Next, we consider the multi-bottleneck system with feedback delays where global stability is often difficult to attain, due to the highly nonlinear nature and the effect of delays. We present two sufficient conditions to guarantee *local asymptotic stability* of the system and note that these results are for general multiple-bottleneck scenarios. Numerical results with Matlab and simulation results with NS-2 [60] have validated the analytical results with an example of two-bottleneck topology. The theoretical findings can be used as a guideline for tuning the system parameters to maintain network stability and enhance system performance, and the analytical and simulation results provide important insight to understand the stability and performance of multi-bottleneck networks.

The remainder of the chapter is organized as follows. In Sec. 5.2, we provide background on the fluid model for stability analysis of the Internet, building on which we develop a general model for multi-bottleneck scenarios. We investigate in Sec. 5.3 the stability properties with delay-free marking, and prove the global asymptotic stability of the fluid model system by using Lyapunov stability theory and LaSalle's Invariance Principle. Sec. 5.4 studies the multi-bottleneck system considering feedback delays. Stability properties of multiple-bottleneck systems are studied by applying the singularly perturbed techniques are given in Sec. 5.5 and delay-dependent LMI criteria for the stability of singularly perturbed AIMD/RED systems with multiple bottlenecks are obtained. Numerical results by MATLAB and simulation results by NS-2 are presented in Sec. 5.6. Sec. 5.7 gives a brief review of related work, followed by concluding remarks in Sec. 5.8.

5.2 Multiple-Bottleneck Network Model

A general scenario of a multiple-bottleneck AIMD/RED system is shown in Fig. 5.1. In the system, AIMD flows pass through multiple links which causes more than one congested routers. The thick lines with arrow in the figure represent the volume of the traffic load on each link and the traffic load becomes smaller each time after passing through a congested router. Assume that a packet can only be marked at most once, following the idea of modeling in [27], based on the modeling idea of single-bottleneck systems, a multiple-bottleneck AIMD/RED system that contains N groups of AIMD flows and M congested links can be mathematically modeled as follows:

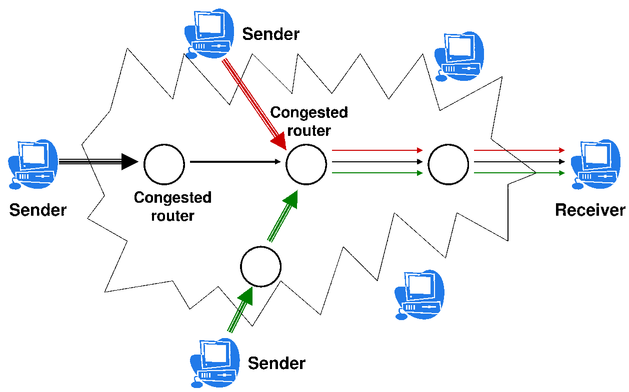

Figure 5.1: General Case of a Multiple-Bottleneck Network

$$
\begin{aligned}
\frac{dW_1(t)}{dt} &= \frac{\alpha_1}{R_1(t)} - \frac{2(1-\beta_1)}{1+\beta_1} W_1(t) \frac{W_1(t-\tau_1)}{R_1(t-\tau_1)} \\
&\qquad \times \textstyle\sum_{i\in r(1)} (K_{p_i} q_i(t-\tau_1)), \\
\cdots\cdots \quad & \cdots\cdots \quad \cdots\cdots \quad \cdots\cdots \\
\frac{dW_N(t)}{dt} &= \frac{\alpha_N}{R_N(t)} - \frac{2(1-\beta_N)}{1+\beta_N} W_N(t) \frac{W_N(t-\tau_N)}{R_N(t-\tau_N)} \\
&\qquad \times \textstyle\sum_{j\in r(N)} (K_{p_j} q_j(t-\tau_N)), \\
\frac{dq_1(t)}{dt} &= \begin{cases} \displaystyle\sum_{n\in f(1)} \frac{N_n W_n(t)}{R_n(t)} - C_1, & q_1 > 0, \\ \{ \displaystyle\sum_{n\in f(1)} \frac{N_n W_n(t)}{R_n(t)} - C_1, \}^+, & q_1 = 0, \end{cases} \\
\cdots\cdots \quad & \cdots\cdots \quad \cdots\cdots \quad \cdots\cdots \\
\frac{dq_M(t)}{dt} &= \begin{cases} \displaystyle\sum_{m\in f(M)} \frac{N_m W_m(t)}{R_m(t)} - C_M, & q_M > 0, \\ \{ \displaystyle\sum_{m\in f(M)} \frac{N_m W_m(t)}{R_m(t)} - C_M, \}^+, & q_M = 0. \end{cases}
\end{aligned} \tag{5.1}
$$

where $r(i)$, i=1, $\cdots$, N, denotes the set of congested routers that flow i passes through, and $f(m)$, m=1, $\cdots$, M, denotes the set of flows that pass through the congested router m.

5.3 Stability Analysis with Delay-free Marking

In this section, we study the dynamics of the multi-bottleneck networks in the absence of feedback delays by using Lyapunov stability theory and LaSalle's Invariance Principle. Assume that the round-trip time R_i is time-invariant, i.e., $R_i(t) = R_i$ for $i = 1, 2, \cdots, N$. We shall show that the equilibrium point of this delay-free system is globally asymptotically stable for all positive gains.

For delay-free marking multiple-bottleneck AIMD/RED system, the equilibrium point ($W_1^*, \cdots, W_N^*, q_1^*, \cdots, q_M^*$) can be obtained by

$$\begin{aligned}
&2(1-\beta_1)\cdot(W_1^*)^2(\textstyle\sum_{i\in r(1)}(K_{p_i}q_i^*) = \alpha_1(1+\beta_1),\\
&\cdots\cdots \quad \cdots\cdots \quad \cdots\cdots \quad \cdots\cdots\\
&2(1-\beta_N)\cdot(W_N^*)^2(\textstyle\sum_{j\in r(N)} K_{p_j}q_j^*) = \alpha_N(1+\beta_N),\\
&\textstyle\sum_{n\in f(1)} N_n\cdot W_n^*/R_n = C_1,\\
&\cdots\cdots \quad \cdots\cdots\\
&\textstyle\sum_{m\in f(M)} N_m\cdot W_m^*/R_m = C_M.
\end{aligned} \tag{5.2}$$

One observation is that, if all flows have the same AIMD parameter pair, the flow that traverses more bottlenecks always suffers more packet losses than other flows, and its window size is always smaller than those of others.

Remark 1.: The analysis throughout this chapter is about the stability property of the equilibrium point of system (5.1). Since the equilibrium point is typically in the desired operating region of the system, its stability property, i.e., the convergence of system trajectories to the equilibrium point, will guarantee network performance in terms of packet loss, delay, and jitter.

With the transformed variables $\tilde{W}_i(t)=W_i(t)-W_i^*$, for $i = 1, \cdots, N$; $\tilde{q}_j(t) = q_j(t) - q_j^*$, for $j = 1, \cdots, M$; we can use the following Lyapunov function to establish the asymptotic stability of delay-free marking system:

$$\begin{aligned} & V(\tilde{W}_1(t), \cdots, \tilde{W}_N(t), \tilde{q}_1(t), \cdots, \tilde{q}_M(t)) \\ & = \frac{1}{2}\sum_{i=1}^{N}\frac{(1+\beta_i)N_i}{(1-\beta_i)\tilde{W}_i^{*2}}\tilde{W}_i^2(t) + \frac{1}{2}\sum_{j=1}^{M}K_{p_j}\tilde{q}_j^2(t). \end{aligned} \tag{5.3}$$

The time-derivative of V along the solution of system (5.1) is non-positive, i.e., $\dot{V} \leq 0$. By applying LaSalle's Invariance Principle, all the trajectories converge to the unique equilibrium point of system (5.1). Thus, the global asymptotic stability of system (5.1) is obtained. The results can be summarized by the following theorem.

Theorem 5.1 *For any $K_{p_1}>0$, $\cdots$, $K_{p_M}>0$, the equilibrium point of the delay-free marking AIMD/RED system is globally asymptotically stable for any positive pairs (α_1, β_1), $\cdots$, (α_N, β_N) and any positive R_1, $\cdots$, R_N.*

Proof: With the transformed variables $\tilde{W}_i(t)=W_i(t)-W_i^*$, for $i = 1, \cdots, N$; $\tilde{q}_j(t) = q_j(t) - q_j^*$, for $j = 1, \cdots, M$; the delay-free marking system becomes

$$
\begin{aligned}
\dot{\tilde{W}}_1(t) = & - \frac{2(1-\beta_1)}{1+\beta_1}\frac{(\tilde{W}_I(t)+W_1^*)^2}{R_1}(\sum_{i\in r(1)} K_{p_i}\tilde{q}_i(t)) \\
& - \frac{2(1-\beta_1)}{1+\beta_1}\frac{\tilde{W}_1^2(t)+2W_1^*\tilde{W}_1(t)}{R_1}(\sum_{i\in r(1)} K_{p_i}q_i^*)), \\
\cdots \quad & \cdots \quad \cdots\cdots \quad \cdots\cdots \quad \cdots\cdots \\
\dot{\tilde{W}}_N(t) = & - \frac{2(1-\beta_N)}{1+\beta_N}\frac{(\tilde{W}_N(t)+W_N^*)^2}{R_N}(\sum_{j\in r(N)} K_{p_j}\tilde{q}_j(t)) \\
& - \frac{2(1-\beta_N)}{1+\beta_N}\frac{\tilde{W}_N^2(t)+2W_N^*\tilde{W}_N(t)}{R_N}(\sum_{j\in r(N)} K_{p_j}q_j^*)), \\
\dot{\tilde{q}}_1(t) = & \sum_{n\in f(1)} \frac{N_n\cdot\tilde{W}_n(t)}{R_n}, \\
\cdots \quad & \cdots \quad \cdots\cdots \\
\dot{\tilde{q}}_M(t) = & \sum_{m\in f(M)} \frac{N_m\cdot\tilde{W}_m(t)}{R_m}.
\end{aligned} \tag{5.4}
$$

with the equilibrium point $(\tilde{W}_1,\,\cdots,\,\tilde{W}_N,\,\tilde{q}_1,\,\cdots\,\tilde{q}_M) = (0,\,0,\,\cdots,\,0,\,0)$.

With system (5.4), we choose Lyapunov function with the following form,

$$
\begin{aligned}
& V(\tilde{W}_1(t),\,\cdots,\,\tilde{W}_N(t),\,\tilde{q}_1(t),\,\cdots,\,\tilde{q}_M(t)) \\
& = \frac{1}{2}\sum_{i=1}^{N}\frac{(1+\beta_i)N_i}{(1-\beta_i)\tilde{W}_i^{*2}}\tilde{W}_i^2(t) + \frac{1}{2}\sum_{j=1}^{M} K_{p_j}\tilde{q}_j^2(t).
\end{aligned} \tag{5.5}
$$

Computing the time-derivative of V along the solution of system (5.4) gives,

$$
\begin{aligned}
\dot{V} &= \sum_{i=1}^{N} \frac{(1+\beta_i)N_i}{(1-\beta_i)\tilde{W}_i^{*2}} \tilde{W}_i(t)\dot{\tilde{W}}_i + \sum_{j=1}^{M} K_{p_j} \tilde{q}_j(t)\dot{\tilde{q}}_j \\
&= -\sum_{k=1}^{N} \frac{N_k}{W_k^{*2} R_k} \cdot \tilde{W}_k^2(t)(\tilde{W}_k(t) + 2W_k^*) \cdot \sum_{i\in r(k)} K_{p_i}(\tilde{q}_i(t) + q_i^*).
\end{aligned}
$$

Note that $\tilde{W}_k(t) + W_k^* = W_k(t) \geq 0$ for $k = I, \cdots, N$; and $\tilde{q}_i(t) + q_i^* = q_i(t) \geq 0$ for $i = 1, \cdots, M$; which implies $\dot{V} \leq 0$. Thus, we prove that the equilibrium point of system (5.4) is stable. Next, we show the globally asymptotic stability of the system by applying LaSalle's Invariance Principle. Consider the set of states where $\dot{V} = 0$,

$$
\begin{aligned}
\mathcal{M}: \ = \{ \quad & (\tilde{W}_1, \cdots, \tilde{W}_N, \tilde{q}_1, \cdots, \tilde{q}_M) : \dot{V} = 0 \ \} \\
= \{ \quad & (\tilde{W}_1, \cdots, \tilde{W}_N, \tilde{q}_1, \cdots, \tilde{q}_M) : \\
& \tilde{W}_1 = \cdots = \tilde{W}_N = 0; \\
& \text{or } \tilde{q}_1 = -q_1^*, \cdots, \tilde{q}_M = -q_M^*. \ \}.
\end{aligned}
$$

Applying LaSalle's Invariance Principle [51, 53], trajectories of (5.4) converge to the largest invariant set contained in $\mathcal{M}$. We then prove that the only invariant set contained in $\mathcal{M}$ is the equilibria $(0, 0, \cdots, 0, 0)$. If $(\tilde{W}_1(t), \cdots, \tilde{W}_N(t), \tilde{q}_1(t), \cdots \tilde{q}_M(t))$ is equal to $(0, \cdots, 0, \tilde{q}_1(t), \cdots, \tilde{q}_M(t))$ or $(\tilde{W}_1(t), \cdots, \tilde{W}_N(t), -q_1^*, \cdots - q_M^*)$, we can then conclude that $(\tilde{W}_1(t^+), \cdots, \tilde{W}_N(t^+), \tilde{q}_1(t^+), \cdots \tilde{q}_M(t^+))$ is not in $\mathcal{M}$ by applying (5.4), which implies that no trajectory can stay in $\mathcal{M}$, other than the equilibrium point $(0, 0, \cdots, 0, 0)$. Therefore, the equilibrium point of system (5.4) is asymptotically stable.□

In the above analysis, the AIMD parameter pairs for all the flows in group i, $i = 1, \cdots, N$, are the same. In reality, there may be heterogeneous AIMD flows within one group. As an example, we consider the case when two types of AIMD flows are within the group I: N_{I1} AIMD (α_{I1}, β_{I1}) flows denoted by W_{I1}, and N_{I2} AIMD (α_{I2}, β_{I2}) flows denoted by W_{I2}, with round trip-time R_{I1} and R_{I2}, respectively. In this case, we can still obtain the globally asymptotic stability by choosing the following proper Lyapunov function and LaSalle's Invariance Principle.

Assume that there are two types of AIMD flows within the group I: N_{I1} AIMD (α_{I1}, β_{I1}) flows denoted by W_{I1}, and N_{I2} AIMD (α_{I2}, β_{I2}) flows denoted by W_{I2}, with round trip-time R_{I1} and R_{I2}, respectively. Then these flows can be modeled as follows,

$$\begin{aligned} \frac{dW_{I1}(t)}{dt} &= \frac{\alpha_{I1}}{R_{I1}} - \frac{2(1-\beta_{I1})}{1+\beta_{I1}} \frac{W_{I1}^2(t)}{R_{I1}} (\sum_{i \in r(I)} K_{p_i} q_i(t)), \\ \frac{dW_{I2}(t)}{dt} &= \frac{\alpha_{I2}}{R_{I2}} - \frac{2(1-\beta_{I2})}{1+\beta_{I2}} \frac{W_{I2}^2(t)}{R_{I2}} (\sum_{i \in r(I)} K_{p_i} q_i(t)). \end{aligned} \tag{5.6}$$

We can then obtain the global asymptotic stability by choose the following Lyapunov function,

$$\begin{aligned} & V(\tilde{W}_{I1}(t), \tilde{W}_{I2}(t), \cdots, \tilde{W}_N(t), \tilde{q}_1(t), \cdots, \tilde{q}_M(t)) \\ &= \frac{1}{2} \frac{(1+\beta_{I1})N_{I1}}{(1-\beta_{I1})\tilde{W}_{I1}^{*2}} \tilde{W}_{I1}^2(t) + \frac{1}{2} \frac{(1+\beta_{I2})N_{I2}}{(1-\beta_{I2})\tilde{W}_{I2}^{*2}} \tilde{W}_{II2}^2(t) \\ & \quad + \frac{1}{2} \sum_{i \neq I} \frac{(1+\beta_i)N_i}{(1-\beta_i)\tilde{W}_i^{*2}} \tilde{W}_i^2(t) + \frac{1}{2} \sum_{j=1}^{M} K_{p_j} \tilde{q}_j^2(t). \end{aligned} \tag{5.7}$$

Using the similar analysis as in Theorem 5.1, global asymptotic stability for this case can be proved. The same conclusion can be drawn for more general cases, i.e., when more than two types of AIMD flows in each group are sharing the link capacities. The corresponding mathematical models can be constructed along similar lines as above, by extending the model to higher dimensions to include more terms, each representing another kind of flow.

Remark 2.: Note that a similar analysis can be carried out for more general cases, i.e., when there are more than two types of AIMD flows in each group sharing the link capacities. For this, the corresponding mathematical models can be constructed along similar lines as above, by extending the model (5.1) to higher dimensions to include more terms, each representing a type of flow.

5.4 Stability Analysis with Feedback Delays

5.4.1 Stability Criteria for General Multiple-Bottleneck Systems

In this section, we study the stability properties of the delayed system (5.1) in Section 5.2. With ever-increasing link capacity and appropriate congestion control mechanism, variation of queuing delays becomes relatively small to propagation delays. In fact, recent work [48] reveals that the variable nature of RTT due to queueing delay variation helps to stabilize the TCP/RED system. Therefore, we can ignore the effect of the delay jitter on the round-trip time and derive sufficient conditions for the asymptotic stability of multiple-bottleneck system assuming RTT to be constant. Clearly, these sufficient conditions will be still applicable if RTT is actually time-varying.

The equilibrium points $(W_1^*, \cdots, W_N^*, q_1^*, \cdots, q_M^*)$ of system (5.1) are defined by (5.2) with $R_i = \tau_i = R_i^*$ for $i = 1, \cdots, N$, where $R_i^* = T_{p_i} + \sum_{j \in r(i)} \frac{q_j^*}{C_j}$.

Due to the highly nonlinear nature and the effect of delays in the system, no suitable Lyapunov function could be constructed to prove global asymptotic stability of the equilibrium. We linearize system (5.1) about the equilibrium point and write it in the following form,

$$\dot{x}(t) = \bar{A}x(t) + \sum_{i=1}^{N} \bar{B}_i x(t - R_i^*), \tag{5.8}$$

with $x=(\tilde{W}_1(t),\, \cdots,\, \tilde{W}_N(t),\, \tilde{q}_1(t),\, \cdots,\, \tilde{q}_M(t))^T$, $\bar{A}=\begin{bmatrix} A_{11} & 0 \\ A_{21} & A_{22} \end{bmatrix}$, $\bar{B}=\begin{bmatrix} B_{i11} & B_{i12} \\ 0 & 0 \end{bmatrix}$,

where A_{ij}, B_{i11} and B_{i12} are known real constant matrices with appropriate dimensions with following forms:

$$A_{11}=\begin{bmatrix} -\frac{\alpha_1}{R_1^* W_1^*} & 0 & \cdots & 0 \\ 0 & -\frac{\alpha_2}{R_2^* W_2^*} & \cdots & 0 \\ \vdots & \vdots & \ddots & \vdots \\ 0 & 0 & \cdots & -\frac{\alpha_N}{R_N^* W_N^*} \end{bmatrix}, \qquad (A_{21})_{ij} = \begin{cases} \dfrac{N_j}{R_j^*}, & if \quad j \in r(i), \\ 0, & otherwise, \end{cases}$$

$$(A_{22})_{ij} = \begin{cases} -\dfrac{1}{C_j} \displaystyle\sum_{l \in f(i)} \dfrac{N_l W_l^*}{R_l^{*2}}, & for \quad i = j, \\ -\dfrac{1}{C_j} \displaystyle\sum_{l \in f(i) \cap f(j)} \dfrac{N_l W_l^*}{R_l^{*2}}, & otherwise, \end{cases}$$

$$(B_{i11})_{jk} = \begin{cases} -\dfrac{\alpha_i}{R_i^* W_i^*}, & for \quad j = k = i, \\ 0, & otherwise, \end{cases}$$

$$(B_{i12})_{jk} = \begin{cases} -\dfrac{2(1-\beta_i)}{1+\beta_i} \dfrac{W_i^{*2}}{R_i^*} K_{pk}, & for \quad j = i \; and \; k \in f(i), \\ 0, & otherwise. \end{cases}$$

It can be checked by the Routh Criterion that $\bar{A}$ is a Hurwitz matrix, which implies that for any positive definite matrix Q, there exists positive definite matrix P, such that $\bar{A}^T P + P\bar{A} = -Q$. We next give some sufficient conditions for the local asymptotic stability of system (5.1) by applying the direct method of Lyapunov. Let $M=\sqrt{\lambda_{\max}(P)/\lambda_{\min}(P)}$, where $\lambda(P)$ denotes eigenvalues of matrix P, we can obtain a sufficient condition to guarantee the local asymptotic stability of the multiple-bottleneck system.

Theorem 5.2 *If there exists positive definite P, Q satisfying $\bar{A}^T P + P\bar{A}{=}-Q$ such that matrix $Q - 2M \cdot (\sum_{i=1}^{N} \|P\bar{B}_i\|) \cdot I$ is positive definite, then the equilibrium point of (5.1) is locally asymptotically stable.*

Proof: With (5.8), we choose Lyapunov function $V(x) = x^T P x$, then

$$\begin{aligned}
\dot{V} &= \dot{x}^T P x + x^T P \dot{x} \\
&= [\bar{A}x(t) + \textstyle\sum_{i=1}^{N} \bar{B}_i x(t - R_i^*)]^T P x + x^T P[\bar{A}x(t) + \textstyle\sum_{i=1}^{N} \bar{B}_i x(t - R_i^*)] \\
&= x^T(t)(\bar{A}^T P {+} P\bar{A})x(t) {+} 2\sum_{i=1}^{N} x^T(t{-}R_i^*)\bar{B}_i^T P x(t) \\
&= -x^T(t)Qx(t) {+} 2\sum_{i=1}^{N} x^T(t{-}R_i^*)\bar{B}_i^T P x(t).
\end{aligned}$$

Let $R^*{=}\max\{R_1^*, \cdots, R_N^*\}$. Applying the Lyapunov-Razumikhin condition, with $\mu{>}1$ such that

$$V(\xi) \le \mu^2 V(t), \qquad \text{for} \quad t - R^* \le \xi \le t,$$

which implies that $\|x(\xi)\| \le M{\cdot}\mu{\cdot}\|x(t)\|$.

Thus,

$$\begin{aligned}\dot{V} &\leq -x^T(t)Qx(t)+2\|x(t-R^*)\|\,(\sum_{i=1}^{N}\|\bar{B}_i^T P\|)\,\|x(t)\| \\ &\leq -x^T(t)[Q-2\mu\, M\,(\sum_{i=1}^{N}\|P\bar{B}_i\|)\,I]x(t),\end{aligned}$$

thereby establishing the asymptotic stability of system (5.1). □

Observe that the Lyapunov-Razumikhin condition is used in Theorem 5.2 to deal with the delayed terms in $\dot{V}$. Lyapunov functional is another method that can be applied when studying the stability of delayed systems. Our next result gives another sufficient condition for the local asymptotic stability of system (5.1) in terms of linear matrix equality by applying the method of Lyapunov functional.

Theorem 5.3 *If there exist positive definite P, Q satisfying $\bar{A}^T P + P\bar{A} = -Q$ and positive definite G_i for $i = 1, \cdots, N$ such that the following matrix is positive definite,*

$$\begin{bmatrix} Q-\sum_{i=1}^{N} G_i & -PB_1 & \cdots & -PB_N \\ -B_1^T P & G_1 & 0 & 0 \\ \vdots & 0 & \ddots & 0 \\ -B_N^T P & 0 & 0 & G_N \end{bmatrix} > 0,$$

then the equilibrium point of (5.1) is locally asymptotically stable.

Proof: With (5.8), we choose Lyapunov functional

$$V(x) = x^T Px + \sum_{i=1}^{N}\int_{t-R_i^*}^{t} x^T(s)G_i x(s)ds,$$

then

$$\begin{aligned}
\dot{V} &= x^T(t)(\bar{A}^T P + P\bar{A})x(t) + 2\sum_{i=1}^{N} x^T(t-R_i^*)\bar{B}_i^T P x(t) \\
&\quad + x^T(t)(\sum_{i=1}^{N} G_i)x(t) - \sum_{i=1}^{N} x^T(t-R_i^*)G_i x(t-R_i^*) \\
&= -x^T(t)(Q - \sum_{i=1}^{N} G_i)x(t) + 2\sum_{i=1}^{N} x^T(t-R_i^*)B_i^T P x(t) \\
&\quad - \sum_{i=1}^{N} x^T(t-R_i^*)G_i x(t-R_i^*) \\
&= -(x^T(t), x^T(t-R_1^*), \cdots, x^T(t-R_N^*)) \cdot \\
&\quad D \cdot (x^T(t), x^T(t-R_1^*), \cdots, x^T(t-R_N^*))^T,
\end{aligned}$$

where D denotes the matrix $\begin{bmatrix} Q - \sum_{i=1}^{N} G_i & -PB_1 & \cdots & -PB_N \\ -B_1^T P & G_1 & 0 & 0 \\ \vdots & 0 & \ddots & 0 \\ -B_N^T P & 0 & 0 & G_N \end{bmatrix}$. Thus, system (5.1) is locally asymptotically stable if D is positive definite. □

It is worth pointing out that sufficient conditions derived in Theorems 5.2 and 5.3 are both given in terms of linear matrix inequalities (LMI). These conditions can be easily assessed by applying the LMI Control Toolbox with Matlab [67].

In general, Theorems 5.2 and 5.3 shed some light on how the network parameters impact the network stability. Specifically, we have the following intuitive interpretation of the conditions in these theorems. To guarantee the local asymptotic stability of system (5.1), $\dot{V}$ in Theorems 5.2 and 5.3 is required to be negative definite. It can be seen from the proof that the more negative $\bar{A}^T P + P\bar{A}$ and the smaller $\|P\bar{B}_i\|, i = 1, \cdots, N$, the more likely $\dot{V}<0$. In other words, the term $\bar{A}^T P + P\bar{A}$ should be dominant in $\dot{V}$ and the absolute values of $\lambda(\bar{A})$ are expected to be sufficiently large. Notice that $\bar{A}$

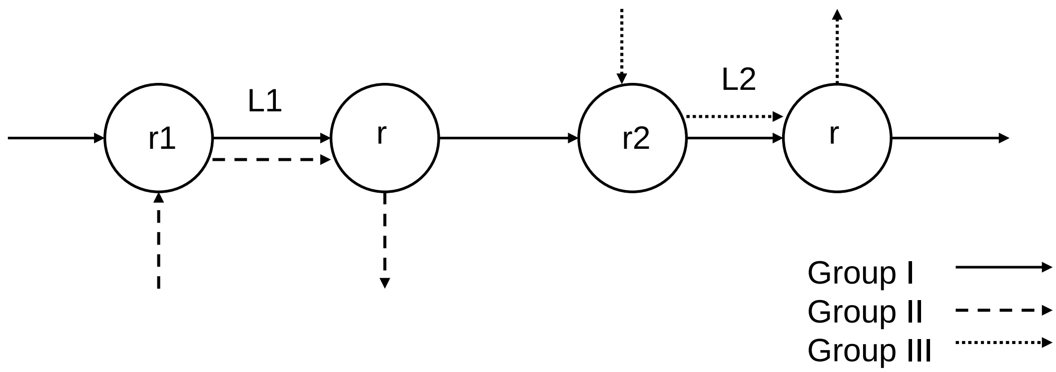

Figure 5.2: Multiple-Bottleneck Topology

has been checked to be a Hurwitz matrix and W_i^*, $i{=}I, \cdots, N$ has the form of RC/N. From the expression of $\bar{A}$ and $\bar{B}_i$, we know that the smaller the terms R_i^*, $i = 1, \cdots, N$, C_j, $j = 1, \cdots, M$, the larger the absolute values of $\lambda(\bar{A})$ and the smaller the $\|PB_i\|$, and hence the better the chance that the system is asymptotically stable. These observations are also consistent with those in [9]: TCP/RED will become unstable when delay increases or when link capacity increases.

5.4.2 Case Study: A Class of Two-Bottleneck Topology

In this section, we consider a basic multi-bottleneck scenario, as depicted in Fig. 5.2. Three groups of flows are sharing the links between four routers. AIMD flows in group I compete with flows in group II over link L_1, and also compete with 50 flows in group III over link L_2. We assume all routers are RED enabled and there is no packet loss and delay jitter in the non-bottleneck links. All routers are RED enabled. Links L_1 and L_2 are bottlenecks with the capacity of C_1 and C_2, respectively. The round-trip delays for the three groups of traffic are R_1, R_2, and R_3, respectively. The results with this topology are also applicable to the scenarios when the three groups of flows traverse other non-bottleneck links before/after they enter/leave L_1 or L_2.

In this multi-bottleneck topology, let K_{p_1} and K_{p_2} denote the marking probability on L_1 and L_2, and (α_1, β_1), (α_2, β_2) and (α_3, β_3) be AIMD parameter pairs for the three groups of flows, respectively. For the first group of flows, the marking probabilities on L_1 and L_2 are $p_1(t-R_1) = K_{p_1}q_1(t-R_1)$ and $p_2(t-R_1) = K_{p_2}q_2(t-R_1)$, respectively. Since we assume that a packet can only be marked at most once, the probability of a flow I packet receiving a mark is $p_1(t-R_1)+p_2(t-R_1)-p_1(t-R_1)p_2(t-R_1)$. The marking probability can be approximated by $p_1(t-R_1)+p_2(t-R_1)$ given that p_1 and p_2 are very small. The closed-loop dynamics can be modeled as follows:

$$
\begin{aligned}
\frac{dW_I(t)}{dt} &= \frac{\alpha_1}{R_1(t)} - \frac{2(1-\beta_1)}{1+\beta_1}W_I(t)\frac{W_I(t-\tau_1)}{R_1(t-\tau_1)}(K_{p_0}q_0(t-\tau_1)+K_{p_2}q_2(t-\tau_1)),\\
\frac{dW_{II}(t)}{dt} &= \frac{\alpha_2}{R_2(t)} - \frac{2(1-\beta_2)}{1+\beta_2}W_{II}(t)\frac{W_{II}(t-\tau_2)}{R_2(t-\tau_2)}K_{p_0}q_0(t-\tau_2),\\
\frac{dW_{III}(t)}{dt} &= \frac{\alpha_3}{R_3(t)} - \frac{2(1-\beta_3)}{1+\beta_3}W_{III}(t)\frac{W_{III}(t-\tau_3)}{R_3(t-\tau_3)}K_{p_2}q_2(t-\tau_3),\\
\frac{dq_1(t)}{dt} &= \begin{cases} \dfrac{N_1W_I(t)}{R_1(t)} + \dfrac{N_2W_{II}(t)}{R_2(t)} - C_1, & q_0 > 0,\\[2ex] \{\dfrac{N_1W_I(t)}{R_1(t)} + \dfrac{N_2W_{II}(t)}{R_2(t)} - C_1\}^+, & q_0 = 0,\end{cases}\\
\frac{dq_2(t)}{dt} &= \begin{cases} \dfrac{N_1W_I(t)}{R_1(t)} + \dfrac{N_3W_{III}(t)}{R_3(t)} - C_2, & q_2 > 0,\\[2ex] \{\dfrac{N_1W_I(t)}{R_1(t)} + \dfrac{N_3W_{III}(t)}{R_3(t)} - C_2\}^+, & q_2 = 0.\end{cases}
\end{aligned}
\tag{5.9}
$$

Next, we give a numerical example to get a more concrete sense of the sufficient conditions in Theorem 5.2 on local asymptotic stability for the AIMD/RED system with heterogeneous delays. Let $N_1 = N_2 = N_3 = 5$, $C_1 = 3 \times 10^3$ packet/sec, $C_2 = 5 \times 10^3$ packet/sec with $K_{p1} = K_{p2} = 0.0005$. Choose $(\alpha_1,\ \beta_1)$=$(1,\ 0.5)$ with $T_{p1} = 0.020$ sec, $(\alpha_2,\ \beta_2) = (0.2,\ 0.875)$ with T_{p2}=0.013 sec and $(\alpha_3,\ \beta_3)$=$(1,\ 0.5)$ with T_{p3}=0.007 sec, respectively. Solving the LMI in Theorem 5.2 with Matlab Control Toolbox, one feasible solution we obtain is as follow: positive definite matrix

$$Q = 10^3 \times \begin{bmatrix} 4.2596 & -1.2369 & 2.3752 & -1.8226 & -1.9184 \\ -1.2369 & 4.5479 & -3.1861 & -2.0736 & 0.8033 \\ 2.3752 & -3.1861 & 2.8241 & 0.5329 & -1.2195 \\ -1.8226 & -2.0736 & 0.5329 & 2.4057 & 0.6722 \\ -1.9184 & 0.8033 & -1.2195 & 0.6722 & 0.8817 \end{bmatrix} \text{ and}$$

$$P = \begin{bmatrix} 2.217 & -2.6696 & 2.4213 & 0.3497 & -1.091 \\ -2.669 & 4.9555 & -3.8606 & -1.3247 & 1.439 \\ 2.421 & -3.8606 & 3.3280 & 0.9250 & -1.279 \\ 0.349 & -1.3247 & 0.9250 & 0.6115 & -0.229 \\ -1.091 & 1.4386 & -1.2789 & -0.2295 & 0.559 \end{bmatrix}.$$

We can also check that the eigenvalues of matrix $Q - 2M\,(\|PB_1\| + \|PB_2\| + \|PB_3\|)I$ are : $1.0e + 003 \times [9.0769, 5.8269, 0.0088, 0.0044, 0.0001]$, which implies that $Q - 2M\,(\|PB_1\| + \|PB_2\| + \|PB_3\|)I$ is positive definite. Thus, the condition of Theorem 5.2 holds and the system is locally asymptotically stable. Simulation results using the same parameters will be given in Sec. 5.6.

Remark 3.: Notice that Theorems 5.2 and 5.3 give two different sets of sufficient conditions for the asymptotic stability of system (5.9). These conditions can be easily checked by the LMI Toolbox, which allow us to use any of them at our convenience.

Remark 4.: Using the similar idea of this section, we can obtain the local stability of the network when it is shared by more than three groups of flows as well. Mathematical models can be established following the idea in Sec. 5.2 and the technique used in this section can be applied to obtain sufficient conditions, in terms of LMI, for asymptotic stability of any given scenarios.

Remark 5.: We note that the results in this section are for local stability only, whereas the results obtained in Sec. 5.3 are for global stability. This is due to the difficulty in constructing a suitable Lyapunov-type function for the nonlinear multiple-bottleneck AIMD/RED system with heterogeneous delays. A plausible approach to resolve this issue is to develop a sequence of upper and lower bounds of system trajectories and use these bounds in Razumikhin's theorem to derive conditions for global stability in the presence of heterogeneous delays, and our study along this line is underway. Studying the stability properties of the general case of multiple-bottleneck AIMD/RED networks by directly using the model (5.1) is an important open issue for further investigation.

5.5 Delay-Dependent Stability Analysis using Singular Perturbation Approach

In this section, we take the mathematical model of AIMD/RED systems with multiple bottlenecks and feedback delays into the novel frame of singularly perturbed systems. Stability properties of multiple-bottleneck systems are studied by applying the singularly perturbed techniques. Delay-dependent LMI criteria for the stability of singularly perturbed AIMD/RED systems with multiple bottlenecks are obtained, and the existence of the sufficiently small parameters that guarantee the asymptotic stability of the system considered above is also demonstrated.

5.5.1 Singularly Perturbed Multiple-Bottleneck Systems

We consider a multiple-bottleneck AIMD/RED system that contains N groups of AIMD flows and M congested links. The corresponding mathematical model for this system, which has been proposed in Sec. 5.2, is described as (5.1).

Notice that in system (5.1), the term $\frac{dq_j(t)}{dt}$ changes much faster than $\frac{dW_i(t)}{dt}$, especially when N_i is large, i.e., window size is slow variable and queue length is fast variable in the system. We assume all groups in system (5.1) contain the number of AIMD flows with the same order, i.e., $O(N_1) \sim O(N_2) \sim \cdots \sim O(N_N)$. Let $\bar{N} = \sum_{i=1}^{N} N_i/N$, and $1/\bar{N}$ is then a small real number in $(0, 1]$. Take $\varepsilon = 1/\bar{N}$ and $\lambda_i = N_i/\bar{N}$, $\frac{dq_j(t)}{dt}$, $j = 1, \cdots M$, $\frac{dq_j(t)}{dt}$ in the original system, (5.1) can be rewritten as,

$$\varepsilon \dot{q}_j(t) = \begin{cases} \sum\limits_{n \in f(j)} \dfrac{\lambda_n W_n(t)}{R_n(t)} - C_j/\bar{N}, & q_j > 0, \\ \\ \{\sum\limits_{n \in f(j)} \dfrac{\lambda_n W_n(t)}{R_n(t)} - C_j/\bar{N}, \}^+, & q_j = 0. \end{cases} \tag{5.10}$$

Hence, the multiple-bottleneck AIMD/RED system with the queue length described in (5.10) has been taken into the frame of *singularly perturbed systems* [68, 71] with heterogeneous feedback delays.

We then linearize the singularly perturbed multiple-bottleneck system about the equilibrium point $(W_1^*, \cdots, W_N^*, q_1^*, \cdots, q_M^*)$. Take $x(t) = (W_1(t), \cdots, W_N(t))^T$ and

$y(t) = (q_1(t), \cdots, q_M(t))^T$, the obtained linearized singularly perturbed system with delays is as follows:

$$\begin{bmatrix} \dot{x}(t) \\ \varepsilon\dot{y}(t) \end{bmatrix} = \begin{bmatrix} A_{11} & 0 \\ A_{21} & A_{22} \end{bmatrix} \begin{bmatrix} x(t) \\ y(t) \end{bmatrix} + \sum_{i=1}^{N} \begin{bmatrix} B_{i11} & B_{i12} \\ 0 & 0 \end{bmatrix} \begin{bmatrix} x(t-R_i^*) \\ y(t-R_i^*) \end{bmatrix}, \tag{5.11}$$

where $x(t) \in R^N$ and $y(t) \in R^M$ are slow- and fast-state vectors, respectively. ε is a singular perturbation parameter. $R_i^* \geq 0$ are time delays on $x(t)$ and $y(t)$. A_{ij}, B_{i11} and B_{i12} are known real constant matrices with appropriate dimensions with following forms:

$$A_{11}= \begin{bmatrix} -\frac{\alpha_1}{R_1^* W_1^*} & 0 & \cdots & 0 \\ 0 & -\frac{\alpha_2}{R_2^* W_2^*} & \cdots & 0 \\ \vdots & \vdots & \ddots & \vdots \\ 0 & 0 & \cdots & -\frac{\alpha_N}{R_N^* W_N^*} \end{bmatrix},$$

$$(A_{21})_{ij} = \begin{cases} \dfrac{\lambda_j}{R_j^*}, & if \quad j \in r(i), \\ 0, & otherwise, \end{cases}$$

$$(A_{22})_{ij} = \begin{cases} -\dfrac{1}{C_j} \displaystyle\sum_{l\in f(i)} \dfrac{\lambda_l W_l^*}{R_l^{*2}}, & for \quad i = j, \\ -\dfrac{1}{C_j} \displaystyle\sum_{l\in f(i)\cap f(j)} \dfrac{\lambda_l W_l^*}{R_l^{*2}}, & otherwise, \end{cases}$$

$$(B_{i11})_{jk} = \begin{cases} -\dfrac{\alpha_i}{R_i^* W_i^*}, & for \quad j = k = i, \\ 0, & otherwise, \end{cases}$$

$$(B_{i12})_{jk} = \begin{cases} -\dfrac{2(1-\beta_i)}{1+\beta_i}\dfrac{W_I^{*2}}{R_i^*} K_{pk}, & for \quad j = i \; and \; k \in f(i), \\ 0, & otherwise. \end{cases}$$

It can be checked that A_{11} and A_{22} both are Hurwitz, which is important to establish sufficient conditions for the stability of system (5.11) for all small enough ε and R_i^*.

5.5.2 Stability Analysis

To facilitate the discussion, we introduce the following lemmas for later use.

Lemma 5.4 *[70] Let* $\mathtt{x} \in R^n$ *and* $\mathtt{y} \in R^n$ *be real vectors, then for any positive definite matrix* $X = X^T > 0$*, the inequality* $-2\mathtt{x}^T\mathtt{y} \le \mathtt{x}^T X^{-1}\mathtt{x} + \mathtt{y}^T X \mathtt{y}$ *holds.*

Lemma 5.5 *For any constants* a *and* b *and any functions* f *and* g*, the following result holds:*

$$\frac{d}{dt}\int_a^b \int_{f(t,\,\theta)}^{g(t,\,\theta)} F(s)ds d\theta$$
$$= \int_a^b \left(F(g(t,\,\theta))\frac{\partial}{\partial t}g(t,\,\theta) - F(f(t,\,\theta))\frac{\partial}{\partial t}f(t,\,\theta)\right) d\theta.$$

We first focus on the necessary condition for the stability of the system (5.11) as $\varepsilon \to 0$ and $R_i^* \to 0$.

The reduced-order delay-free system of the $(N+M)$th-order system (5.11) is given as $\varepsilon \to 0$ and $R_i^* \to 0$.

$$\dot{x}_s(t) = A_{11}x_s(t) + \sum_{i=1}^{N} \begin{bmatrix} B_{i11} & B_{i12} \end{bmatrix} \begin{bmatrix} x_s(t) \\ y_s(t) \end{bmatrix}, \tag{12a}$$

$$0 = A_{21}x_s(t) + A_{22}y_s(t). \tag{12b}$$

Note that A_{22}^{-1} exists because A_{22} is Hurwitz,

$$y_s(t) = -A_{22}^{-1}A_{21}x_s(t) \tag{5.13}$$

is the unique solution of (12b). Substituting (5.13) into (12a) results in the unique Nth order system.

$$\dot{x}_s(t) = A_0 x_s(t), \tag{5.14}$$

where $A_0 := A_{11} + \sum_{i=1}^{N} \bar{B}_i$, $\bar{B}_i := B_{i11} - B_{i12}A_{22}^{-1}A_{21}$.

Then we have the following necessary condition:

Theorem 5.6 *Let system (5.11) be stable for all small enough ε and R_i^*, then A_0 is Hurwitz. In other words, there exists $P_0 = P_0^T > 0$ such that the following LMI holds.*

$$P_0A_0 + A_0^TP_0 < 0. \tag{5.15}$$

Proof: It is clear that this result is given as the limits of ε and R_i^* both go to zero.

In the remainder of the section, sufficient conditions are derived for system (5.11). We first define the following similarity transformation [69, 71].

$$\begin{bmatrix} x(t) \\ \eta(t) \end{bmatrix} = \begin{bmatrix} I_N & 0 \\ L(\varepsilon) & I_M \end{bmatrix} \begin{bmatrix} x(t) \\ y(t) \end{bmatrix}, \tag{5.16}$$

where $L(\varepsilon)$ is obtained by solving the following linear algebraic equation:

$$A_{21} - A_{22}L(\varepsilon) + \varepsilon L(\varepsilon)A_{11} = 0. \tag{5.17}$$

Lemma 5.7 *[71] There exists a small constant $\bar{\varepsilon}$ such that for all $\varepsilon \in (0,\ \bar{\varepsilon})$, the linear algebraic equation (5.17) admits the unique solution $L = L(\varepsilon)$ that can be expressed as*

$$L = L(\varepsilon) = A_{22}^{-1}A_{21} + O(\varepsilon). \tag{5.18}$$

By using the similarity transformation (5.16) and lemma 5.7, system (5.11) can be rewritten as:

$$\begin{aligned}\begin{bmatrix} \dot{x}(t) \\ \varepsilon\dot{\eta}(t) \end{bmatrix} &= \begin{bmatrix} A_{11} & 0 \\ 0 & A_{22} \end{bmatrix} \begin{bmatrix} x(t) \\ \eta(t) \end{bmatrix} \\ &\quad + \sum_{i=1}^{N} \begin{bmatrix} \tilde{B}_{i11} & B_{i12} \\ L\tilde{B}_{i11} & LB_{i12} \end{bmatrix} \begin{bmatrix} x(t-R_i^*) \\ \eta(t-R_i^*) \end{bmatrix},\end{aligned} \tag{5.19}$$

where $\tilde{B}_{i11} := B_{i11} - B_{i12}L$.

Sufficient conditions are obtained as follows for asymptotic stability of system (5.11).

Theorem 5.8 *Given $\varepsilon > 0$, $R_i^* > 0$, system (5.11) is asymptotically stable if there exist $P_1 = P_1^T > 0$, $P_2 = P_2^T > 0$, $Q_{1i} = Q_{1i}^T > 0$, $Q_{2i} = Q_{2i}^T > 0$, $X_{1i} = X_{1i}^T > 0$ and*

$X_{2i} = X_{2i}^T > 0$, $i = 1, \ldots, N$ *such that the LMI*

$$\Gamma := \begin{bmatrix} \Phi & \Delta_1 & \cdots & \Delta_N & \Theta_1 & \Theta_1 & \cdots & \Theta_N & \Theta_N \\ \Delta_1^T & \Lambda_1 & \cdots & \Lambda_{1N} & 0 & 0 & \cdots & 0 & 0 \\ \vdots & \vdots & \ddots & \vdots & \vdots & \vdots & \ddots & \vdots & \vdots \\ \Delta_N^T & \Lambda_{N1} & \cdots & \Lambda_N & 0 & 0 & \cdots & 0 & 0 \\ \Theta_1^T & 0 & \cdots & 0 & -X_{11} & 0 & \cdots & 0 & 0 \\ \Theta_1^T & 0 & \cdots & 0 & 0 & -X_{12} & \cdots & 0 & 0 \\ \vdots & \vdots & \ddots & 0 & \vdots & \vdots & \ddots & \vdots & \vdots \\ \Theta_N^T & 0 & \cdots & 0 & 0 & 0 & \cdots & -X_{1N} & 0 \\ \Theta_N^T & 0 & \cdots & 0 & 0 & 0 & \cdots & 0 & -X_{2N} \end{bmatrix} < 0,$$

where

$$\begin{aligned}\Phi &:= \Phi(\varepsilon,\ R_1^*,\ \dots,R_N^*)\\ &= \Psi + \sum_{i=1}^{N}\left(P\begin{bmatrix}\tilde{B}_{i11} & 0\\ L\tilde{B}_{i11} & 0\end{bmatrix} + \begin{bmatrix}\tilde{B}_{i11} & 0\\ L\tilde{B}_{i11} & 0\end{bmatrix}^T P\right)\\ &+\sum_{i=1}^{N} R_i^*\begin{bmatrix}A_{11}^T\\ 0\end{bmatrix} X_{1i}\begin{bmatrix}A_{11} & 0\end{bmatrix},\end{aligned}$$

$$\Psi := \begin{bmatrix}P_1A_{11}+A_1^TP_1+\sum_{i=1}^{N}Q_{1i} & 0\\ 0 & P_2A_{22}+A_{22}^TP_2+\sum_{i=1}^{N}Q_{2i}\end{bmatrix},$$

$$\Lambda_i := -\begin{bmatrix}Q_{1i} & 0\\ 0 & Q_{2i}\end{bmatrix} + \begin{bmatrix}\tilde{B}_{i11}^T\\ B_{i12}^T\end{bmatrix}\left(\sum_{k=1}^{N}R_k^*X_{2k}\right)\begin{bmatrix}\tilde{B}_{i11} & B_{i12}\end{bmatrix},$$

$$\Lambda_{ij} := \begin{bmatrix}\tilde{B}_{i11}^T\\ B_{i12}^T\end{bmatrix}\left(\sum_{k=1}^{N}R_k^*X_{2k}\right)\begin{bmatrix}\tilde{B}_{j11} & B_{j12}\end{bmatrix},\ i\neq j,$$

$$\Delta_i := P\begin{bmatrix}0 & B_{i12}\\ 0 & LB_{i12}\end{bmatrix},\ \Theta_i := \sqrt{R_i^*}P\begin{bmatrix}\tilde{B}_{i11}\\ L\tilde{B}_{i11}\end{bmatrix},$$

$$P := \begin{bmatrix}P_1 & 0\\ 0 & P_2\end{bmatrix}.$$

Proof: The main idea of the proof for Theorem 5.8 is as follows.

Consider the following Lyapunov-Krasovskii function

$$\begin{aligned}V(z(t)) = \quad & x^T(t)P_1x(t) + \varepsilon\eta^T(t)P_2\eta(t)\\ + \quad & \textstyle\sum_{i=1}^{N}\int_{t-R_i^*}^{t} z^T(s)Q_iz(s)ds + W(t),\end{aligned} \tag{5.20}$$

where $W(t) := W_1(t) + W_2(t)$,

$$W_1(t) := \sum_{i=1}^{N} \int_{-R_i^*}^{0} \int_{t+\theta}^{t} z^T(s) \begin{bmatrix} A_{11}^T \\ 0 \end{bmatrix} \times X_{1i} \begin{bmatrix} A_{11} & 0 \end{bmatrix} z(s) ds d\theta,$$

$$W_2(t) := \sum_{i=1}^{N} \int_{-R_i^*}^{0} \int_{t+\theta}^{t} \left(\sum_{j=1}^{N} z^T(s - R_j^*) \begin{bmatrix} \tilde{B}_{jii}^T \\ B_{j12}^T \end{bmatrix} \right) \times X_{2i} \left(\sum_{k=1}^{N} \begin{bmatrix} \tilde{B}_{kii} & B_{k12} \end{bmatrix} z(s - R_k^*) \right) ds d\theta,$$

$$z(t) := \begin{bmatrix} x(t) \\ \eta(t) \end{bmatrix}, \; Q_i := \begin{bmatrix} Q_{1i} & 0 \\ 0 & Q_{2i} \end{bmatrix},$$

$$Q_{1i} = Q_{1i}^T > 0, \; Q_{2i} = Q_{2i}^T > 0,$$

$$X_{1i} = X_{1i}^T > 0, \; X_{2i} = X_{2i}^T > 0.$$

With the Lyapunov-Krasovskii function defined as (5.20) and system (5.11), we have

$$\begin{aligned}
\frac{dV(z(t))}{dt} &= x^T(t)(P_1A_{11}+A_{11}^TP_1)x(t)+\eta^T(t)(P_2A_{22}+A_{22}^TP_2)\eta(t) \\
&+ 2x^T(t)P_1\sum_{i=1}^{N}\left[\begin{array}{cc}\tilde{B}_{i11} & B_{i12}\end{array}\right]z(t-R_i^*) \\
&+ 2\eta^T(t)P_2\sum_{i=1}^{N}L\left[\begin{array}{cc}\tilde{B}_{i11} & B_{i12}\end{array}\right]z(t-R_i^*) \\
&+ \sum_{i=1}^{N}[z^T(t)Q_iz(t)-z^T(t-R_i^*)Q_iz(t-R_i^*)] \\
&+ \frac{dW(t)}{dt}.
\end{aligned} \tag{5.21}$$

Integrating $\dot{x}(t)$ in system (5.19) from $t-R_i^*$ to t results in

$$\begin{aligned}
x(t-R_i^*) &= x(t)-\int_{t-R_i^*}^{t}\left[\begin{array}{cc}A_{11} & 0\end{array}\right]z(s)ds \\
&- \sum_{j=1}^{N}\int_{t-R_i^*}^{t}\left[\begin{array}{cc}\tilde{B}_{j11} & B_{j12}\end{array}\right]z(t-R_j^*)ds.
\end{aligned} \tag{5.22}$$

Substituting (5.22) into (5.21), we obtain that

$$
\begin{aligned}
&\frac{dV(z(t))}{dt} \\
&= z^T(t)\Psi z(t) + 2z^T(t)\sum_{i=1}^{N}\Delta_i z(t-R_i^*) \\
&\quad +2z^T(t)P\sum_{i=1}^{N}\begin{bmatrix} \tilde{B}_{i11} & 0 \\ & \\ L\tilde{B}_{i11} & 0 \end{bmatrix} z(t) \\
&\quad +2z^T(t)P\sum_{i=1}^{N}\begin{bmatrix} \tilde{B}_{i11} \\ L\tilde{B}_{i11} \end{bmatrix}\left(-\int_{t-R_i^*}^{t}\begin{bmatrix} A_{11} & 0 \end{bmatrix} z(s)ds\right) \\
&\quad +2z^T(t)P\sum_{i=1}^{N}\begin{bmatrix} \tilde{B}_{i11} \\ L\tilde{B}_{i11} \end{bmatrix}\times\left(-\sum_{j=1}^{N}\int_{t-R_i^*}^{t}\begin{bmatrix} \tilde{B}_{j11} & B_{j12} \end{bmatrix} z(t-R_j^*)ds\right) \\
&\quad -\sum_{i=1}^{N} z^T(t-R_i^*)Q_i z(t-R_i^*) + \frac{dW(t)}{dt}.
\end{aligned}
\tag{5.23}
$$

It follows from the inequality of lemma 5.4 that

$$
\begin{aligned}
&\frac{dV(z(t))}{dt} \\
= \;& z^T(t)\Psi z(t) + 2z^T(t)\sum_{i=1}^{N}\Delta_i z(t-R_i^*) \\
+ \;& 2z^T(t)P\sum_{i=1}^{N}\begin{bmatrix}\tilde{B}_{i11} & 0 \\ L\tilde{B}_{i11} & 0\end{bmatrix} z(t) \\
+ \;& z^T(t)\sum_{i=1}^{N}R_i^* P\begin{bmatrix}\tilde{B}_{i11} \\ L\tilde{B}_{i11}\end{bmatrix}(X_{1i}^{-1}+X_{2i}^{-1})\begin{bmatrix}\tilde{B}_{i11}^T & \tilde{B}_{i11}^T L^T\end{bmatrix} Pz(t) \\
+ \;& \sum_{i=1}^{N}\int_{t-R_i^*}^{t} z^T(s)\begin{bmatrix}A_{11}^T \\ 0\end{bmatrix} X_{1i}\begin{bmatrix}A_{11} & 0\end{bmatrix} z(s)ds \\
+ \;& \sum_{i=1}^{N}\int_{t-R_i^*}^{t}\left(\sum_{j=1}^{N} z^T(s-R_j^*)\begin{bmatrix}\tilde{B}_{jii}^T \\ B_{j12}^T\end{bmatrix}\right)X_{2i}\left(\sum_{k=1}^{N}\begin{bmatrix}\tilde{B}_{kii} & B_{k12}\end{bmatrix} z(s-R_k^*)\right)ds \\
- \;& \sum_{i=1}^{N} z^T(t-R_i^*)Q_i z(t-R_i^*) + \frac{dW(t)}{dt}.
\end{aligned}
\tag{5.24}
$$

On the other hand we have

$$
\begin{aligned}
&\frac{dW(t)}{dt} \\
&:= \sum_{i=1}^{N} \int_{-R_i^*}^{0} \frac{d}{dt}\left(\int_{t+\theta}^{t} z^T(s) \left[\begin{array}{c} A_{11}^T \\ 0 \end{array} \right] \right. \\
&\qquad \left. \times X_{1i} \left[\begin{array}{cc} A_{11} & 0 \end{array} \right] z(s) ds \right) d\theta \\
&\quad + \sum_{i=1}^{N} \int_{-R_i^*}^{0} \frac{d}{dt}\left(\int_{t+\theta}^{t} \left(\sum_{j=1}^{N} z^T(s-R_j^*) \left[\begin{array}{c} \tilde{B}_{jii}^T \\ B_{j12}^T \end{array} \right] \right) \right. \\
&\qquad \left. \times X_{2i} \left(\sum_{k=1}^{N} \left[\begin{array}{cc} \tilde{B}_{kii} & B_{k12} \end{array} \right] z(s-R_k^*) \right) ds \right) d\theta \\
&:= \sum_{i=1}^{N} R_i^* z^T(t) \left[\begin{array}{c} A_{11}^T \\ 0 \end{array} \right] X_{1i} \left[\begin{array}{cc} A_{11} & 0 \end{array} \right] z(t) \\
&\quad + \sum_{i=1}^{N} R_i^* \left(\sum_{j=1}^{N} z^T(t-R_j^*) \left[\begin{array}{c} \tilde{B}_{jii}^T \\ B_{j12}^T \end{array} \right] \right) \\
&\qquad \times X_{2i} \left(\sum_{k=1}^{N} \left[\begin{array}{cc} \tilde{B}_{kii} & B_{k12} \end{array} \right] z(t-R_k^*) \right) \\
&\quad - \sum_{i=1}^{N} \int_{t-R_i^*}^{t} z^T(s) \left[\begin{array}{c} A_{11}^T \\ 0 \end{array} \right] \times X_{1i} \left[\begin{array}{cc} A_{11} & 0 \end{array} \right] z(s) ds \\
&\quad - \sum_{i=1}^{N} \int_{t-R_i^*}^{t} \left(\sum_{j=1}^{N} z^T(s-R_j^*) \left[\begin{array}{c} \tilde{B}_{jii}^T \\ B_{j12}^T \end{array} \right] \right) \times X_{2i} \left(\sum_{k=1}^{N} \left[\begin{array}{cc} \tilde{B}_{kii} & B_{k12} \end{array} \right] z(s-R_k^*) \right) ds.
\end{aligned}
$$

Then, we have

$$\begin{aligned}
&\frac{dV(z(t))}{dt} \\
&\leq z^T(t)\Xi z(t) + 2z^T(t)\sum_{i=1}^{N}\Delta_i z(t-R_i^*) \\
&\quad + \sum_{i=1}^{N} R_i^* \left(\sum_{j=1}^{N} z^T(t-R_j^*) \begin{bmatrix} \tilde{B}_{jii}^T \\ B_{j12}^T \end{bmatrix}\right) \\
&\qquad \times X_{2i}\left(\sum_{k=1}^{N} \begin{bmatrix} \tilde{B}_{kii} & B_{k12} \end{bmatrix} z(t-R_k^*)\right) \\
&\quad - \sum_{i=1}^{N} z^T(t-R_i^*) Q_i z(t-R_i^*),
\end{aligned} \tag{5.25}$$

where

$$\begin{aligned}
\Xi := \Phi + \sum_{i=1}^{N} R_i^* P \begin{bmatrix} \tilde{B}_{i11} \\ L\tilde{B}_{i11} \end{bmatrix} (X_{1i}^{-1} + X_{2i}^{-1}) \\
\times \begin{bmatrix} \tilde{B}_{i11}^T & \tilde{B}_{i11}^T L^T \end{bmatrix} P.
\end{aligned}$$

Therefore, we obtain

$$\frac{dV(z(t))}{dt} \leq w^T(t)\Pi w(t). \tag{5.26}$$

where

$$\begin{aligned}
\Pi &:= \begin{bmatrix} \Xi & \Delta_1 & \cdots & \Delta_N \\ \Delta_1^T & \Lambda_1 & \cdots & \Lambda_{1N} \\ \vdots & \vdots & \ddots & \vdots \\ \Delta_N^T & \Lambda_{N1} & \cdots & \Lambda_N \end{bmatrix}, \\
w(t) &:= \begin{bmatrix} z^T(t) & z^T(t-R_1^*) & \cdots & z^T(t-R_N^*) \end{bmatrix}.
\end{aligned}$$

Finally, using Schur complement for matrix inequality $\Pi < 0$ results in $\Gamma < 0$. This completes the proof of the theorem. □

Furthermore, sufficient conditions for robust asymptotic stability of system (5.11) is given in the following corollary.

Corollary 5.9 *If there exist* $\bar{P}_1 = \bar{P}_1^T > 0$, $\bar{P}_2 = \bar{P}_2^T > 0$, $\bar{Q}_{1i} = \bar{Q}_{1i}^T > 0$ *and* $\bar{Q}_{2i} = \bar{Q}_{2i}^T > 0$ *such that the LMI*

$$\bar{\Pi} := \begin{bmatrix} \bar{\Phi} & \bar{\Delta}_1 & \cdots & \bar{\Delta}_N \\ \bar{\Delta}_1^T & -\bar{Q}_1 & \cdots & 0 \\ \vdots & \vdots & \ddots & \vdots \\ \bar{\Delta}_N^T & 0 & \cdots & -\bar{Q}_N \end{bmatrix} < 0, \tag{5.27}$$

where

$$\bar{\Phi} := \begin{bmatrix} \bar{P}_1 A_{11} + A_1^T \bar{P}_1 + \sum_{i=1}^{N} \bar{Q}_{1i} & 0 \\ 0 & \bar{P}_2 A_{22} + A_{22}^T \bar{P}_2 + \sum_{i=1}^{N} \bar{Q}_{2i} \end{bmatrix}$$
$$+ \sum_{i=1}^{N} \left(\bar{P} \begin{bmatrix} \bar{B}_i & 0 \\ A_{22}^{-1} A_{21} \bar{B}_i & 0 \end{bmatrix} + \begin{bmatrix} \bar{B}_i & 0 \\ A_{22}^{-1} A_{21} \bar{B}_i & 0 \end{bmatrix}^T \bar{P} \right),$$
$$\bar{\Delta}_i := \bar{P} \begin{bmatrix} 0 & B_{i12} \\ 0 & A_{22}^{-1} A_{21} B_{i12} \end{bmatrix},$$
$$\bar{Q}_i := \begin{bmatrix} \bar{Q}_{1i} & 0 \\ 0 & \bar{Q}_{2i} \end{bmatrix}, \ \bar{P} := \begin{bmatrix} \bar{P}_1 & 0 \\ 0 & \bar{P}_2 \end{bmatrix}.$$

then there exist small enough $\bar{\varepsilon}$ *and* $\bar{R}$ *such that for all* $\varepsilon \in (0, \bar{\varepsilon})$ *and* $R_i^* \in (0, \bar{R})$*, system (5.11) is asymptotically stable.*

It is worth pointing out that sufficient conditions (5.20) and (5.27) derived in Theorem 5.8 are both given in terms of linear matrix inequalities. These conditions can be easily assessed by applying the LMI Control Toolbox with Matlab.

Remarks: The singular perturbation approach applied in system (5.11) provides two distinct advantages. First, this approach demonstrates the existence of small singular perturbation parameter and time delays that guarantee the asymptotic stability of the system. Second, when time delays are sufficiently small, asymptotic stability can be guaranteed by checking LMI (5.27), whose order is much smaller than (5.20) and needs less computation. Mathematically deriving the bounds of singular perturbation parameter and time delays is an important problem, for which no general solution has been found. This issue is not addressed in the current work.

5.6 Numerical Results and Performance Evaluation

With the two-bottleneck topology described in Sec. 5.4, we first obtain the system evolution trajectories by using *Matlab* to verify the asymptotic stability proved in Secs. 5.3 and 5.4. Network simulator, NS-2, is then used to further study the performance of the systems.

5.6.1 Numerical Results

System without feedback delays

Figs. 5.3 - 5.5 show the traces of window size and queue length under the topology of Fig. 5.2, modeled by (5.9). The capacity of L_1 is $C_1 = 1 \times 10^5$ packet/sec, that of

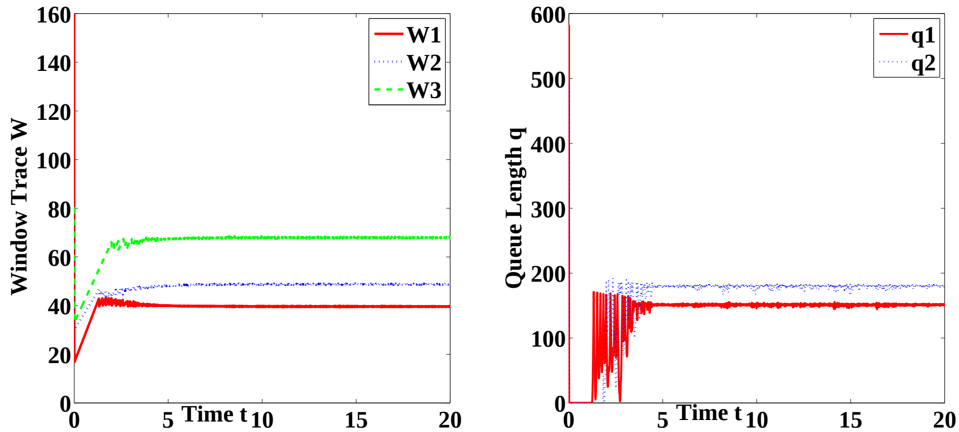

(a) Window trace (b) Queue length

Figure 5.3: Homogeneous TCP flows, delay-free

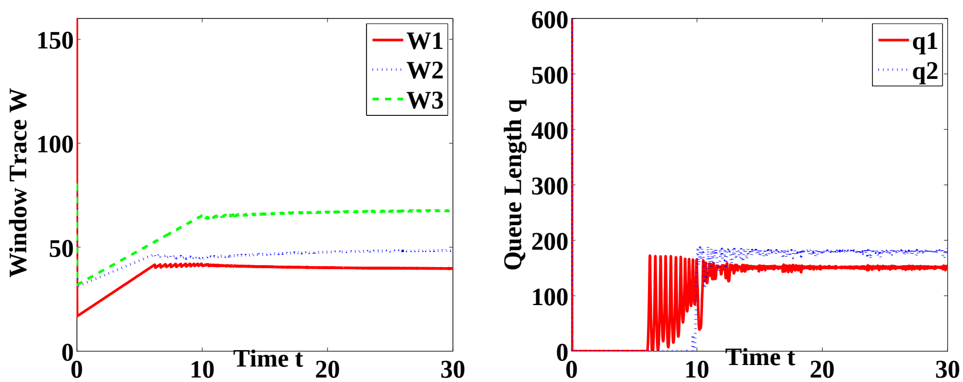

(a) Window trace (b) Queue length

Figure 5.4: Homogeneous AIMD(0.2, 0.875) flows, delay-free

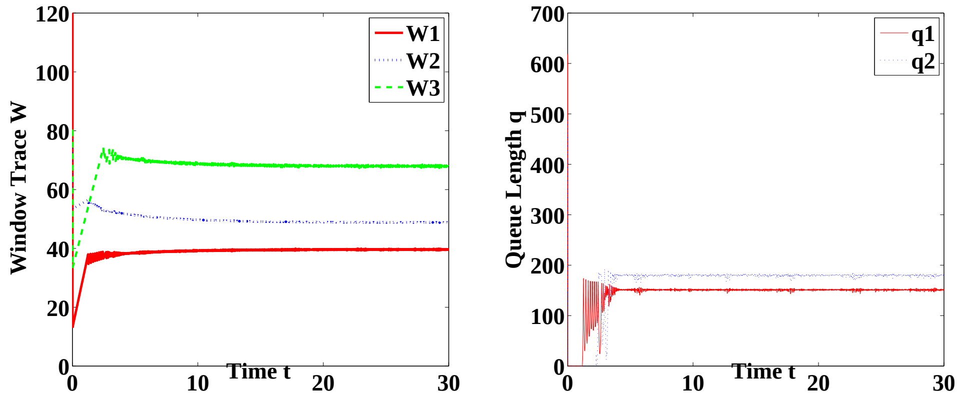

(a) Window trace (b) Queue length

Figure 5.5: TCP and AIMD(0.2, 0.875) flows, delay-free

L_2 is $C_2 = 12 \times 10^4$ packet/sec. The number of flows in each groups are $N_1 = 80$, $N_2 = 60$ and $N_3 = 50$, respectively. The deterministic round trip times of these groups are $T_{p_1} = 0.05$ sec, $T_{p_2} = 0.08$ sec and $T_{p_3} = 0.06$ sec, respectively. We choose $K_{p_1} = 0.0006$, $K_{p_2} = 0.0008$, Q_{min1}=150 packets and Q_{min2}=180 packets.

In Fig. 5.3, all flows are TCP flows, i.e., $(\alpha, \beta) = (1, 0.5)$. In Fig. 5.4, all flows are AIMD flows with the same parameter pair, $(\alpha, \beta) = (0.2, 0.875)$. W_i in Fig. 5.3 (a) and Fig. 5.4 (a) represents the average window size of flows in the i-th group, and q_1 and q_2 in Fig. 5.3 (b) and Fig. 5.4 (b) represent the bottleneck queue lengths at r_1 and r_2, respectively. It can be seen that both the average window sizes and queue lengths converge to constants in steady state. Although the convergence speed of homogeneous TCP flows is faster than that of homogeneous AIMD flows, their average windows and the average queue lengths in steady state are the same.

We further investigate the case that different groups of flows use different AIMD

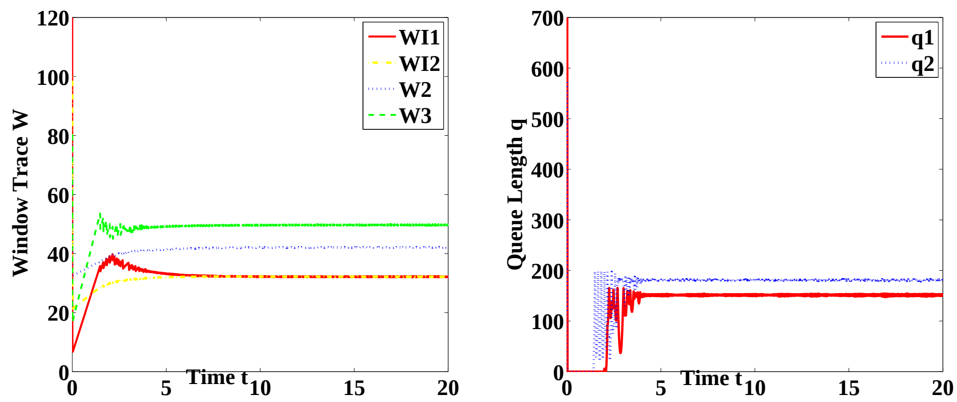

(a) Window trace (b) Queue length

Figure 5.6: TCP and AIMD(0.2,0.875) flows, heterogeneous traffic in group I

parameters. The flow parameters of the three groups in Fig. 5.5 are $(\alpha_1, \beta_1) = (1, 0.5)$, $(\alpha_2, \beta_2) = (0.2, 0.875)$ and $(\alpha_3, \beta_3) = (1, 0.5)$, respectively. The numerical results show that the average window sizes of the three groups of flows and queue lengths of the two bottleneck routers converge to constants. Since all the trajectories are asymptotically stable, thereby validating Theorem 5.1. In addition, the average window sizes of each groups in Figs. 5.3-5.5 are the same in steady state, which means AIMD $(0.2, 0.875)$ flows are TCP-friendly.[1] This property can be further illustrated in the following case.

The traces of window size and queue lengths when there are two different classes of flows in group I are shown in Fig. 5.6, which is modeled by (5.6). Here the number of flows within each group is chosen as $N_{11} = N_{12} = 40$, $N_2 = 60$ and $N_3 = 50$.

[1] *TCP-friendliness* is defined as the average throughput of non-TCP-transported flows over a large time scale does not exceed that of any conformable TCP-transported ones under the same circumstance [47]. It has been shown that if an AIMD flow with the parameter pair satisfying the condition $\frac{\alpha(1+\beta)}{1-\beta} = 3$, the AIMD flow is TCP-friendly [12, 27].

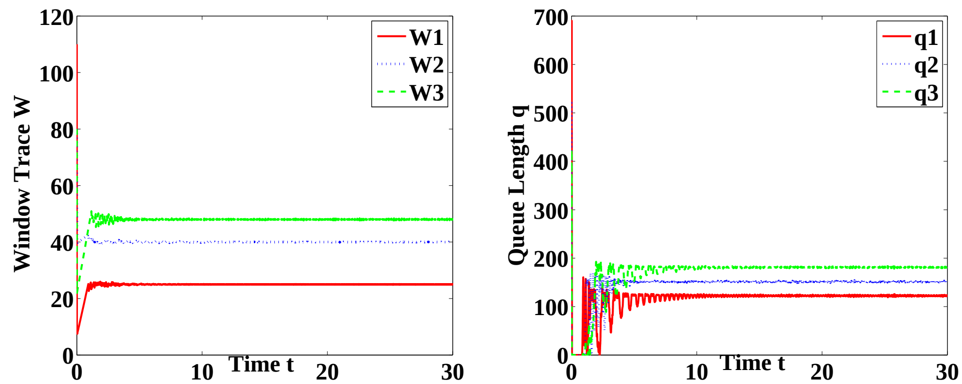

(a) Window trace (b) Queue length

Figure 5.7: TCP and AIMD(0.2, 0.875) flows, delay-free, three bottleneck links

Their deterministic RTTs are $T_{p_{11}} = 0.05$ sec, $T_{p_{12}} = 0.04$ sec, $T_{p_2} = 0.06$ sec and $T_{p_3} = 0.04$ sec, respectively. Also, we have $C_1 = 1 \times 10^5$ packet/sec and $C_2 = 1.2 \times 10^5$ packet/sec as in Figs. 5.3 - 5.5 with $K_{p_1} = 0.0006$ and $K_{p_2} = 0.0008$. The AIMD parameter pairs in this case are $(\alpha_{11}, \beta_{11}) = (\alpha_3, \beta_3) = (1, 0.5)$ and $(\alpha_{12}, \beta_{12}) = (\alpha_2, \beta_2) = (0.2, 0.875)$, respectively. It can be seen that both the window size and queue length are asymptotically stable and are consistent with our analysis, and the AIMD(0.2, 0.875) flows are truly TCP-friendly.

Figs. 5.7 and 5.8 show how the window size and queue length evolve when the link capacity of rr_2 for group I flows, C_3, is so small that the link rr_2 becomes the third bottleneck. Consequently, there are three bottlenecks in the network under the topology shown in Fig. 5.2. We choose $N_1 = 80$, $N_2 = 60$ and $N_3 = 50$, $C_1 = 8 \times 10^4$ packet/sec, $C_2 = 1 \times 10^5$ packet/sec and $C_3 = 4 \times 10^4$ packet/sec with $K_{p_1} = 0.0004$, $K_{p_2} = 0.0006$ and $K_{p3} = 0.0008$, respectively. The deterministic RTTs are chosen as $T_{p_1} = 0.05$ sec, $T_{p_2} = 0.06$ sec and $T_{p_3} = 0.04$ sec. In Fig. 5.7, $(\alpha_1, \beta_1) = (\alpha_3, \beta_3) = (1, 0.5)$, and

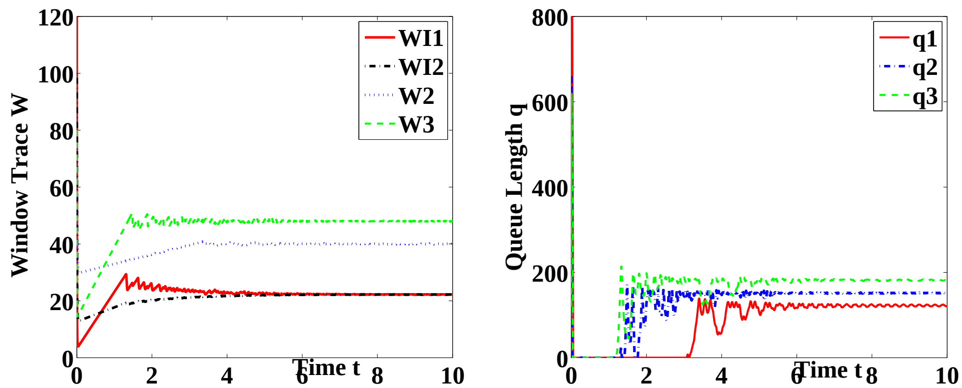

(a) Window trace (b) Queue length

Figure 5.8: TCP and AIMD(0.2,0.875) flows, delay-free, three bottleneck links

$(\alpha_2,\, \beta_2) = (0.2,\, 0.875)$. In Fig. 5.8, there are two types of flows in group I, with $N_{11} = 40$, $N_{12} = 40$; and $T_{p_{11}} = 0.05\,$sec, $T_{p_{12}} = 0.04\,$sec. Other parameters are chosen as $(\alpha_{11},\, \beta_{11}) = (\alpha_3,\, \beta_3) = (1,\, 0.5)$, $(\alpha_{12},\, \beta_{12}) = (\alpha_2,\, \beta_2) = (0.2,\, 0.875)$. We can observe the property of the asymptotic stability of these systems from the numerical results.

System with feedback delays

Figs. 5.5 - 5.8 show the asymptotic stability of the multiple-bottleneck system without feedback delays, in which the property of stability is global. Figs. 5.9 - 5.11 illustrate the local asymptotic stability of the system with feedback delays. We choose $N_1 = N_2 = N_3 = 5$, $C_1 = 3 \times 10^3$ packet/sec, $C_2 = 5 \times 10^3$ packet/sec with $K_{p_1} = K_{p_2} = 0.0005$. The deterministic RTTs for the flows are chosen as $T_{p_1} = 0.020\,$sec, $T_{p_2} = 0.013\,$sec and $T_{p_3} = 0.007\,$sec, respectively. The parameters used are the same as those in the numerical example of Theorem 5.2. In Fig. 5.9, $(\alpha_i,\, \beta_i) = (1,\, 0.5)$ for $i = 1, 2, 3$; in

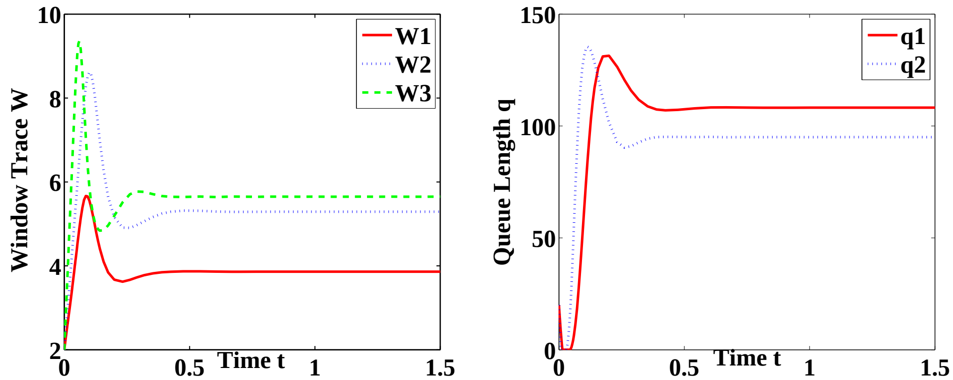

(a) Window trace (b) Queue length

Figure 5.9: Homogeneous TCP flows, with feedback delay

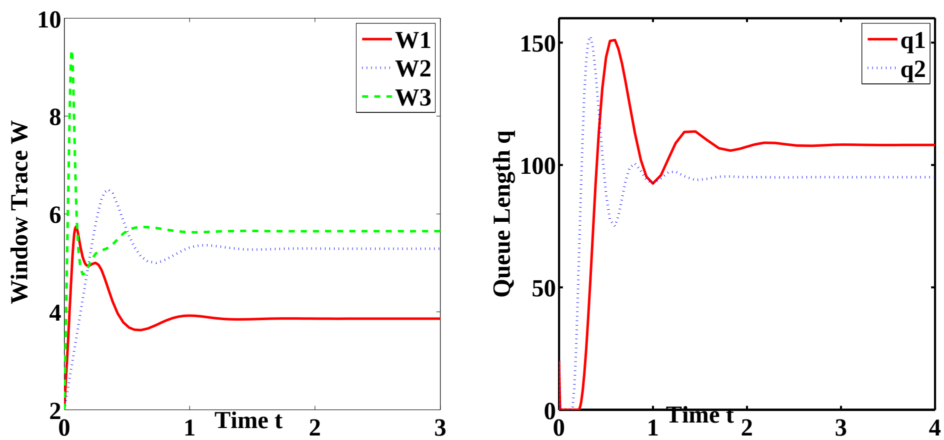

(a) Window trace (b) Queue length

Figure 5.10: Homogeneous AIMD flows, with feedback delay

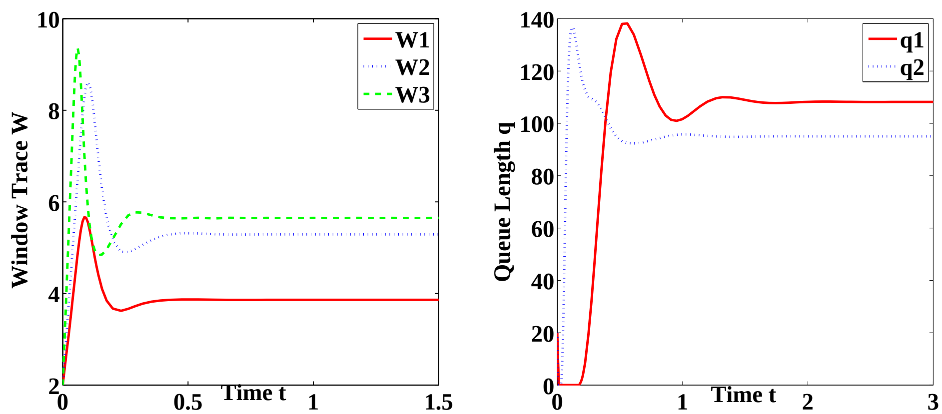

(a) Window trace (b) Queue length

Figure 5.11: TCP and AIMD flows, with feedback delay

Fig. 5.10, $(\alpha_i,\ \beta_i) = (0.2,\ 0.875)$ for $i = 1, 2, 3$; and in Fig. 5.11, $(\alpha_1,\ \beta_1) = (\alpha_3,\ \beta_3) = (1,\ 0.5)$, $(\alpha_2,\ \beta_2) = (0.2,\ 0.875)$. As shown in the figures, all the trajectories are locally asymptotically stable, and the numerical results validate the theorems.

In the last part of this section, we give an example of an unstable multiple-bottleneck RED network. We choose $N_1 = N_3 = 4$, $N_2 = 8$, $C_1 = 1000$ packet/sec, $C_2 = 1000$ packet/sec with $K_{p_1} = K_{p_2} = 0.05$ and $(\alpha_i,\ \beta_i) = (1,\ 0.5)$ for $i = 1, 2, 3$ with $T_{p_1} = 0.03$ sec, $T_{p_2} = 0.03$ sec and $T_{p_3} = 0.04$ sec. This case has been shown unstable in [61] and it is consistent with our results in Fig. 5.12. It is easy to check that this case does not satisfy the conditions of Theorems 5.2 and 5.3.

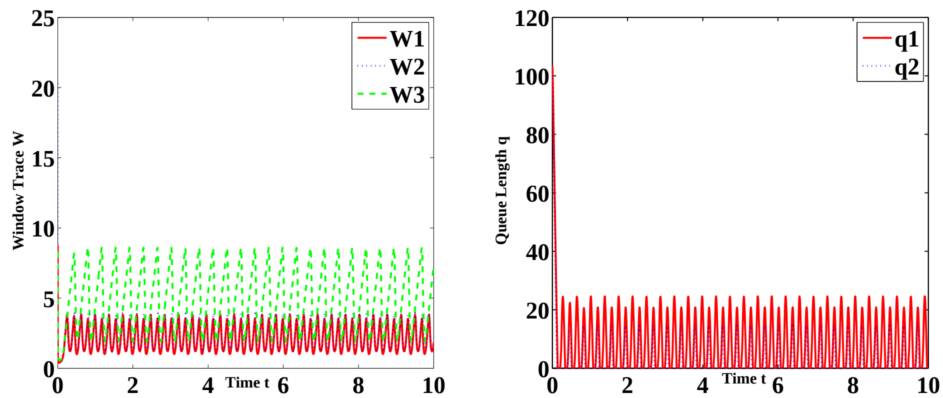

(a) Window trace (b) Queue length

Figure 5.12: Homogeneous TCP flows: unstable case

5.6.2 Simulation Results

We use network simulator (NS-2) to further study the performance of the AIMD/RED system with realistic protocols and network topologies. The same multiple-bottleneck topology as in Fig. 5.2 is used in the simulations.

We first validate a theoretically stable setting. The parameters used are the same as those used for Fig. 5.11. It should be mentioned that, since the fluid model describes the *ensemble average*s of window size and queue length, the asymptotically stable property applies to the ensemble averages or time averages over a round. Here, a round is defined as the time interval between two instants at which the sender reduces its window size consecutively. Therefore, we focus on the time averages of the window size and queue length over a round. Fig. 5.13 shows that the time averages of the flow window sizes and queue lengths are converging to certain values, i.e., their time averages over a round are asymptotically stable. The average window sizes in the NS-2 simulation results are

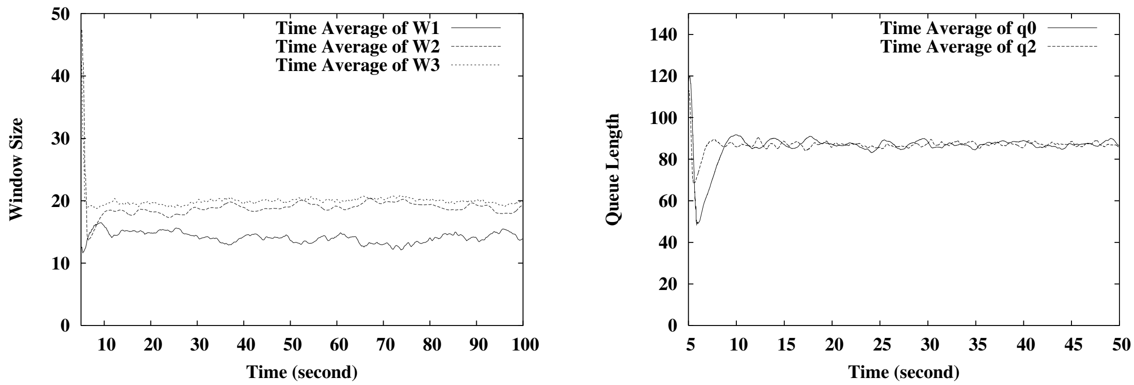

(a) Window trace (b) Queue length

Figure 5.13: Simulation results for a stable system

slightly larger than the numerical results. This is because the numerical simulations with Matlab ignore the queuing delay in RTTs, which under-estimates the window size.

We also run the simulation for the unstable case with the same parameters as those used in Fig. 5.12, and the results are shown in Fig. 5.14. It can be seen that even averaging over a round, the window sizes and queue lengths are still highly oscillating. The simulation results validate the analytical ones.

5.7 Related Work

Internet stability analysis has recently received much attention. In particular, the stability of TCP systems has been studied from the point of window-based flow control [9, 7, 19, 23, 25, 26, 27] and rate control [64, 65]. New control mechanisms such as those in [35] are also proposed for the Internet, aiming to achieve quick convergence to efficiency, stability, fair bandwidth sharing, and low packet loss rate.

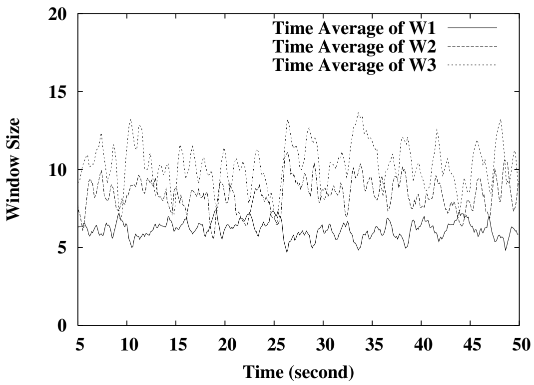

(a) Window trace

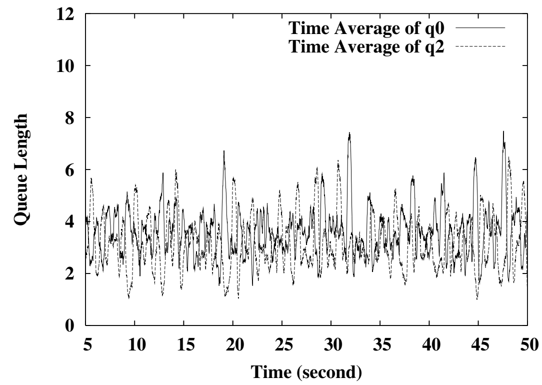

(b) Queue length

Figure 5.14: Simulation results for an unstable system

In practice, it is very likely that heterogeneous flows with different round-trip delays may undergo multiple bottlenecks. To date, little work has been done on the stability and analysis of multiple-bottleneck networks. It has been shown in [61] that RED configuration based on a single-bottleneck assumption may not prevent traffic instability when congestion occurs in two different locations of the network simultaneously. Recent work [62] studied a class of TCP/RED multiple-bottleneck model and tried to avoid network congestion by imposing some restrictions of AQM parameters. In this chapter, we study the general case of multiple-bottleneck AIMD/RED systems and obtain sufficient conditions for the asymptotic stability with and without feedback delays. It is illustrated that appropriate system parameters can be chosen to make the system asymptotically stable.

5.8 Summary and Future Discussions

In this chapter, we have developed a class of general AIMD/RED models for multi-bottleneck systems, and have studied stability properties for the models with delay-free marking and with heterogeneous delays, respectively. We have proved the global asymptotic stability for the multiple-bottleneck AIMD/RED systems without feedback delay, and then derived sufficient conditions or the local asymptotic stability of multiple-bottleneck AIMD/RED systems with heterogeneous delays, by applying the methods of Lyapunov functional and Lyapunov function with the Razumikhin condition. These results are obtained for general multiple-bottleneck scenarios and provide important guidelines for setting system parameters that guarantee the efficient utilization of network resources in multi-bottleneck networks without excessive delay jitter. We are currently investigating sufficient conditions for establishing global stability in the presence of heterogeneous delays, by developing a sequence of upper and lower bounds of system trajectories and applying these bounds in Razumikhin's Theorem. The generalization of stability analysis for networks with mesh topologies will also be an interesting future research direction.

Chapter 6

Conclusions and Future Work

In this chapter, we conclude the thesis by summarizing main research results and proposing future work.

6.1 Main Research Results

The goal of congestion control mechanisms is to use the network resources as efficiently as possible, that is, attain the highest possible throughput while maintaining a low loss ratio and small delay. The research work is centered on finding ways to address these types of problems and provide guidelines for predicting and controlling network performance, through the use of suitable mathematical tools and control analysis.

- We first systematically studied the stability of a class of generalized AIMD/RED system and obtained sufficient conditions for asymptotic stability of both homogeneous- and heterogeneous-flow systems with and without feedback delay by using direct

Lyapunov and Lyapunov-Razumikhin method. Our study reveals the relationship between the AIMD parameters and the average window size of competing AIMD flows. Consequently, the TCP-friendly condition is derived. The analytical and simulation results can help us to better understand the stability and performance of AIMD/RED system.

- Even though previous research indicated that the AIMD/RED system may not be asymptotically stable when the time delay or the link capacity becomes large, as long as the system operates near its desired equilibrium, small oscillations are acceptable, and the network performance is still satisfactory. Motivated by this, we studied the practical stability of the homogeneous- and heterogeneous-flow AIMD/RED systems with feedback delays, and obtained theoretical bounds on the AIMD flow window size and the RED queue length. Our analytical and simulation results provide important insights on which system parameters contribute to higher oscillations of the system and the derived theoretical bounds can be used as a guideline to set up the system parameters to enhance system efficiency with bounded delay and loss. These results can also help to predict and control the system performance for Internet with higher data rate links multiplexed with more flows with different parameters.

- A realistic network normally accommodate flows that undergo multiple bottleneck. It has been known that the network system with multiple-bottleneck links could be unstable even if its system parameters are set the same as those in a stable single-bottleneck system. Because of this reason, we studied the stability of the general AIMD/RED system with multiple bottlenecks. A general model for multi-bottleneck scenarios was first developed and sufficient conditions for the asymptotic stability of multiple-bottleneck systems with and without heterogeneous delays were derived. These conditions can be easily assessed by using LMI Toolbox.

6.2 Future Work

Congestion control is a topic that has drawn attentions of many researchers, and it has also become a facet of daily life for Internet users. The emergence and development of new Internet technologies have brought with them new problems which need to be solved. In this section, we identify several potential research directions from this thesis for future work.

- Global stability analysis of Multiple-Bottleneck Systems

  Intuitively, the Internet system is stable if all transmitted packets will be eventually processed by the link and reach the intended destination. Stability problems have been investigated for the Internet models with a single-bottleneck. As the Internet is becoming a more diverse system, most flows traverse multiple bottlenecks. The theoretical and performance analysis for the multiple-bottleneck network is becoming more and more necessary.

  Local stability results for multiple-bottleneck systems constitute one aspect of the work in this thesis. But when considering the uncertain factors and unpredictable changes in the Internet, the guarantee of convergence associated with a global stability result carries significant weight. To address this problem, a plausible approach is to apply the iterative method and construct monotone sequences that converge to the trivial solution of the system.

- Bound estimates of Multiple-bottleneck systems

  For the vast-scale Internet, the single bottleneck topology may no longer be representative and a flow may traverse multiple links with non-negligible packet losses. As long as the system operates near its desired equilibrium, small oscillations are acceptable, the overall system efficiency can still be very high, and the network performance is still satisfactory. Therefore, besides stability analysis, another important research issue is to study the bounds of the multiple-bottleneck network.

  Upper and lower bounds estimates for single-bottleneck systems form one important chapter of this thesis. However, so far, there is no result for the bounds estimates of multiple-bottleneck systems because of the difficulties in modeling and theoretical analysis. We are going to solve this issue by applying the method of comparison theory and approximation technique. The study of this topic will be theoretically original and of great practical value for controlling, predicting and enhancing the system performance

- Adding impulsive control in the congestion control mechanism

  Abrupt changes at selected moment can be expressed in terms of impulses. Existent theoretical results have shown that impulsive control can speed up the convergence of a system to its steady state.

  For the Internet congestion, adding proper impulsive control can help the system converge to its steady state more quickly, stay in the desired operating area longer, and even avoid some serious latent congestion. As far as we know, no results for impulsive control to the Internet have been reported. Based on the existing work on the theoretical analysis of impulsive systems, proper controller shall be designed for the Internet congestion

- Modeling and theoretical analysis of TCP/AIMD performance over wireless links

  Although fluid model is successfully applied for performance analysis in wired domain, it is not suitable in wireless networks. Time to successfully transmit a packet in wireless link is not negligible when compared to the total transfer time. With time-varying delay and bandwidth wireless link, the $RTTs$ of each packet is highly variable according to not only the queue length but also the wireless channel state. The fluid traffic model cannot capture this characteristic.

  Because of the wireless link's own characteristics, such as limited bandwidth, high error rate, time-varying and location dependent, mathematically modeling and theoretical analysis of TCP/AIMD performance over wireless links becomes a great challenge. At the time of writing, no related results had been presented on this matter and some of our future efforts will be put on this issue.

6.3 Final Remarks

In this thesis, we systematically studied the widely used AIMD/RED system in the Internet, particularly on system modeling, stability analysis and bounds estimates. Our theoretical analysis provide important insights for in-depth understanding of the congestion control problem, and have shown how to guarantee system efficiency with bounded delay and loss. Results in this thesis can also help to predict and control the system performance for the Internet with higher data rate links multiplexed with heterogeneous flows.

Bibliography

[1] J. Postel, “Transmission Control Protocol,” RFC 793, Sept. 1982.

[2] W. R. Steven, *TCP/IP Illustrated, Volume I.* Addison-Weslry, Reading, MA, Nov. 1994.

[3] V. Jacobson and M. Karels, “Congestion avoidance and control,” *Proc ACM SIGCOMM’88*, pp. 314-329, 1988.

[4] D. M. Chiu and R. Jain, “Analysis of the Increase and Decrease Algorithms for Congestion Avoidance in Computer Networks,” *Computer Networks and ISDN Systems*, Vol. 17, no. 1, pp. 1-14, June 1989.

[5] D. Bertsekas and R. Gallager, *Data Networks* Prentice Hall, NJ. 1987.

[6] R. Srikant, *The mathematics of Internet Congestion Control*, Birkhauser Boston, ISBN: 978-0-8176-3227-4, 2004.

[7] R. Johari and D. K. H. Tan, “End-to-End Congestion Control for the Internet: Delays and Stability,” *IEEE/ACM Transactions on Networking*, Vol. 9, no. 6, pp. 818-832, December 2001.

[8] F. P. Kelly, "Models for a Self-Managed Internet," *Philosoph. Trans. Royal Soc. London*, vol. 358, pp. 2335-2348, 2000.

[9] S. Low, F. Paganini, J. Wang, S. Adlakha and J. C. Doyle, "Dynamics of TCP/RED and a Scalable Control," *IEEE Infocom'02*, vol. 1, pp. 239-248, June 2002.

[10] S. Floyd, M. Handley and J. Padhye, "A Comparison of Equation-Based and AIMD Congestion Control", May 2000. Available `http://www.aciri.org/tfrc/tcp-friendly.TR.ps`.

[11] Y. R. Yang and S. S. Lam, General AIMD Congestion Control. Technical Report TR-2000-09, University of Texas, May 2000. A shorter version appeared in Proceedings of ICNP'00, Osaka, Japan, November 2000.

[12] L. Cai, X. Shen, J. Pan and J. W. Mark, "Performance Analysis of TCP-Friendly AIMD Algorithms for Multimedia Applications," *IEEE Trans. on Multimedia*, Vol. 7, No. 2, pp. 339–355, April 2005.

[13] V. Firoiu and M. Borden, "A Study of Active Queue Management for Congestion Control," *In Proceedings of Infocom*, Vol. 3, pp. 1435-1444, Mar 2000.

[14] S. Floyd and V. Jacobson, "Random Early Detection Gateways for Congestion Avoidance," *IEEE/ACM Transactions on Networking*, Vol. 1, pp. 397-413, August 1993.

[15] D. Lin and R. Morris, "Dynamics of Random Early Detection," *Proceedings of ACM/SIGCOMM*, pp. 127-137, 1997.

[16] F. P. Kelly, A. K. Maulloo and D. K. H. Tan, “Rate Control for Communication Networks: Shadow Prices, Proportional Fairness and Stability,” *Journal of the Operational Research Society,* Vol. 49, No. 3, pp. 237-252, March, 1998.

[17] S. Deb and R. Srikant, “Global Stability of Congestion Controllers for the Internet,” *IEEE Trans. on Automatic Control*, Vol. 48, No. 6, pp. 1055-1060, June 2003.

[18] L. Ying, G. E. Dullerud and R. Srikant, “Global Stability of Internet Congestion Controllers with Heterogeneous Delays,” *American Control Conference*, Vol. 4, pp. 2948-2953, June 2004.

[19] Y. Zhang, S. Kang and D. Loguinov, “Delayed Stability and Performance of Distributed Congestion Control,” *Proc. of the 2004 conference on Applications, technologies, architectures, and protocols for computer communications,* pp. 307-318, 2004.

[20] Z. Wang and F. Paganini, “Global Stability with Time-Delay in Network Congestion Control,” *Proc. IEEE Conf. on Decision and Control,* Vol. 4, pp. 3632-3637, LasVegas, NV, Dec. 2002.

[21] S. Low, “A Duality Model of TCP and Queue Management Algorithms,” *IEEE Trans. on Networking*, Vol. 11, No. 4, pp. 525-536, Aug. 2003.

[22] V. Misra, W. B. Gong and D. Towsley, “Fluid-Based Analysis of a Network of AQM Routers Supporting TCP Flows,” *Proc. of ACM/SIGCOMM*, pp. 151–160, 2000.

[23] C. V. Hollot, V. Misra, D. Towsley and W. B. Gong, “Analysis and Design of Controllers for AQM Routers Supporting TCP Flows,” *IEEE Trans. on Automatic Control*, Vol. 47, No. 6, pp. 945-959, June 2002.

[24] C. V. Hollot, V. Misra, D. Towsley and W. B. Gong, “On Designing Improved Controllers for AQM Routers Supporting TCP Flows,” *Proc. of IEEE INFOCOM*, Anchorage, pp. 1726–1734, April 2001.

[25] C. V. Hollot, V. Misra, D. Towsley and W. B. Gong, “A Control Theoretic Analysis of RED,” *Proc. of IEEE INFOCOM*, Anchorage, pp. 1510–1519, April 2001.

[26] C. V. Hollot and Y. Chait, “Non-Linear Stability Analysis of a Class of TCP/AQM Networks,” *Proc. of IEEE Conference on Decision and Control*, Vol. 3, pp. 2309-2314, Orlando, Florida USA, Dec. 2001.

[27] L. Wang, L. Cai, X. Liu and X. Shen, “Stability and TCP-friendliness of AIMD/RED Systems with Feedback Delays,” *Computer Networks*, Vol. 51, No. 15, pp. 4475-4491, Oct. 2007.

[28] L. Wang, L. Cai, X. Liu and X. Shen, ”Stability and Fairness Analysis of AIMD/RED System with Heterogeneous Delays”, *Proc. of IEEE Globecom*, pp. 1813-1817, Dec. 2007.

[29] L. Wang, L. Cai, X. Liu and X. Shen, “AIMD Congestion Control: Stability, TCP-friendliness, Delay Performance,” *Tech. Rep.*, Mar. 2006. Available `http://www.ece.uvic.ca/~cai/tech-2006.pdf`

[30] L. Wang, L. Cai, X. Liu and X. Shen, “Practical Stability and Bounds of Heterogeneous AIMD/RED System with Time Delay,” *Proc. of IEEE ICC*, Beijing China, pp. 5558-5563, May 2008.

[31] L. Wang, L. Cai, X. Liu and X. Shen, "Boundedness of AIMD/RED Systems with Time Delays," *Tech. Rep.*, Jul. 2007. Available `http://www.ece.uvic.ca/~cai/tech2007.pdf`.

[32] L. Wang, H. Mukaidani, X. Shen and X. Liu, "Delay-Dependent Stability Analysis for Large-Scale Multiple-Bottleneck Systems Using Singular Perturbation Approach", to appear, *Proc. of IEEE Globecom 2008* Available `http://www.math.uwaterloo.ca/~l44wang/tech08.pdf`.

[33] L. Wang, L. Cai, X. Liu, X. Shen and J. Zhang, "Stability Analysis of Multiple-Bottleneck Networks", *submitted to Computer Networks*, January 2008.

[34] Y. Chait, C. V. Hollot, V. Misra, S. Oldak, D. Towsley and W. B. Gong, "Fixed and Adaptive Model-Based Controllers for Active Queue Management," *Proc. of ACC*, Vol. 4, pp. 2981-2986, 2001.

[35] C. Wang, J. Liu, B. Li, K. Sohraby and Y. T. Hou, "LRED: A Robust and Responsive AQM Algorithm Using Packet Loss Ratio Measurement," *IEEE Trans. on Parallel and Distributed Systems*, Vol. 18, No.1, pp. 29-43, January 2007.

[36] D. G. Luenberger, *Introduction to Dynamic Systems: Theory, Models, and Application*, May 1979. ISBN: 0-471-02594-1

[37] V. Firoiu and M. Borden, A Study of Active Queue Management for Congestion Control, *In Proceedings of IEEE Infocom*, 2000.

[38] S. Floyd and V. Jacobson, Random Early Detection gateways for congestion avoidance, *IEEE/ACM Transactions on Networking*, Vol.1, August 1997.

[39] D. Lin and R. Morris, Dynamics of Random Early Detection, *Proceedings of ACM/SIGCOMM*, 1997.

[40] "Configuring Weighted Random Early Detection," *Cisco IOS Release 12.0 Quality of Service Solutions Configuration Guide*, `http://www.cisco.com/en/US/docs/ios/12_0/qos/configuration/guide/qcwred.pdf`

[41] "Configuring Dropping Behavior with RED and WRED," *Juniper Quality of Service Configuration Guide*, `http://www.juniper.net/techpubs/software/erx/junose90/swconfig-qos/html/drop-profiles-config.html`

[42] S. Shakkottai, R. Srikant and S. Meyn, "Bounds on the Throughput of Congestion Controllers in the Presence of Feedback Delay," *IEEE Transactions on Networking*, vol. 11, no. 6, pp. 972-981, Dec. 2003.

[43] Z. Wang and F. Paganini, "Boundedness and Global Stability of a Nonlinear Congestion Control with Delays," *IEEE Transactions on Automatic Control*, vol. 51, no. 9, pp. 1514-1519, Sept. 2006.

[44] L. Ying, G. E. Dullerud and R. Srikant,"Global Stability of Internet Congestion Controllers with Heterogeneous Delays," *IEEE Transactions on Networking*, vol. 14, no. 3, pp. 579-591, Jun. 2006.

[45] S. Deb and R. Srikant, "Global Stability of Congestion Controllers for the Internet," *IEEE Transactions on Automatic Control*, vol. 48, no. 6, pp. 1055-1060, Jun. 2003.

[46] S. Shakkottai and R. Srikant, "How Good are Deterministic Fluid Model of Internet Congestion Control?" *IEEE Infocom'02*, vol. 2, pp. 497-505, Jul. 2002.

[47] S. Floyd and K. Fall, "Promoting the use of end-to-end congestion control in the Internet," *IEEE/ACM Transactions on Networking*, vol. 7, no. 4, pp. 458-472, Aug. 1999.

[48] S. Liu, T. Basar and R. Srikant, "Pitfalls in the Fluid Modeling of RTT Variations in Window-Based Congestion Control," *Proc. of IEEE INFOCOM*, vol. 2, pp. 1002-1012, Miami, Florida USA, March 2005.

[49] V. Lakshmikantham, S. Leela, A. A. Martynyuk, *Practical Stability of Nonlinear System* World Scientific, Nov. 1990, ISBN: 9810203519.

[50] V. Lakshmikantham, X. Liu, *Stability Analysis in Terms of Two Measures* World Scientific, Feb. 1994, ISBN: 9810213891.

[51] H. K. Khalil, *Nonlinear Systems*, Upper Saddle River, N.J.: Prentice Hall, 2002.

[52] S. J. Leon, *Linear Algebra with Applications,* Macmillan Publishing Company, Inc., New York, 1994.

[53] H. K. Hale and S. M. Verduyn Lunel, *Introduction of Functional Differential Equations,* Springer-Verlag, New York, 1993.

[54] A. Halanay, *Differential Equations: Stability, Oscillations, Time Lags,* Academic Press, Inc., New York, 1966.

[55] V. Kolmanovskii and A. Myshkis, *Introduction to the Theory and Applications of Functional Differential Equations,* Kluwer Academic Publishers, 1999.

[56] V. Kolmanovskii and V. Nosov, *Stability of Functional Dierential Equations,* Academic Press, INC, 1986.

[57] Y. Kuang, *Delayed Diffrential Equations with Applications in Population Dynamics*, Academic Press Inc., 1993.

[58] G. Stepan, ”Retarded Dynamical Systems,” *ser. Pitman Research Notes in Mathematics*, Vol. 210. Longman Group, Essex, 1989.

[59] Y. Zhang, *Stability of Hybrid Systems with Time Delay. PhD thesis,* University of Waterloo, ON. Canada, 2004.

[60] S. Floyd and S. McCanne, “Network Simulator,” LBNL public domain software. Available via ftp from ftp.ee.lbl.gov. NS-2 is available in `http://www.isi.edu/nsnam/ns/`.

[61] D. Bauso, L. Giarre and G. Neglia, “Active Queue Management Stability in Multiple Bottleneck Networks,” *IEEE ICC’04*, Vol. 4, pp. 2267-2271, June 2004.

[62] Y. Xiao and M. Lee, ”Nonlinear Control of Active Queue Management for Multiple Bottleneck Network,” *IEICE Transactions on Communications*, Vol. E89B, No. 11, pp. 3108-3113, November 2006.

[63] R. H. Middleton, C. M. Kellett, and R. N. Shorten, ”Fairness and Convergence Results for Additive-Increase Multiplicative-Decrease Multiple-Bottleneck Networks,” *45th IEEE Conference on Decision and Control*, pp. 1864-1869, December 2006.

[64] P. Ranjan, R. J. La and E. H. Abed, “Global Stability Conditions for Rate Control with Arbitrary Communication Delays,” *IEEE/ACM Trans. on Networking*, Vol. 14, No. 1, pp. 94-107, February 2006.

[65] G. Vinnicombe, ”On the stability of networks operating TCP-like congestion control,” *Proc. of the IFAC World Congress,*, 2002.

[66] J. E. Slotine and W. Li, *Applied Nonlinear Control,* Prentice Hall, Englewood Cliffs, NJ, 1991.

[67] P. Gahinet, A. Nemirovski, A. J. Laub and M. Chilali, *LMI Control Toolbox – for Use with Matlab,* The MATH Works Inc., 1995.

[68] Z. Gajic and X. Shen, *Parallel Algorithms for Optimal Control of Large Scale Linear Systems,* Springer-Verlag, 1993, ISBN: 0387198253.

[69] Z.H. Shao, Stability bounds of singularly perturbed delay systems, *IEE Proc.-Control Theory Appl.*, **151**, (2004) pp. 585-588.

[70] E. Fridman, Effects of small delays on stability of singularly perturbed systems, *Automatica*, **38**, (2002) pp. 897-902.

[71] P.V. Kokotović, H.K. Khalil and J. O’Reilly, *Singular Perturbation Methods in Control: Analysis and Design,* SIAM, Philadelphia, 1999.

Author's Publications

1. L. Wang, L. Cai, X. Liu and X. Shen, "Stability and TCP-friendliness of AIMD/RED Systems with Feedback Delays," *Computer Networks*, Vol. 51, No. 15, pp. 4475-4491, Oct. 2007.

2. L. Wang, L. Cai, X. Liu and X. Shen, "Stability and Fairness Analysis of AIMD/RED System with Heterogeneous Delays", *Proc. of IEEE Globecom*, pp. 1813-1817, Dec. 2007.

3. L. Wang, L. Cai, X. Liu and X. Shen, "AIMD Congestion Control: Stability, TCP-friendliness, Delay Performance," *Tech. Rep.*, Mar. 2006. Available at *http://www.ece.uvic.ca/ cai/tech-2006.pdf*

4. L. Wang, L. Cai, X. Liu and X. Shen, "Practical Stability and Bounds of Heterogeneous AIMD/RED System with Time Delay," *Proc. of IEEE ICC*, Beijing China, pp. 5558-5563, May 2008. **(Best Paper Award)**

5. L. Wang, H. Mukaidani, X. Shen and X. Liu, "Delay-Dependent Stability Analysis for Large-Scale Multiple-Bottleneck Systems Using Singular Perturbation Approach", to appear, *Proc. of IEEE Globecom 2008.*

6. L. Wang, X. Liu and X. Shen, "Uniform asymptotic stability of infinite dimensional hybrid dynamical systems", *Proc. of the 4th International DSDIC Conference on Engineering Applications and Computational Algorithms*, pp.837-842, 2005, Watam Press.

7. S. Li, X. Liu and L. Wang, "Robust stabilization of discrete impulsive switched

systems with disturbance", *Dynamics of Continuous, Discrete and Impulsive systems. Ser. A Mathematical Analysis* 13A, pp. 2101–2111, 2006.

8. L. Wang, L. Cai, X. Liu and X. Shen, "Boundedness of AIMD/RED Systems with Time Delays," *Tech. Rep.*, Jul. 2007. Available at *http://www.ece.uvic.ca/ cai*.

9. L. Wang, L. Cai, X. Liu, X. Shen and J. Zhang, "Stability Analysis of Multiple-Bottleneck Networks", *submitted to Computer Networks,* Jan. 2008.

10. L. Wang, L. Cai, X. Liu and X. Shen, "Practical Stability of AIMD/RED Systems with Time Delays," *Submitted to Journal of Communications and Networks,* Jun. 2008.